USGS
science for a changing world

Prepared in cooperation with the University of Minnesota and the Minnesota Geological Survey

Cyclic Injection, Storage, and Withdrawal of Heated Water in a Sandstone Aquifer at St. Paul, Minnesota

Analysis of Thermal Data and Nonisothermal Modeling of Long-Term Test Cycles 1 and 2

U.S. Geological Survey Professional Paper 1530-C

U.S. Department of the Interior
U.S. Geological Survey

Cyclic Injection, Storage, and Withdrawal of Heated Water in a Sandstone Aquifer at St. Paul, Minnesota

By G.N. DEILN[1], M.C. HOYER[2], T.A. WINTERSTEIN[1] *and* R.T. MILLER[3]

Analysis of Thermal Data and Nonisothermal Modeling of Long-Term Test Cycles 1 and 2

U.S. GEOLOGICAL SURVEY PROFESSIONAL PAPER 1530–C

Prepared in cooperation with the University of Minnesota
and the Minnesota Geological Survey

[1] U.S. Geological Surrvey, Mounds View, Minnesota
[2] University of Minnesota, Underground Space Center, Department of Civil Engineering, Minneapolis, Minnesota
[3] Groundwater Investigations, Inc., Pine Bush, New York

U.S. DEPARTMENT OF THE INTERIOR

Gale A. Norton, Secretary

U.S. GEOLOGICAL SURVEY

Charles G. Groat, Director

Mound View, Minnesota, 2002

Library of Congress Cataloging in Publications Data
Delin, G.N., Hoyer, M.C., Winterstein, T.A., and Miller, R.T
Cyclic injection, storage, and withdrawal of heated water in a sandstone aquifer at St. Paul, Minnesota / G.N. Delin, M.C. Hoyer, T.A. Winterstein, and R.T. Miller.
80 p., 28 cm. — (Analysis of thermal data and nonisothermal modeling of long-term test cycles 1 and 2) (U.S. Geological Survey Professional Paper; 1530-C)
"Prepared in cooperation wth the University of Minnesota and the Minnesota Geological Survey."
Includes bibliographic references (p. 79).
ISBN 0-607-99152-6
Supt. of Docs. no.: I 19.16: 1530-C
1. Hot-air heating. 2. Hot water. 3. Water-storage—Minnesota—St. Paul. 4. Aquifers—Minnesota—St. Paul. I. Univesity of Minnesota. II. Minnesota Geological Survey. III. Title. IV. Series. V. Series: U.S. Geological Survey professional paper; 1530-C.
TH7602.M55 2002 92–23497
697'.4—dc20 CIP

For sale by U.S. Geological Survey, Information Services,
Box 25286, Federal Center,
Denver, CO 80225

CONTENTS

Illustrations

Illustrations—Continued

Tables

CONVERSION FACTORS, VERTICAL DATUM, AND ABBREVIATIONS

Multiply	By	To obtain
	Length	
meter (m)	3.281	foot
	Area	
square meter (m^2)	0.0002471	acre
	Volume	
cubic meter (m^3)	6.290	barrel (petroleum, 1 barrel=42 gal)
	Flow rate	
meter per day (m/d))	3.281	foot per day
cubic meter per second (m^3/s)	35.31	cubic foot per second
liter per second (L/s)	15.85	gallon per minute
cubic meter per day (m^3/d)	264.2	gallon per day
	Mass	
kilogram (kg)	2.205	pound avoirdupois
	Pressure	
kilopascal (kPa)	0.1450	pound-force per inch
	Density	
kilogram per cubic meter (kg/m^3)	0.06242	pound per cubic foot
	Energy	
joule	0.0000002	kilowatt-hour
watt per square meter (W/m^2)	8.804×10^{-5}	British thermal unit per square foot per second
watt per cubic meter (W/m^3)	2.684×10^{-5}	British thermal unit per cubic foot per second
joule per meter per day per degree [((J/m)/d)/°C]	1.605×10^{-4}	British thermal unit per foot Celsius per day per degree Fahrenheit
joule per cubic meter per degree [(J/m^3)/°C]	1.491×10^{-5}	British thermal unit per cubic pound avoirdupois per
joule per kilogram per degree [(J/kg)/°C]	2.388×10^{-4}	British thermal unit per pound avoirdupois per degree Fahrenheit
	Hydraulic conductivity	
meter per day (m/d)	3.281	foot per day
	Hydraulic gradient	
meter per kilometer (m/km)	5.27983	foot per mile
	Transmissivity	
meter squared per day (m^2/d)	10.76	foot squared per day

Temperature in degrees Celsius (°C) may be converted to degrees Fahrenheit (°F) as follows: $°F = (1.8 \times °C) + 32$

Sea level: In this report, "sea level" refers to the National Geodetic Vertical Datum of 1929 (NGVD of 1929)—a geodetic datum derived from a general adjustment of the first-order level nets of both the United States and Canada, formerly called Sea Level Datum of 1929.

Altitude, as used in this report, refers to distance above or below sea level.

Transmissivity: The standard unit for transmissivity is cubic foot per day per square foot times foot of aquifer thickness [(ft^3d)/ft^2]ft. In this report, the mathematically reduced form, foot squared per day (ft^2/d), is used for convenience.

Specific conductance is given in microsiemens per centimeter at 25 degrees Celsius (µS/cm at 25 °C).

Concentrations of chemical constituents in water are given either in milligrams per liter (mg/L) or micrograms per liter (µg/L).

NOTE TO USGS USERS: Use of hectare (ha) as an alternative name for square hectometer (hm^2) is restricted to the measurement of small land or water areas. Use of liter (L) as a special name for cubic decimeter (dm^3) is restricted to the measurement of liquids and gases. No prefix other than milli should be used with liter. Metric ton (t) as a name for megagram (Mg) should be restricted to commercial usage, and no prefixes should be used with it.

Cyclic Injection, Storage, and Withdrawal of Heated Water in a Sandstone Aquifer at St. Paul, Minnesota

Analysis of Thermal Data and Nonisothermal Modeling of Long-Term Test Cycles 1 and 2

By G.N. Delin[1], M.C. Moyer[2], T.A. Winterstein[1], and R.T. Miller[3]

ABSTRACT

In May 1980, the University of Minnesota began a project to evaluate the feasibility of storing heated water (150 degrees Celsius) in the Franconia-Ironton-Galesville aquifer (183 to 245 meters below land surface) and later recovering it for space heating. The University's steam-generation facilities supplied high-temperature water for injection. This Aquifer Thermal-Energy Storage system had a doublet-well design in which the injection and withdrawal wells were spaced approximately 250 meters apart. Water was pumped from one of the wells through a heat exchanger, where heat was added or removed. This water was then injected back into the aquifer through the other well.

Two long-term test cycles, consisting of approximately equal durations of injection, storage and withdrawal of about 59 days, were completed. Rates of injection and withdrawal of about 18 liters per second were maintained for each long-term test cycle. Injection temperatures averaged about 108.5 and 117.7 degrees Celsius for long-term test cycles 1 and 2, respectively. Withdrawal temperatures averaged about 75 and 85 degrees Celsius, respectively.

Temperature graphs for selected depths at individual observation wells indicate that the Ironton and Galesville Sandstones received, stored, and yielded more thermal energy than the upper part of the Franconia Formation. Vertical-profile plots and time-graphs during storage indicate that the effects of buoyancy flow were minimal within the aquifer.

A three-dimensional, anisotropic, nonisothermal ground-water-flow and thermal-energy-transport model was constructed to simulate the two long-term test cycles. The only model properties varied during model calibration were longitudinal and transverse thermal dispersivities, which, for final calibration, were simulated as 3.3 and 0.33 meters, respectively. The model was calibrated by comparing model-computed results to: (1) measured temperatures at selected altitudes in five observation wells, (2) measured temperatures at the production well, and (3) calculated thermal efficiencies of the aquifer. Model-computed withdrawal-water temperatures were within about 3 percent of measured values and model-computed aquifer-thermal efficiencies were within about 1 percent of calculated values for the long-term test cycles. On the basis of these data, the model accurately simulates aquifer thermal-energy storage within the Franconia-Ironton-Galesville aquifer.

INTRODUCTION

The University of Minnesota started a project in May 1980 to evaluate use of a confined, sedimentary-bedrock (sandstone) aquifer [about 183 m beneath the St. Paul campus] for thermal-energy storage (fig. 1). The project was funded by the U.S. Department of Energy through Battelle Pacific Northwest Laboratories. Other participants in the project include the Minnesota Energy Agency, the Minnesota Geological Survey, National Biocentrics, Inc., Orr-Schelen-Mayeron and Associates, and the U.S. Geological Survey. The project was designed to evaluate the feasibility and effects of storing high-temperature (150°C) water in the Franconia-Ironton-Galesville aquifer beneath the St. Paul campus and later recovering the heat for water and space heating.

The specific objectives of the U.S. Geological Survey in evaluating Aquifer Thermal-Energy Storage (ATES) were to: (1) develop an understanding of the ground-water-flow system near the site, (2) identify the

[1] U.S. Geological Survey, Mounds View, Minnesota
[2]University of Minnesota, Underground Space Center, Department of Civil Engineering, Minneapolis, Minnesota
[3]Groundwater Investigations, Inc., Pine Bush, New York

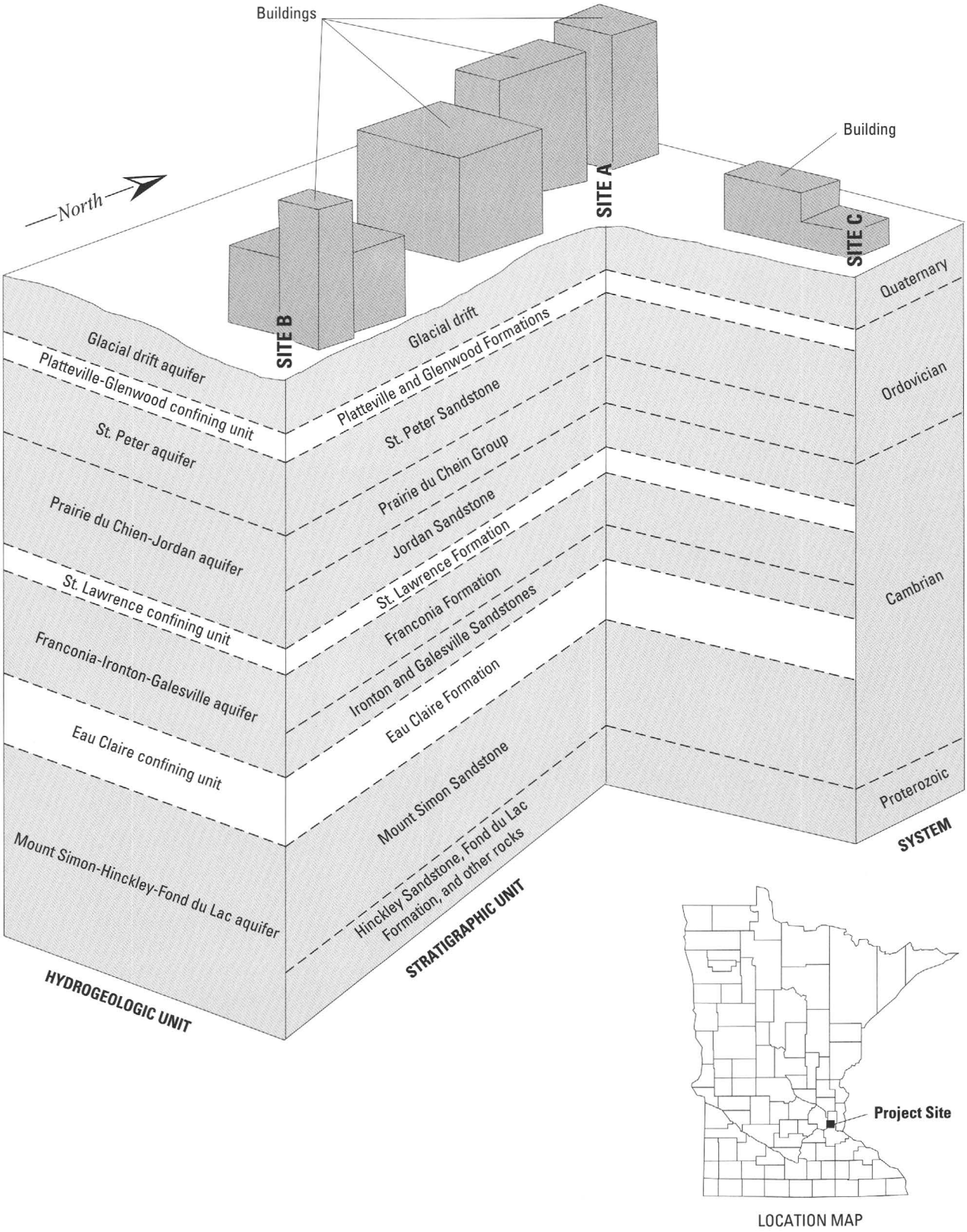

Figure 1. Location and generalized schematic diagram of hydrogeology of the Aquifer Thermal-Energy Storage (ATES) site.

hydraulic properties of the ground-water-flow system that are most important with respect to thermal-energy storage and identify data-collection needs for monitoring and evaluating aquifer-system performance, (3) develop a method to evaluate flow and thermal-energy transport for various cyclic injection and withdrawal schemes and aid in selection of an efficient well-system design, and (4) assist in the collection of hydraulic and thermal data during injection-withdrawal tests and design a data-processing system that will facilitate entry of the data into computer storage. Miller (1984 and 1985) described the anisotropy of the Franconia-Ironton-Galesville aquifer, and preliminary modeling at the ATES site, respectively. Miller and Voss (1986) described the design of the finite-difference grid at the ATES site. Miller and Delin (1993) described (1) analysis of field observations for aquifer characterization and observation-network design, (2) preliminary model analysis to determine model sensitivity to hydraulic and thermal characteristics and to facilitate final model design, and (3) model simulations of the aquifer's thermal efficiency. Miller and Delin (1994) described analysis of the thermal data and nonisothermal modeling for the short-term test cycles. Walton and others (1991) described the geologic and hydrologic setting of the ATES site, the ATES system and its operation during the short-term test cycles, and presented the water chemistry, system flow, and temperature results for the short-term test cycles. Hoyer and others (1991a and 1991b) describe additions to and operation of the ATES system during the first and second long-term test cycles, and present the water chemistry, system flow, and temperature results for the first and second long-term test cycles.

Purpose and Scope

This report describes (1) the collection of hydraulic and thermal data for two long-term test cycles of heated-water injection, storage, and withdrawal; and (2) the analysis and nonisothermal modeling for the two cycles. This report is one in a series that describes the potential for thermal-energy storage within the Franconia-Ironton-Galesville aquifer beneath the St. Paul campus of the University of Minnesota.

Hydrogeologic Setting

The St. Paul metropolitan area is underlain by a stratified sequence of Proterozoic and early Paleozoic sedimentary formations consisting of porous sandstone and fractured dolomite, which can be grouped into four major regional aquifers. The aquifers generally are separated by semipermeable sandstone, siltstone, or shale formations. The major aquifers are the St. Peter, Prairie du Chien-Jordan, Franconia-Ironton-Galesville, and Mount Simon-Hinckley-Fond du Lac (fig. 1).

The St. Peter aquifer consists of the St. Peter Sandstone, which is composed of a light-yellow or white, massive, quartzose, fine- to medium-grained, well-sorted, and friable sandstone. Thin beds of siltstone and shale near the base of the St. Peter Sandstone form a lower confining layer. The upper confining layer, consisting of the Platteville and Glenwood Formations, overlies the St. Peter Sandstone and is in contact with glacial drift. At the test site, the St. Peter aquifer is approximately 57 m below land surface and is 50 m thick. Transmissivity ranges from 220 to 280 m^2/d and the storage coefficient ranges from 9.0×10^{-5} to 9.75×10^{-3}. Porosity ranges from 0.28 to 0.30. The hydraulic gradient was estimated to be 0.006 and the pore velocity was estimated to be 0.18 m/d by Norvitch and others (1973).

The Prairie du Chien-Jordan aquifer consists of the Prairie du Chien Group and the Jordan Sandstone (fig. 1). The Prairie du Chien Group is predominantly a light brownish-gray or buff, sandy, thin- to thick-bedded dolomite that is vuggy and fractured and contains thin layers of interbedded grayish-green shale. The underlying Jordan Sandstone is a white to yellow, quartzose, fine-to coarse-grained sandstone that is massive or thick to thin bedded and varies from friable to well cemented. Despite the differing lithologies, the Prairie du Chien Group and Jordan Sandstone function as one aquifer because there is no regional confining unit between them. At the test site the aquifer is approximately 107 m below land surface and is 69 m thick. The average transmissivity is approximately 1,235 m^2/d, with a porosity of 0.30. The hydraulic gradient was estimated to be approximately 0.005 and the pore velocity was estimated to be 0.30 m/d by Norvitch and Walton (1979).

The St. Lawrence Formation acts as a confining layer between the Prairie du Chien-Jordan and the Franconia-Ironton Galesville aquifers. The St. Lawrence Formation is about 176 m below land surface and is approximately 7 m thick at the test site. It is a gray and greenish-gray, laminated, thin-bedded, dolomite siltstone, silty dolomite, and shale. The porosity ranges from 0.15 to 0.20 and transmissivities range from 1 to 10 m^2/d.

The Franconia-Ironton-Galesville aquifer consists of the Franconia Formation, and the Ironton and Galesville Sandstones. The Franconia Formation is divided into four members: Reno, Mazomanie, Tomah, and Birkmose (Walton and others, 1991). The Reno Member in the upper part of the Franconia is a fine- to very fine-grained, quartz, and glauconitic sandstone. The Reno is divided into two sections and is located approximately between 180 and 183 m and between 193 and 206 m below land surface. The Mazomanie member is in the upper part of the Franconia between the depths of 186–193 m. The Mazomanie also is a fine- to very-fine grained, quartz sandstone, but has minor glauconite content. The Tomah Member in the lower part of the Franconia is an interbedded sequence of fine- to very fine-grained, silty sandstone with interbedded siltstone or shale. The Tomah is located between 206 and 219 m below land surface. The Birkmose Member in the lower part of the Franconia is a dolomitic siltstone with some shale and fine- to very fine-grained glauconitic sandstone interbedded. Based on laboratory permeability tests (Walton and others, 1991), the horizontal hydraulic conductivity of the upper part of the Franconia is about 158 times greater than the hydraulic conductivity of the lower part of the Franconia. Analysis of results of packer tests indicate two hydraulic zones within the Franconia Formation (Miller and Delin, 1993). Based on the distinct differences in grain size, geophysical logs, and hydraulic properties between the upper and lower parts of the Franconia Formation, the upper 14 m of the Franconia was considered an aquifer and the lower 25 m of the Franconia was considered a confining unit. The Ironton Sandstone is white, medium-grained, moderately well-sorted quartz arenite that contains some silt-sized material. The Galesville Sandstone consists of a white to light-gray slightly glauconitic, well- to moderately well-sorted, mostly medium-grained quartzose sandstone. The depth of the Franconia-Ironton-Galesville aquifer beneath the site is about 183 m and its thickness is about 62 m. The total transmissivity is 97.5 m^2/d and the storage coefficient is 2.75×10^{-5}. Transmissivity of the Franconia-Ironton-Galesville aquifer is anisotropic, with the principal axis of transmissivity oriented about 30 degrees east of north. Average porosity ranges from 0.25 to 0.31 with a hydraulic gradient of 0.002 and an estimated pore velocity of 0.05 m/d. The ambient temperature of the ground-water system is typically about 11°C.

The Eau Claire Formation is a confining layer between the Franconia-Ironton Galesville and the Mount Simon-Hinckley-Fond du Lac aquifers.The Eau Claire Formation consists of interbedded siltstone, shale, and fine silty sandstone with a few thin layers of dolomite. The depth of the formation beneath the site is about 245 m and its thickness is about 29 m. Transmissivity ranges from 0.5 to 5 m^2/d and porosity ranges from 0.28 to 0.35 (Norvitch and others, 1973).

The Mount Simon-Hinckley-Fond du Lac aquifer consists of the Mount Simon and Hinckley Sandstones and the Fond du Lac Formation. The Mount Simon Sandstone is fine- to coarse-grained, contains very thin beds of shale, and commonly is gray, white, or pink. The Hinckley Sandstone is fine- to coarse-grained and pale red to light pink. The Fond du Lac Formation contains lenticular beds of fine- to medium-grained arkosic sandstone interbedded with mudstone and is dark red to pink. The top of the aquifer is approximately 274 m below land surface and the aquifer is approximately 60 m thick. The transmissivity is approximately 250 m^2/d and the storage coefficient is about 6×10^5 (Norvitch and others, 1973). The porosity averages 0.25, the hydraulic gradient is 0.0025, and the pore velocity is approximately 0.03 m/d (Norvitch and others, 1973).

Aquifer Selection

The selection of an aquifer for thermal-energy testing was based on the following criteria: (1) minimal use of water from the aquifer in the Twin Cities area, (2) ability of the confining units above and below the aquifer to contain the injected heated water, and (3) the hydrogeologic properties and natural gradients within the aquifer and their effect on the transfer of heat.

Description of Test Facility

The University of Minnesota test facility was a doublet well system in which production wells A and B were spaced approximately 250 m apart (fig. 2). During heat injection, water was pumped from the Franconia-Ironton-Galesville aquifer through production well B (fig. 2), transported through the ion-exchange water softener where hardness was reduced, passed through a heat exchanger where the water was heated, and injected back into the Franconia-Ironton-Galesville aquifer through production well A (fig. 3). During heat withdrawal, water was pumped from the Franconia-Ironton-Galesville aquifer through production well A (fig. 2), transported through a radiator where the water

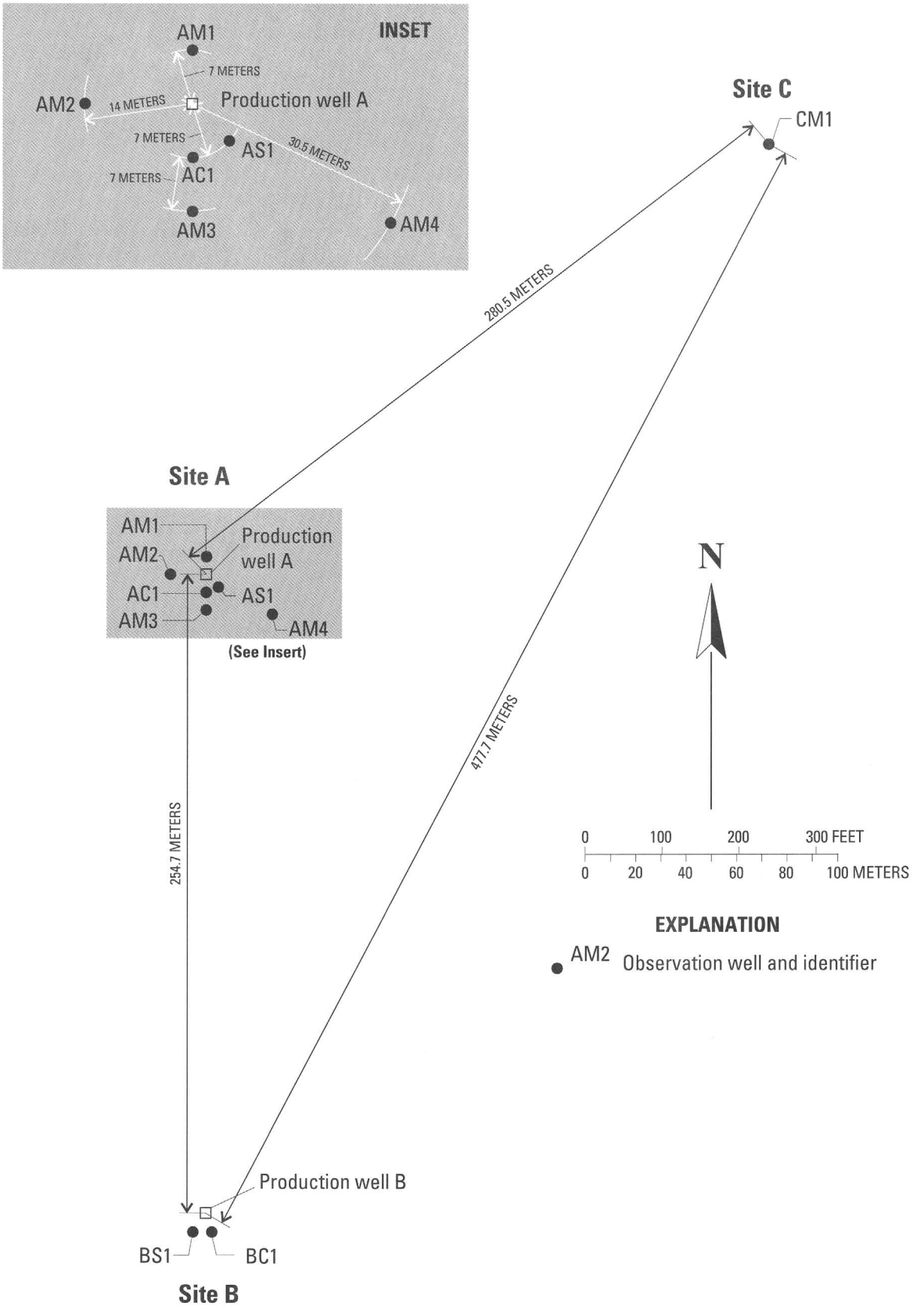

Figure 2. Plan view of the Aquifer Thermal-Energy Storage (ATES) sites.

was cooled, and then injected back into the aquifer through production well B (fig. 3). The system also included piping between the production wells, steam and condensate piping to the campus steam plant, heat exchangers, water treatment facility, observation wells, and instrumentation (fig. 3). The production wells were screened from about 40 to 61 m (Ironton and Galesville Sandstones) and from about 90 to 104 m (upper part of the Franconia Formation) above sea level, respectively (fig. 4; Miller and Delin, 1993). For the long-term test cycles an ion-exchange water softener was added to the system (fig. 3).

The ion-exchange water softener was added to the ATES system to prevent calcium carbonate precipitation in the storage well and aquifer, replacing the above-ground precipitation filters that had been used during the short-term cycles (Walton and others, 1991; Miller and Delin, 1994). The ion-exchange water softener reduced the hardness of the ground water before it was heated, reducing the degree of scaling in the heat exchangers and in the storage well (Hoyer and others, 1991a and 1991b). Use of the water softener allowed the uninterrupted operation of the ATES system during heat injection (Hoyer and others, 1991a and 1991b). During the short-term test cycles, the precipitation filters and the heat exchangers required cleaning after one or two days of injection (Walton and others, 1991; Miller and Delin, 1994).

Temperature and pressure measurements were made in observation wells AM1, AM2, AM3, AM4, and AS1 (figs. 2 and 3). Observation well AM4 was installed 30.5 meters from production well A before the long-term test cycles began to record temperatures near the anticipated maximum extent of the thermal front for the long-term test cycles. Separate wells were installed for temperature and pressure measurements at each location (fig. 4). The altitudes of individual measurement points for the observation wells are also shown in figure 4.

Temperature measurements at production well A were made by use of a type-T (copper-constantan) thermocouple installed within the injection/discharge pipe at the wellhead. Temperature measurements within each of the observation wells (fig. 4) were made by use of as many as 12 type-T thermocouples as described in detail by Miller and Delin (1993). The thermocouples were in 1 or 2 manufactured strings (one containing 8 thermocouples and one containing 4) in protective 3.2-cm- or 5.1-cm- diameter steel casings within the observation wells at the altitudes shown in figure 4. Individual thermocouples were coated with Teflon for resistance to heat, and each 4 or 8 thermocouple string was covered with a stainless steel overbraid to add rigidity and to protect each string as it was lowered into the steel casing. During installation, however, the overbraid tended to twist and kink causing excessive wear to the thermocouple wire where the kinks rubbed on the side of the well casing. Several thermocouples failed because of electrical shorts in thermocouple wires at these points of excessive wear. Temperatures measured by the thermocouples probably were slightly less than the actual temperatures in the aquifer because of conductive heat losses to the well casing; however, these temperature losses were minimal and measured temperatures were considered representative of temperatures in the aquifer.

Submersible pressure transducers were installed to measure pressures in the observation wells. Pressures from 0 to 1,724 kPa could be measured in a temperature range of 10–121°C. Measurement accuracy was ±2 percent of the full-scale output over the compensated temperature range, or a maximum of ±34 kPa at 121°C. The pressure transducers in most observation wells failed shortly after being installed. Several pressure transducers were replaced more than once, only to fail again. Only one pressure transducer functioned during long-term test cycle 1 and none functioned during long-term test cycle 2. Consequently, water levels were measured periodically in the observation wells during the long-term test cycles. Water-level data are reported in Hoyer and others (1991a and 1991b).

All temperature and pressure-transducer data were transmitted through buried cables to a central data logger that measured data on electrostatic paper and nine-track computer tape. The operation of the data logger and the computer programs written to reduce the stored data are described in detail by Czarnecki (1983). Minor modification of the data-logger entries and the data-reduction program were required with the addition of observation well AM4 for the long-term test cycles. Some data were lost during the test cycles as a result of occasional failure of individual data-logger channels.

Individual data-collection points will be referred to in this report by their observation-well location with respect to production well A and by their vertical position within each observation well as referenced to sea level. Reference to sea level as a datum is justified because over the very small area of the site, the formations are essentially flat-lying.

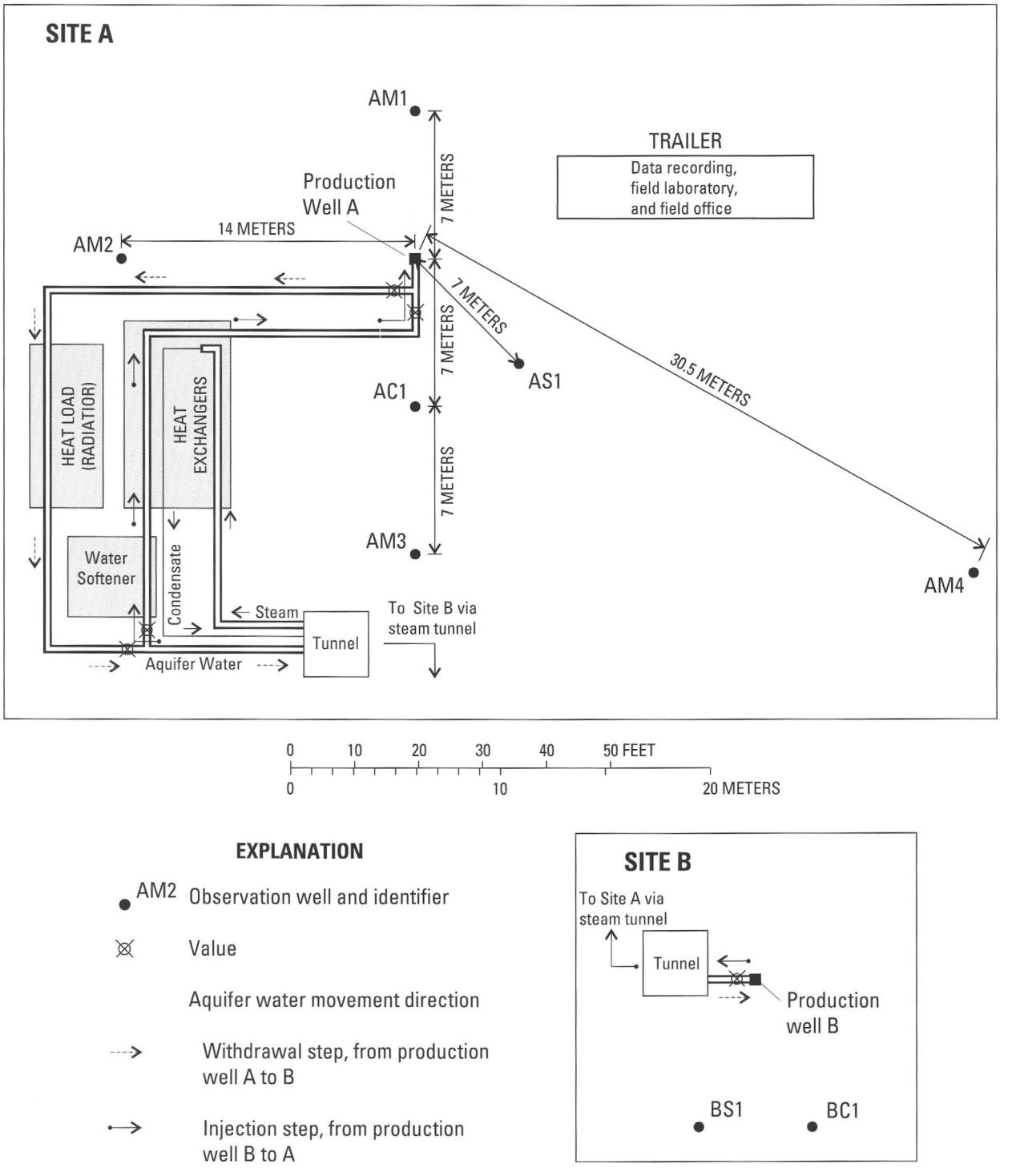

Figure 3. Schematic diagram of sites A and B at the Aquifer Thermal-Energy Storage (ATES) site. (Modified from Walton and others, 1991).

Downhole gyroscopic surveys were conducted in several observation wells to determine deviations of each well bore with respect to land surface position (Hoyer and others, 1991a; Miller and Delin, 1993). The bottoms of some wells deviate from their land-surface locations by as much as 8 m horizontally (fig. 5). These horizontal deviations were considered during interpretation of temperature data.

LONG-TERM TEST CYCLES 1 AND 2

Following completion of the ATES short-term test cycles (Walton and others, 1991; Miller and Delin,

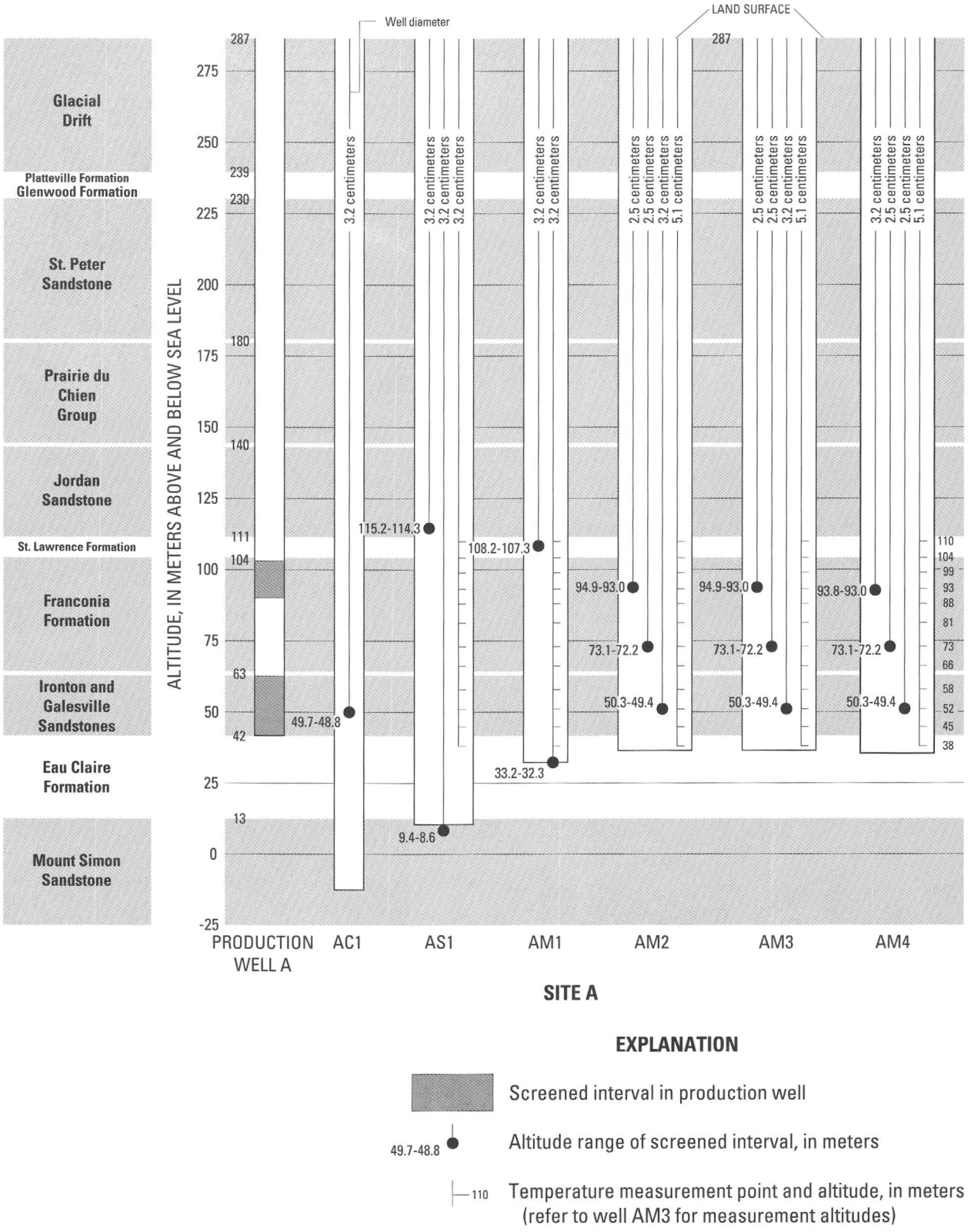

Figure 4. Depths of screened intervals of observation wells, Thermal-Energy Storage (ATES) site. (Horizontal

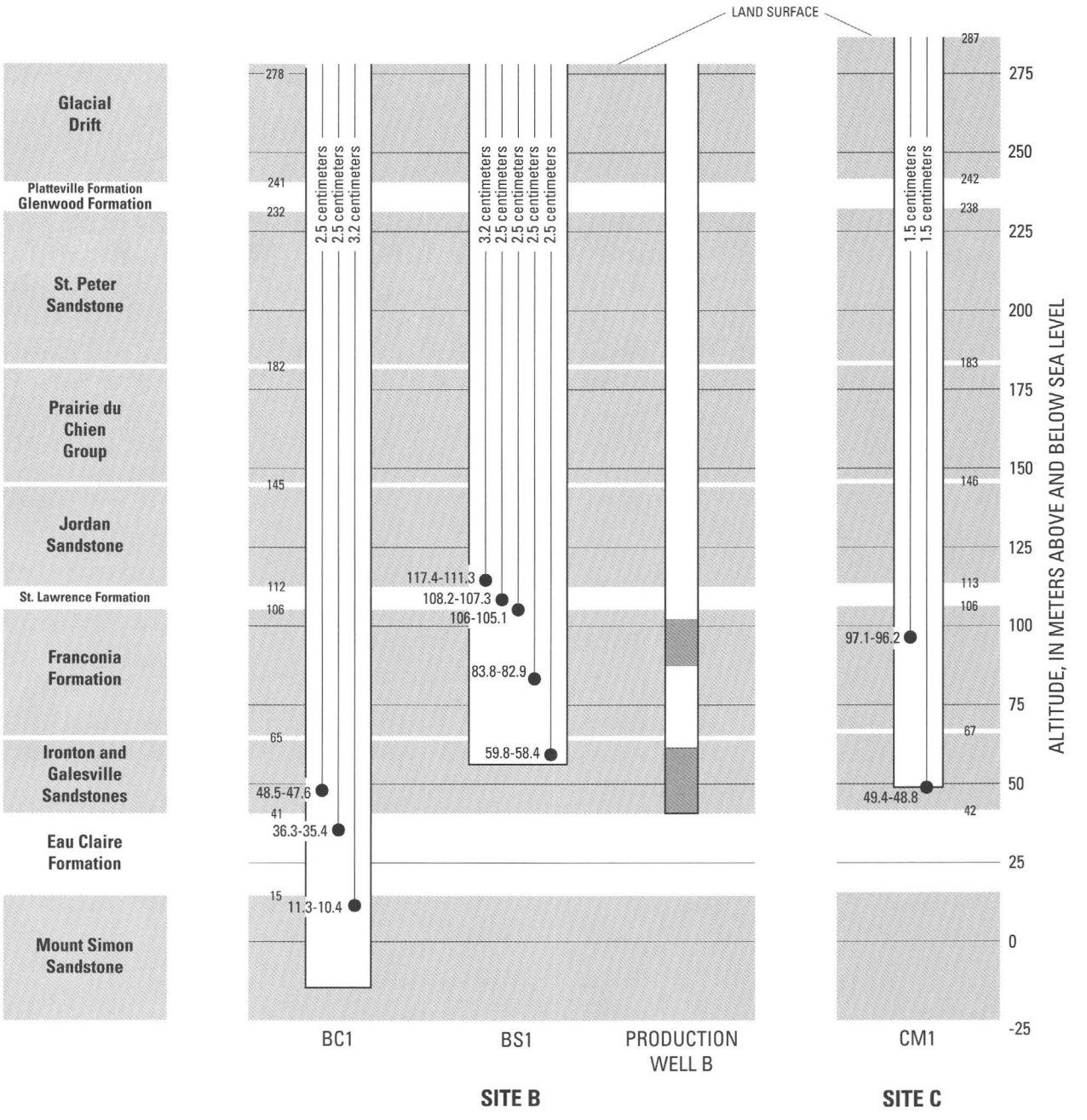

stratigraphy, and location of measurement points of the Aquifer arrangement of wells is arbitrary and not to scale.)

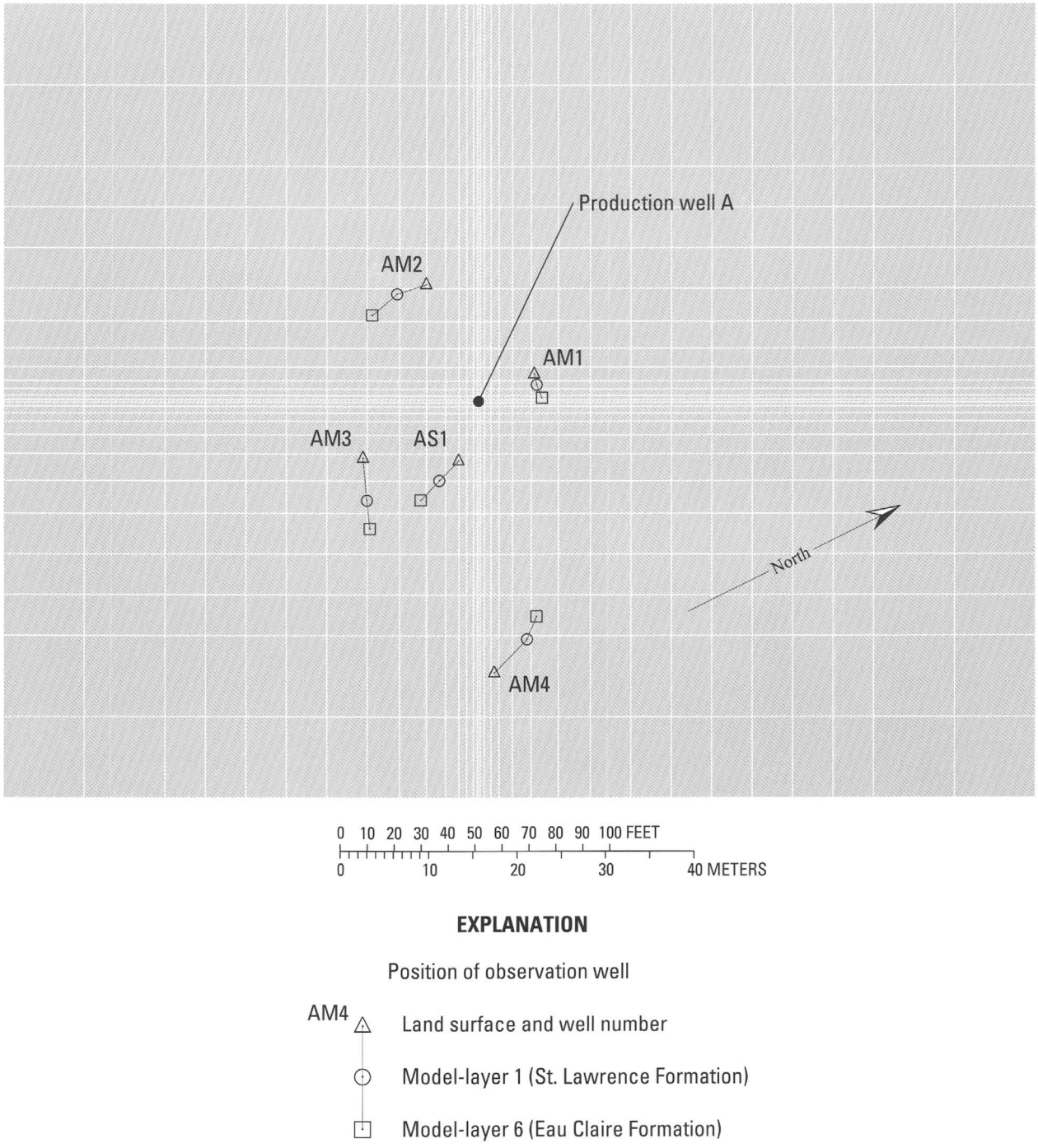

Figure 5. Model grid and position of observation wells at various depths.

1994), addition of an ion-exchange water softener, and addition of observation well AM4, testing of the ATES system continued with two long-term test cycles of heated-water injection, storage, and withdrawal. Each cycle was planned to be approximately 180 days long; the injection, storage, and withdrawal periods for each cycle each were to be approximately 60 days in duration.

The first long-term test cycle was conducted from November 1984 through May 1985; the second long-term test cycle from October 1986 through April 1987. The duration, average rate of injection and withdrawal, and average temperature of injection and withdrawal for long-term test cycles 1 and 2 are shown in table 1. A third long-term test cycle, not described in this report, during

which recovered water was sent to a heat exchanger in a campus building for use, was conducted from October 1989 through March 1990 (Hoyer and others, 1994).

Table 1. Summary of duration, average rates of injection and withdrawal, and average temperatures of injection, storage, and withdrawal for long-term test cycles 1 and 2

	Phase duration (days)	Average flow rate (liters per second)	Average temperature (degrees Celsius)
	Long-term test cycle 1		
Injection	[1]59.1	18.0	108.5
Storage	61.0		
Withdrawal	[2]58.0	18.4	74.7
	Long-term test cycle 2		
Injection	[3]59.3	18.3	117.7
Storage	59.1		
Withdrawal	[4]59.7	17.9	85.1

[1]Over a period of 76 days.
[2]Over a period of 58.8 days.
[3]Over a period of 65.0 days.
[4]Over a period of 59.8 days.

Operation of the ATES system during long-term test cycles 1 and 2 was relatively trouble free. Unlike the short-term test cycles, when injection was interrupted to clean the filters after 1 or 2 days, flow was maintained for many days at relatively constant temperatures during the long-term test cycles with few interruptions. The source water temperature varied smoothly and the temperature of the injected water was controlled by the temperature controller, or varied as a response to the capacity of the heat exchanger (Hoyer and others, 1991a and 1991b). Injection was interrupted eight times during long-term test cycle 1, and five times during long-term test cycle 2. Withdrawal was interrupted once during each cycle by an electrical outage. Interruptions during the injection phases resulted from malfunctioning of the ion-exchange water softener, freezing of pressure shutoff valves, and shutdowns for repairs. A detailed description of the operation of the long-term test cycles is given in Hoyer and others (1991a and 1991b).

ANALYSIS OF THERMAL DATA FOR LONG-TERM TEST CYCLES 1 AND 2

The following sections of the report summarize and interpret the thermal data for the long-term test cycles and describe the movement of heat and the changes in temperature in relation to the hydraulic and thermal properties of the aquifer and confining units. Thermal data are presented in graphs having temperature plotted as a function of time and in graphs of temperature profiles of observation wells at the start and end of each phase of the cycles. Discussion and possible explanations are given for measured trends at individual observation wells and measurement points.

Temperature as a Function of Time

Graphs of temperature as a function of time since each test cycle began were used to evaluate temperature front arrivals, temperature trends, maximum temperatures, and transient thermal effects at specific points within the aquifer. These graphs were particularly useful at points where aquifer properties change between measuring points. Temperatures measured at the wellhead in production well A and in observation wells AM1, AS1, AM2, AM3, and AM4 are presented. Figures 6 through 11 present temperatures for periods of injection, storage, and withdrawal for long-term test cycle 1; figures 12 through 17 present temperatures for injection, storage, and withdrawal periods for long-term test cycle 2. Relatively small temperature fluctuations, which represent intermittent failure of thermocouples due to insulation wear at kinks in the thermocouple wires or electronic noise in the data logger, are evident in some of the graphs for the observation wells and should be ignored. An example of this type of noise is evident in the graph of the 73.1-m thermocouple between days 3 and 10. Temperatures are not plotted for thermocouples that failed during the long-term test cycles. Temperatures for production well A were measured at the wellhead, not within the Franconia-Ironton-Galesville aquifer. Therefore, temperatures for production well A indicate when injection or withdrawal of heated water took place, and when injection or withdrawal was interrupted (figs. 6 and 12). When water was not flowing through the wellhead, as during periods of storage and during interruptions to injection or withdrawal, temperatures in production well A rapidly decreased to the air temperature at the time, below 50°C. Temperatures measured during storage periods, therefore, represent air temperatures and are not representative of temperatures in the Franconia-Ironton-Galesville aquifer.

A temperature front is hereinafter defined as the first temperature increase or decrease measured at a thermocouple, which defines the beginning of a trend of increasing or decreasing temperatures. Identifying the first arrival time of a temperature front was imprecise when the temperature changes were small and when the

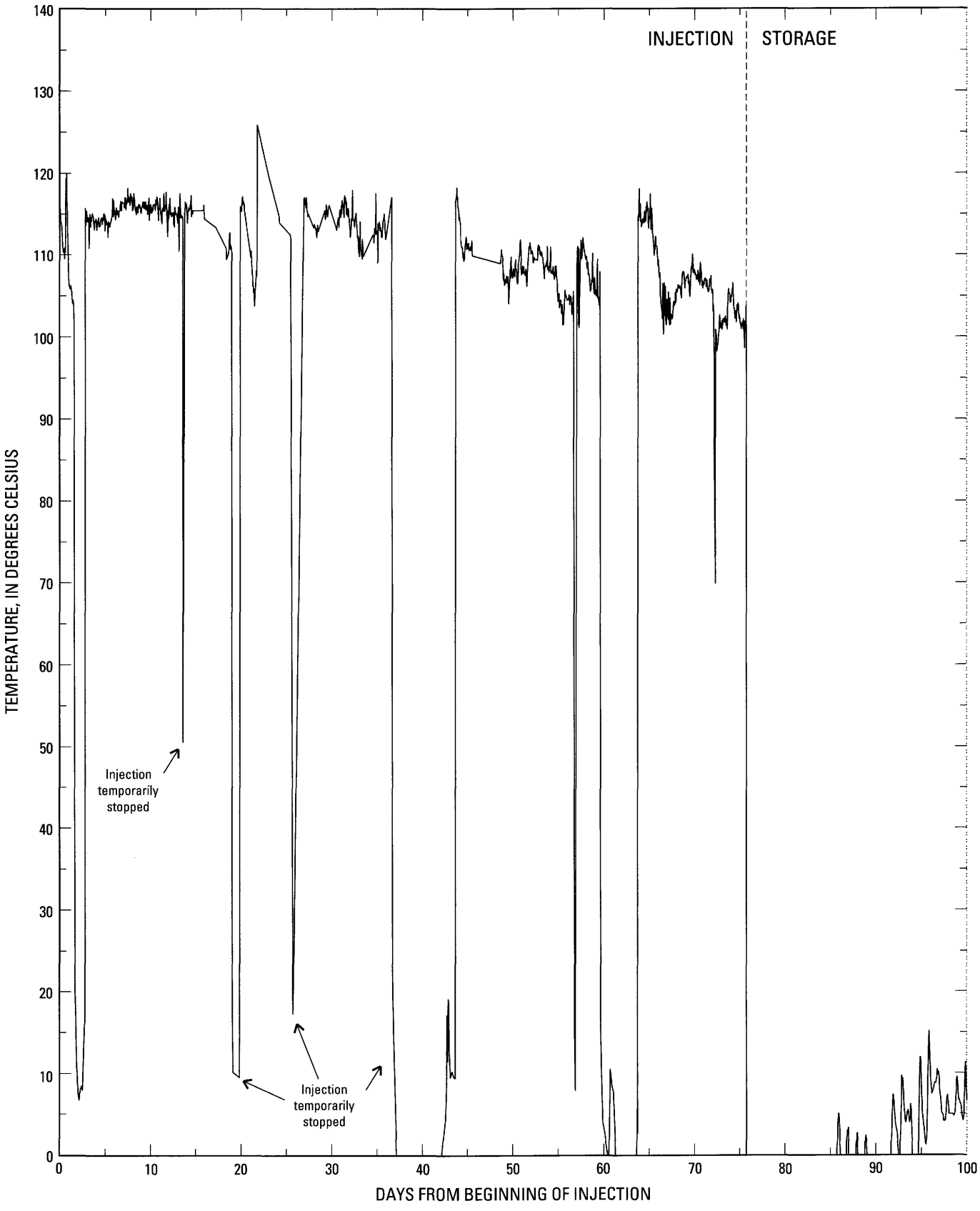

Figure 6. Temperatures at the wellhead in production well A

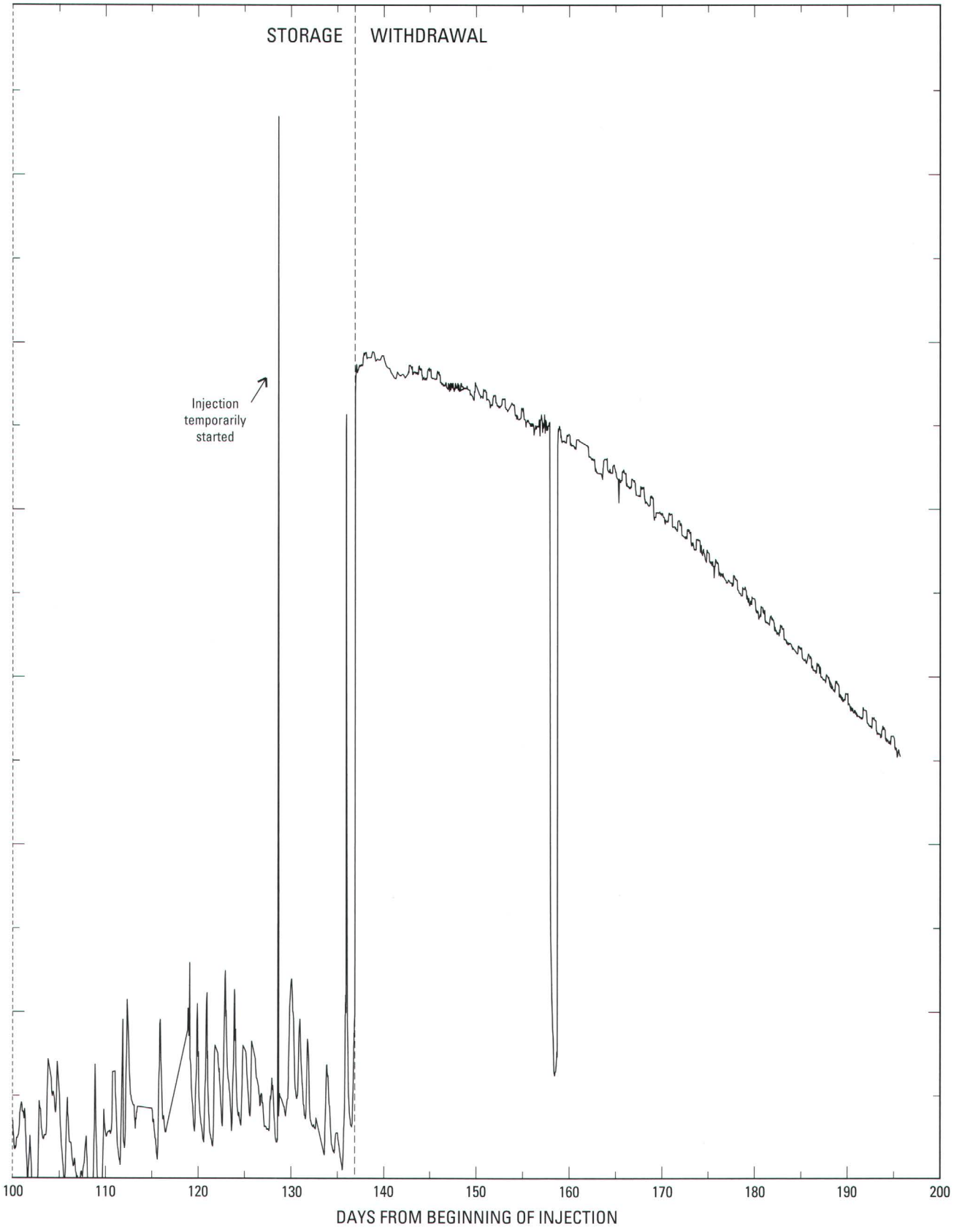

during long-term test cycle 1, November 1984 through May 1985.

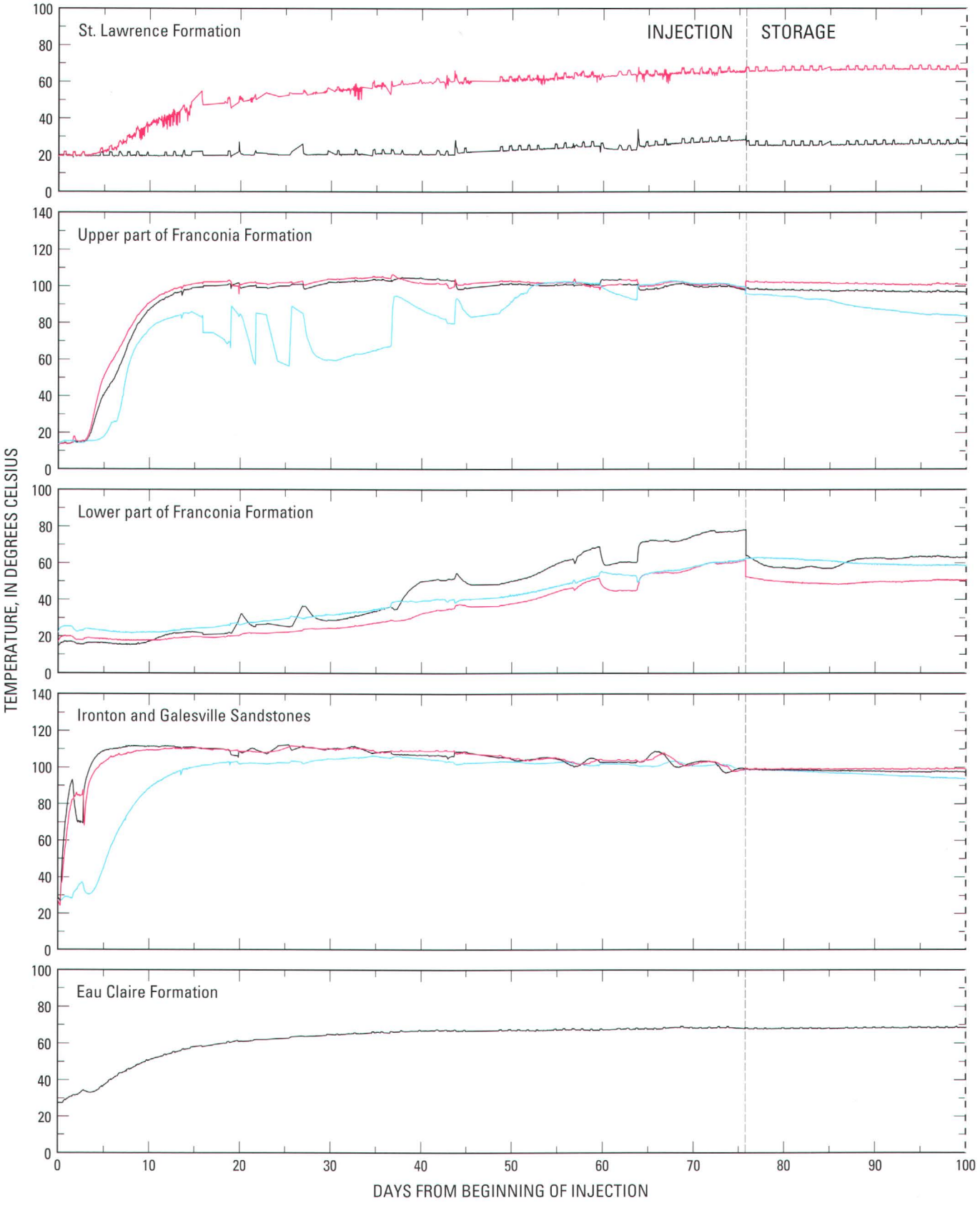

Figure 7. Temperatures in observation well AM1 during

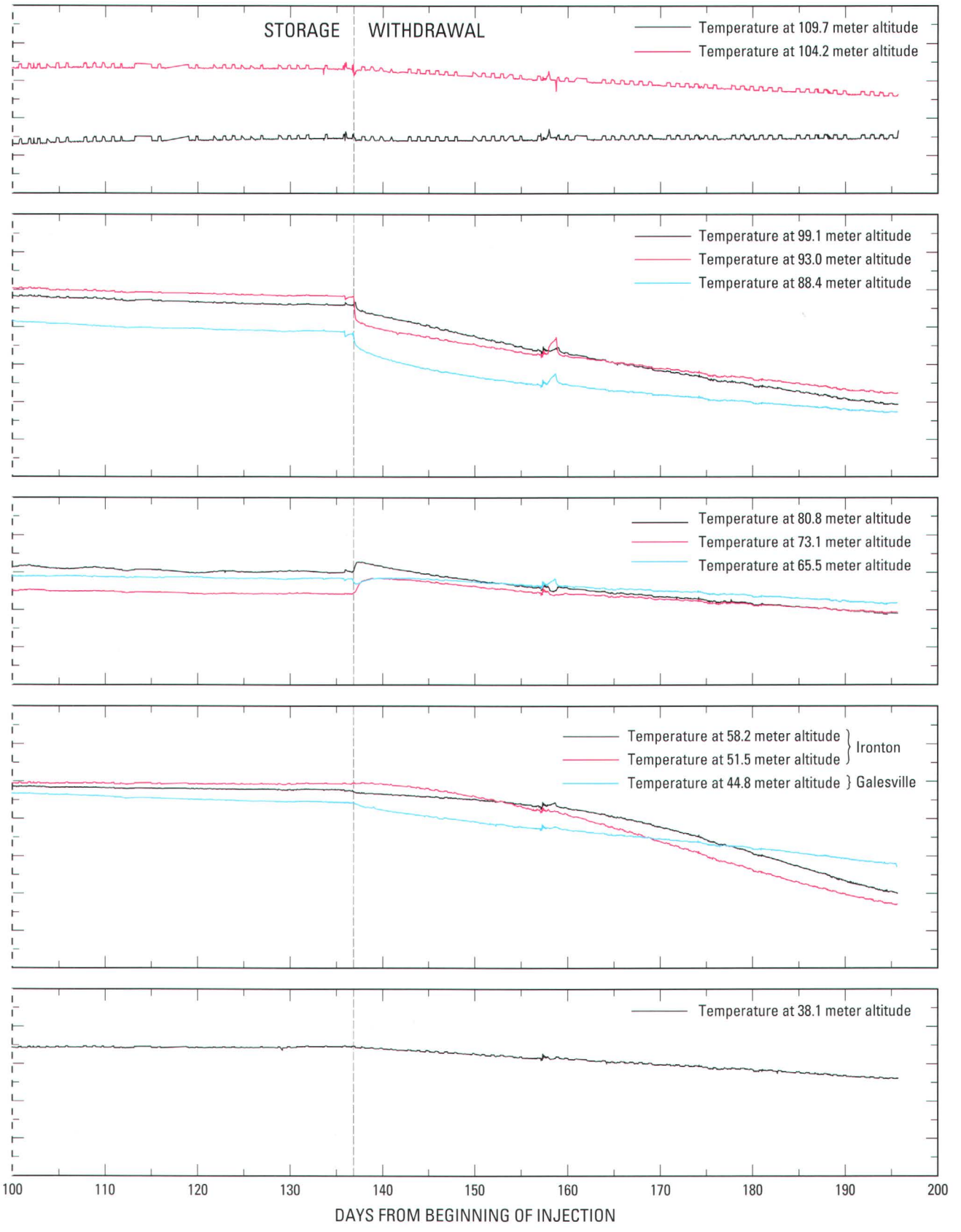

long-term test cycle 1, November 1984 through May 1985.

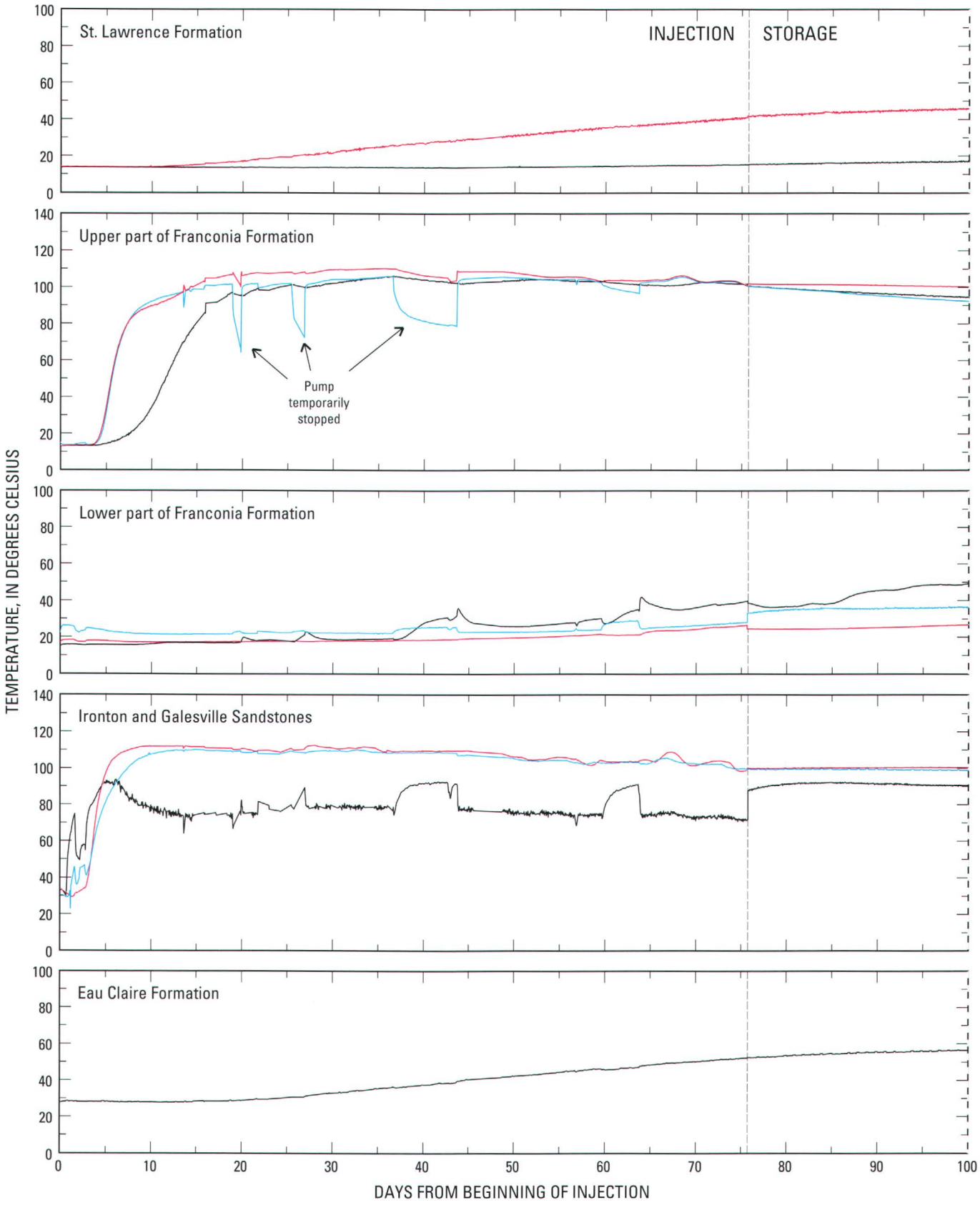

Figure 8. Temperatures in observation well AS1 during

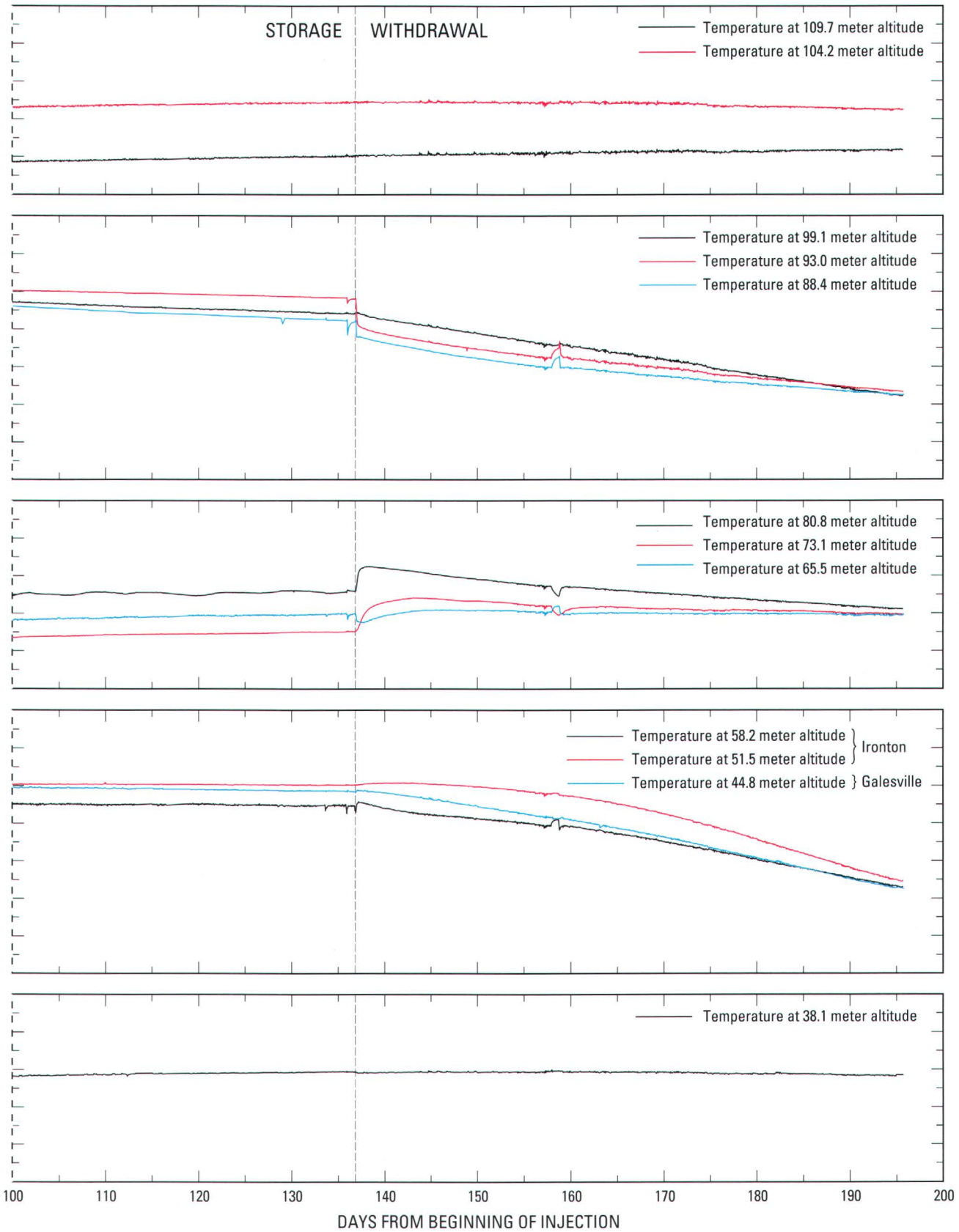

long-term test cycle 1, November 1984 through May 1985.

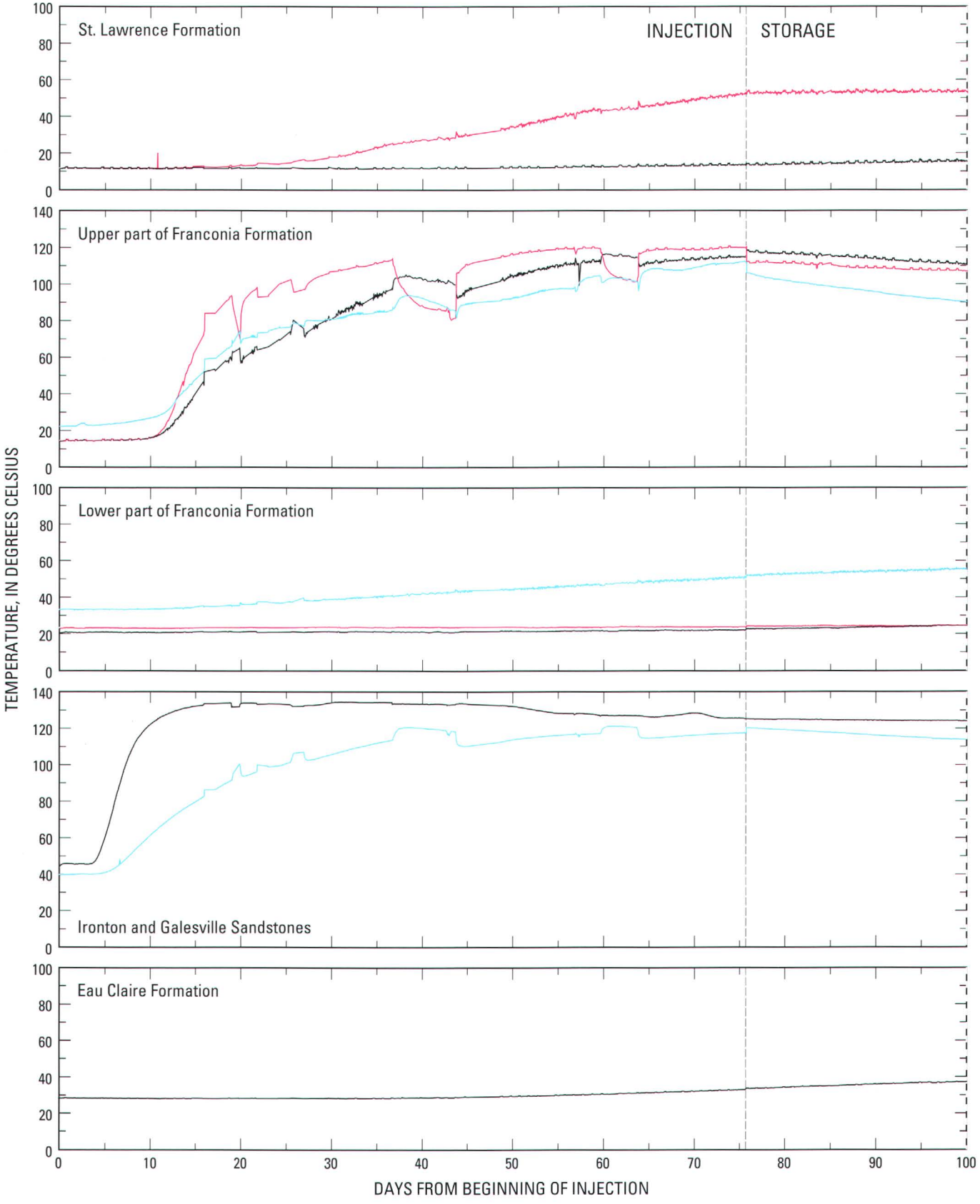

Figure 9. Temperatures in observation well AM2 during

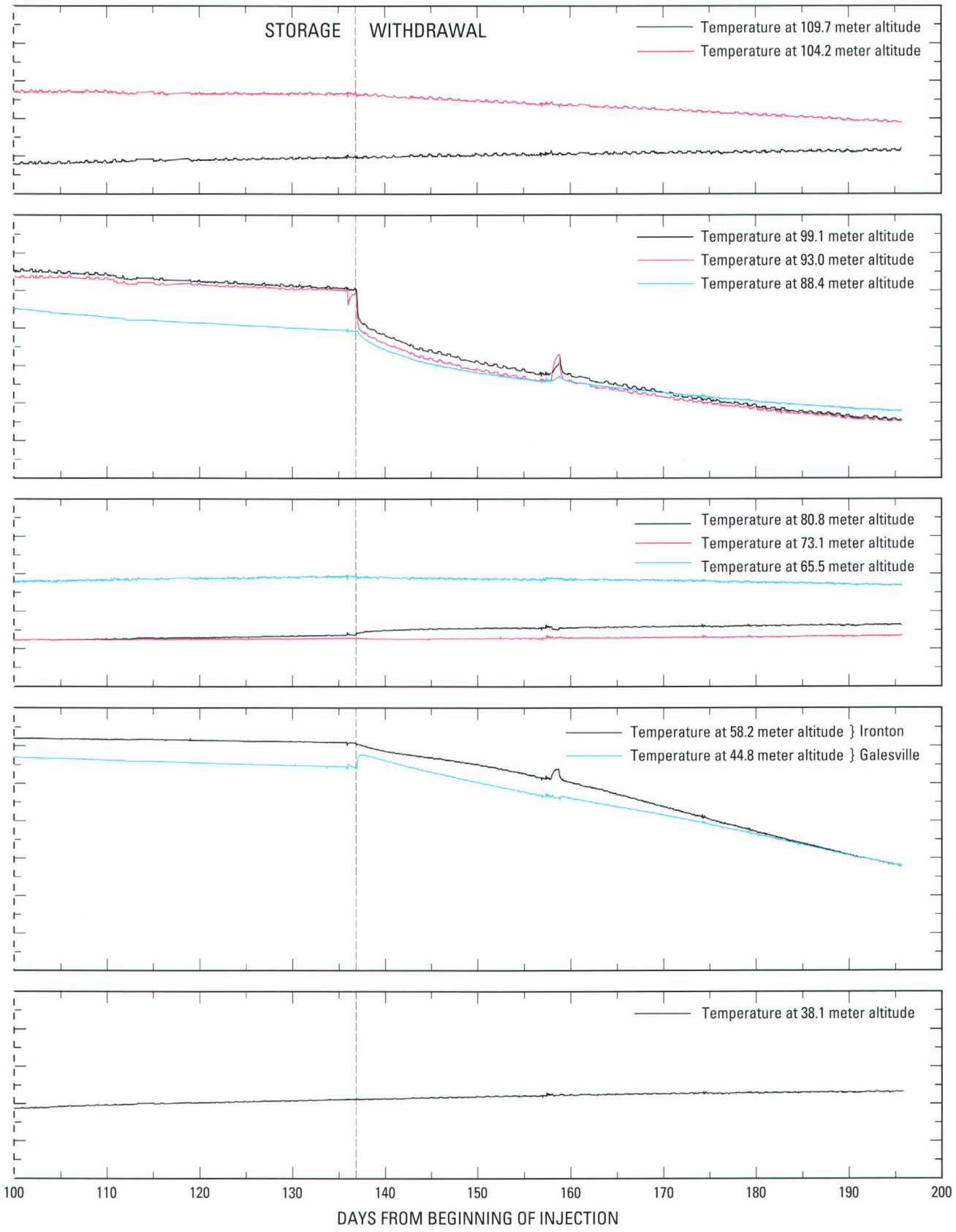

long-term test cycle 1, November 1984 through May 1985.

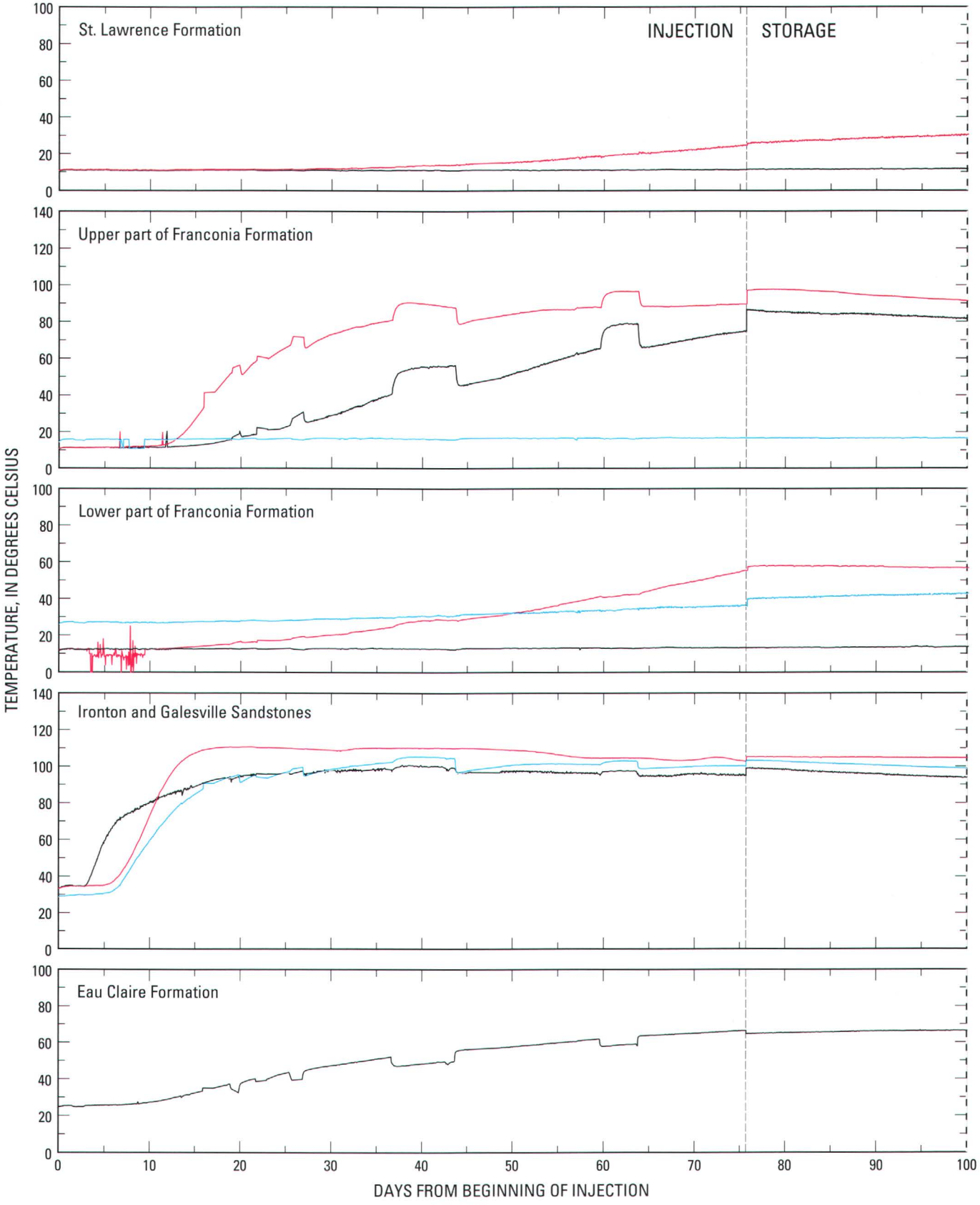

Figure 10. Temperatures in observation well AM3 during

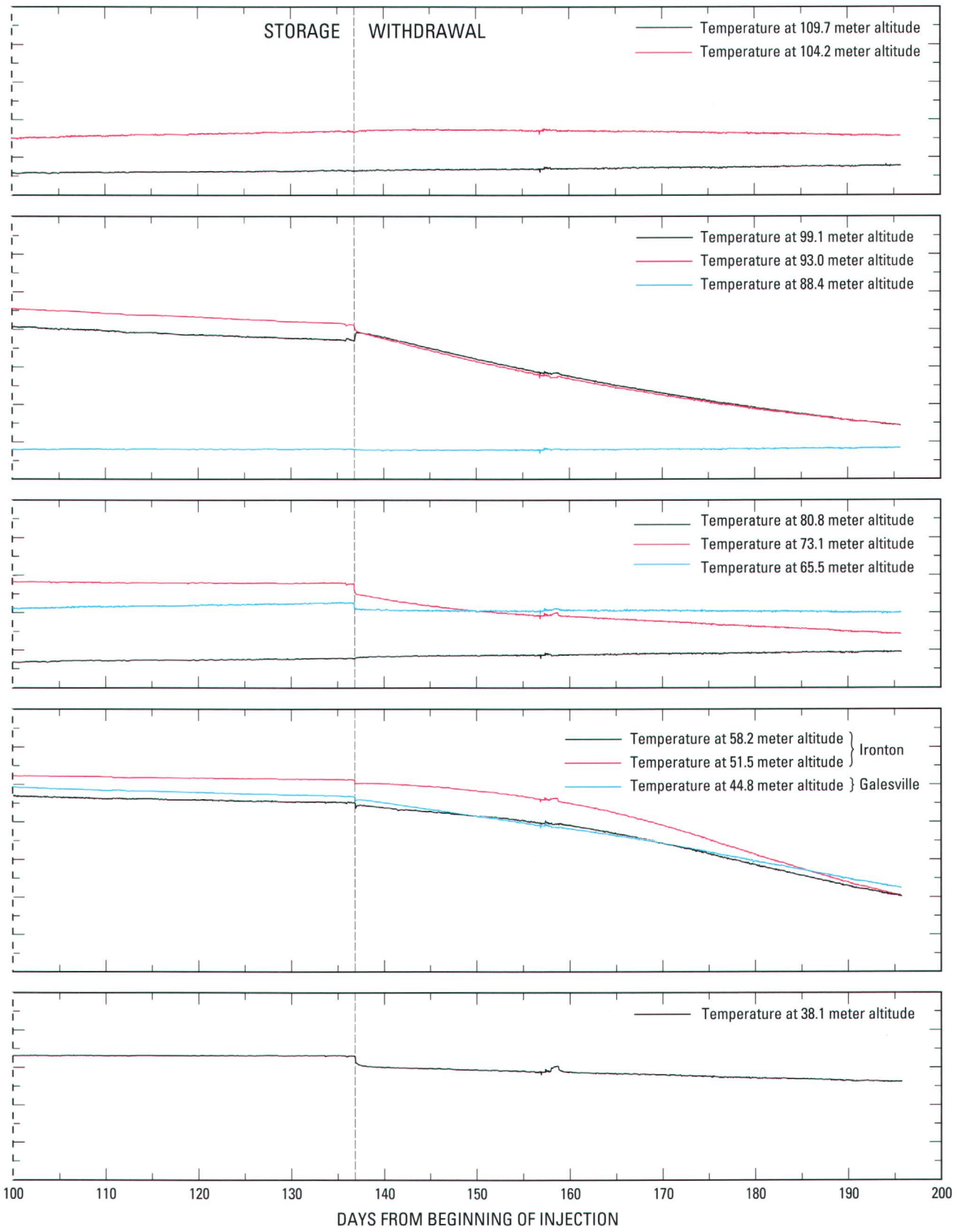

long-term test cycle 1, November 1984 through May 1985.

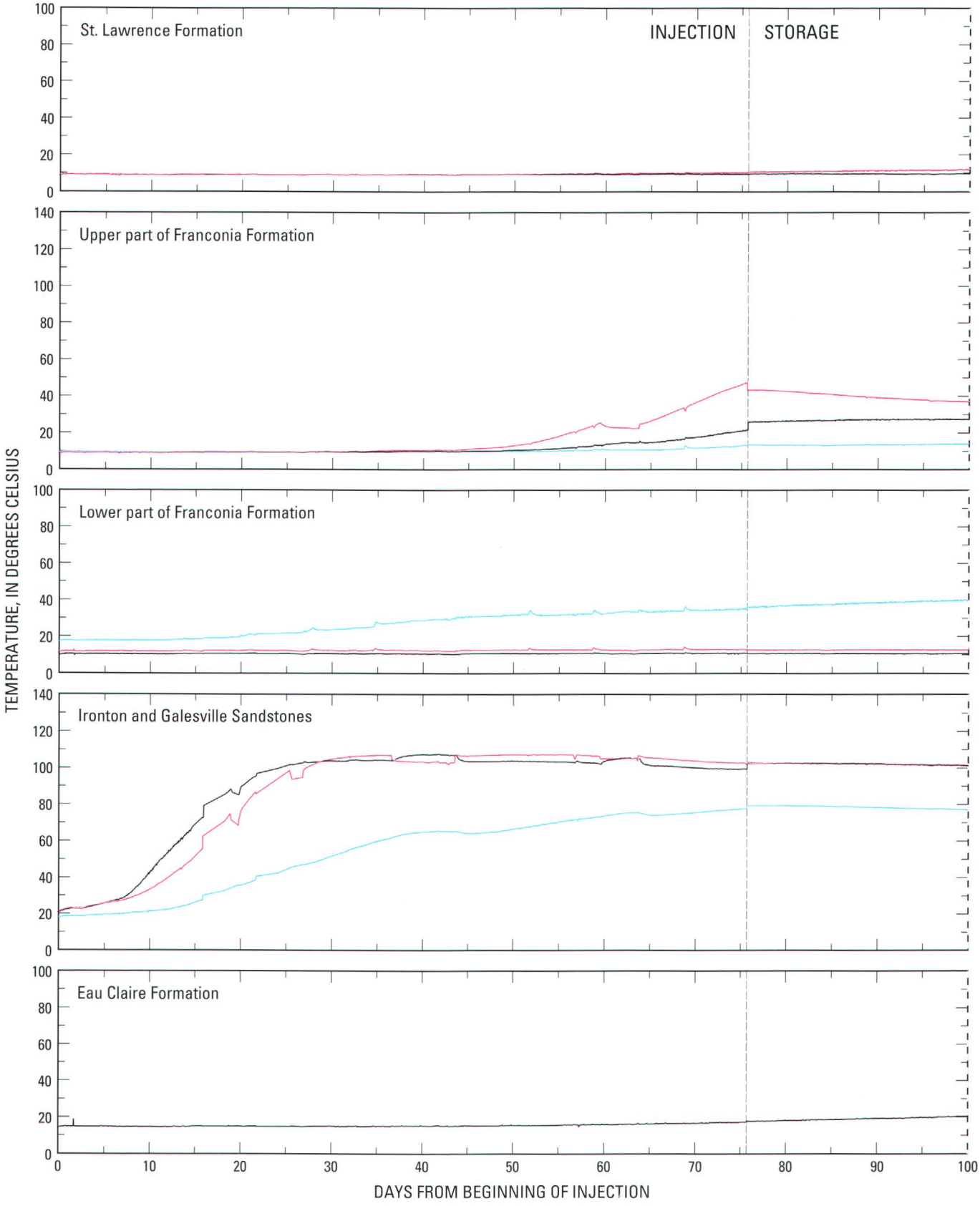

Figure 11. Temperatures in observation well AM4 during

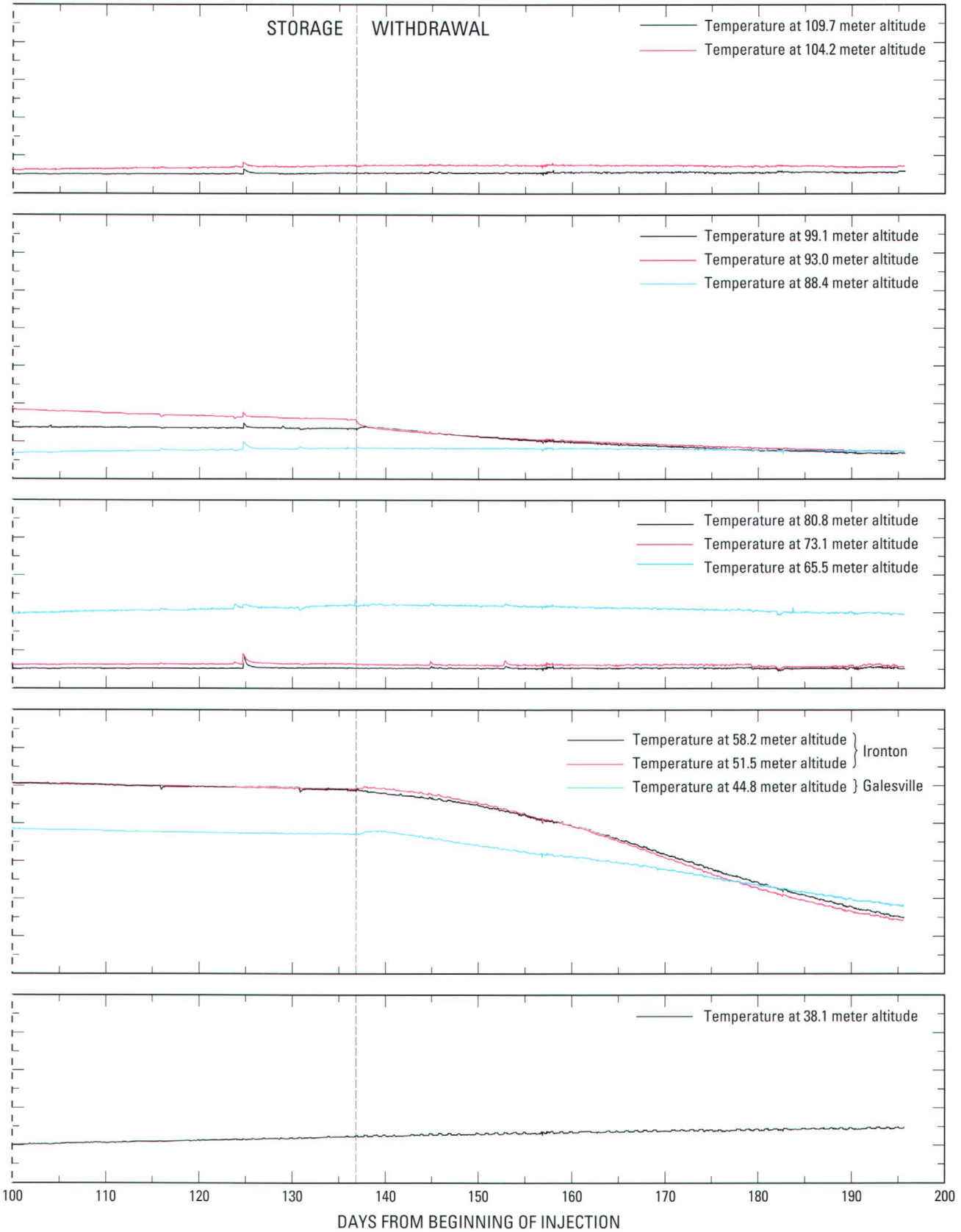

long-term test cycle 1, November 1984 through May 1985.

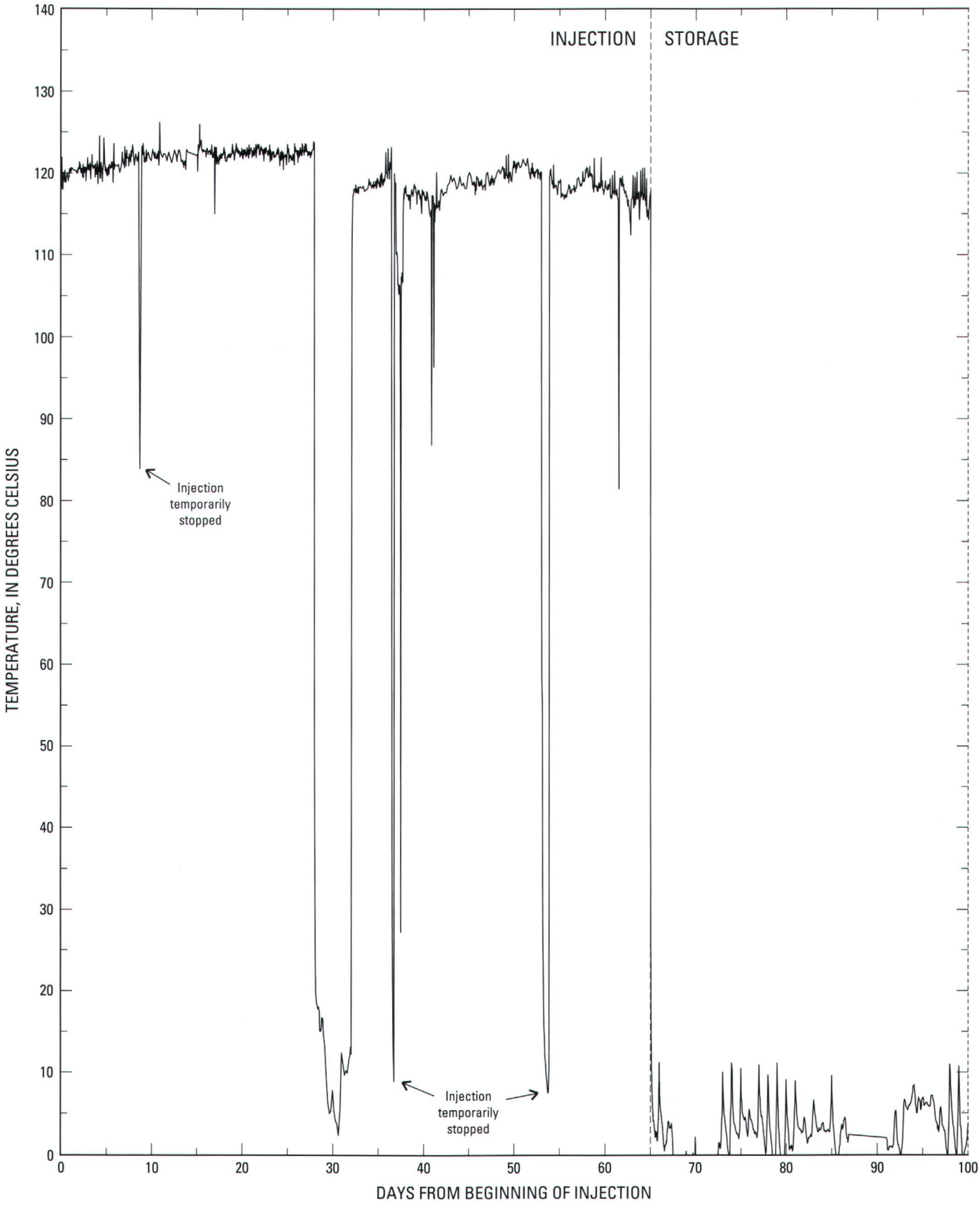

Figure 12. Temperatures in production well A during

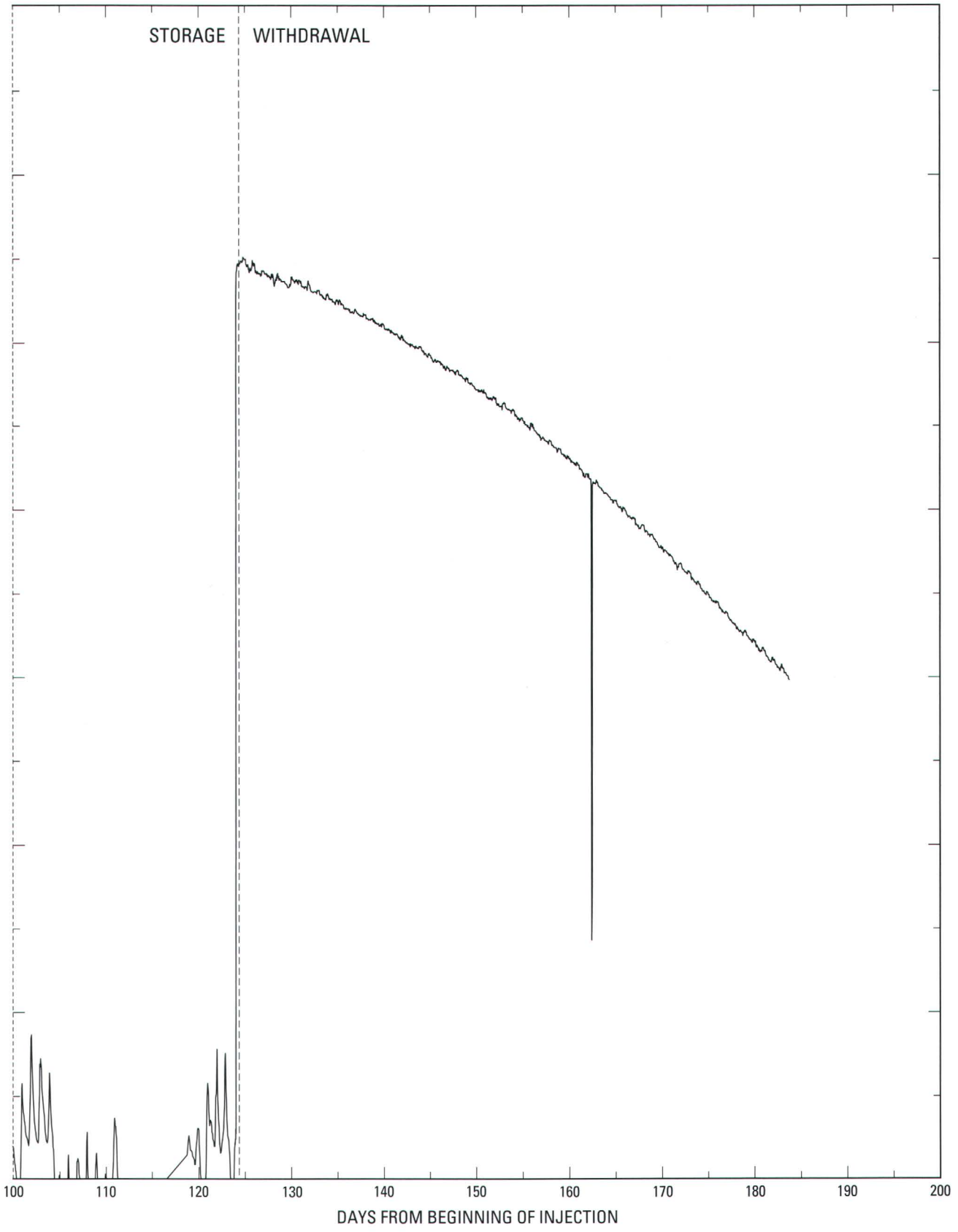

long-term test cycle 2, October 1986 through April 1987.

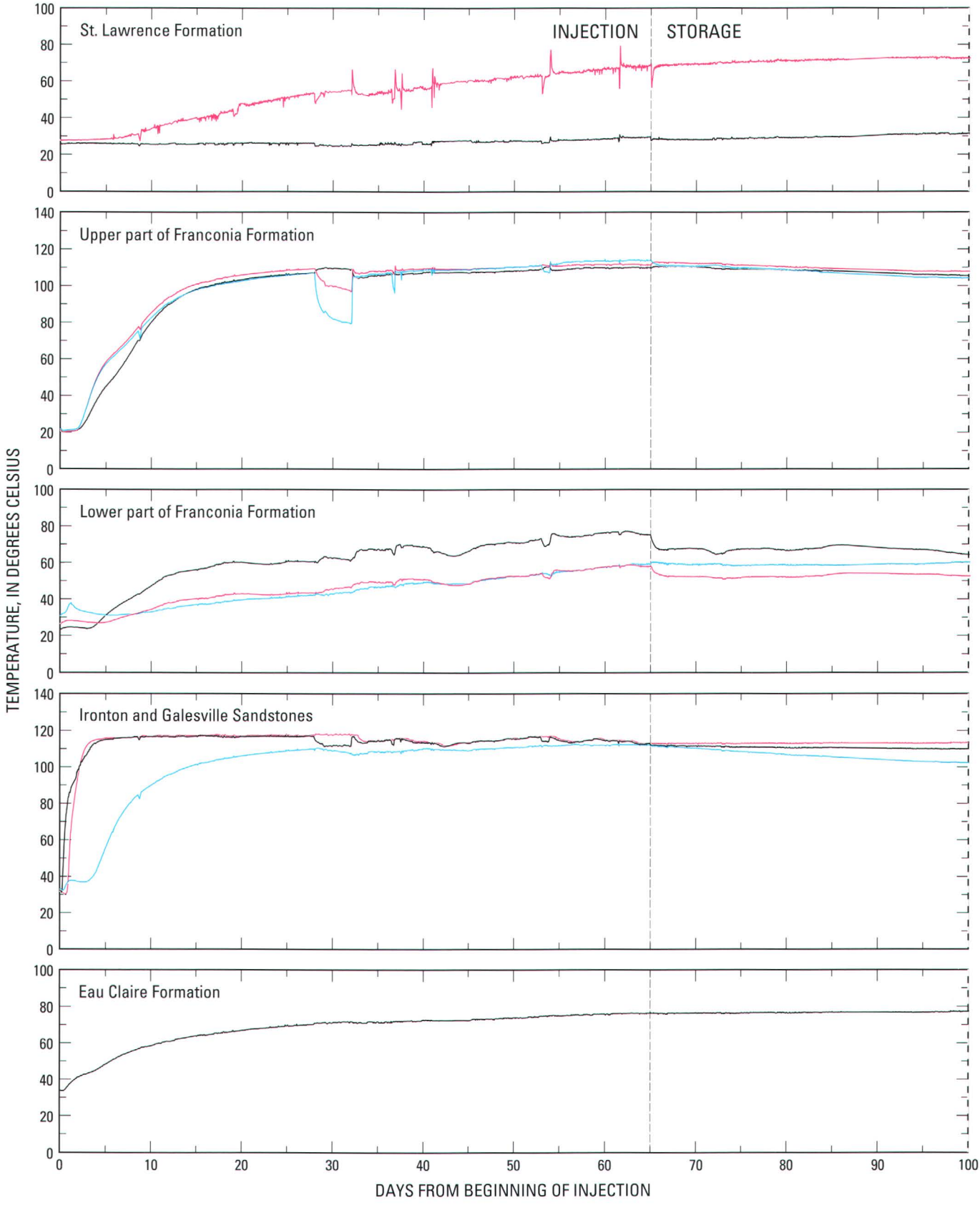

Figure 13. Temperatures in observation well AM1 during

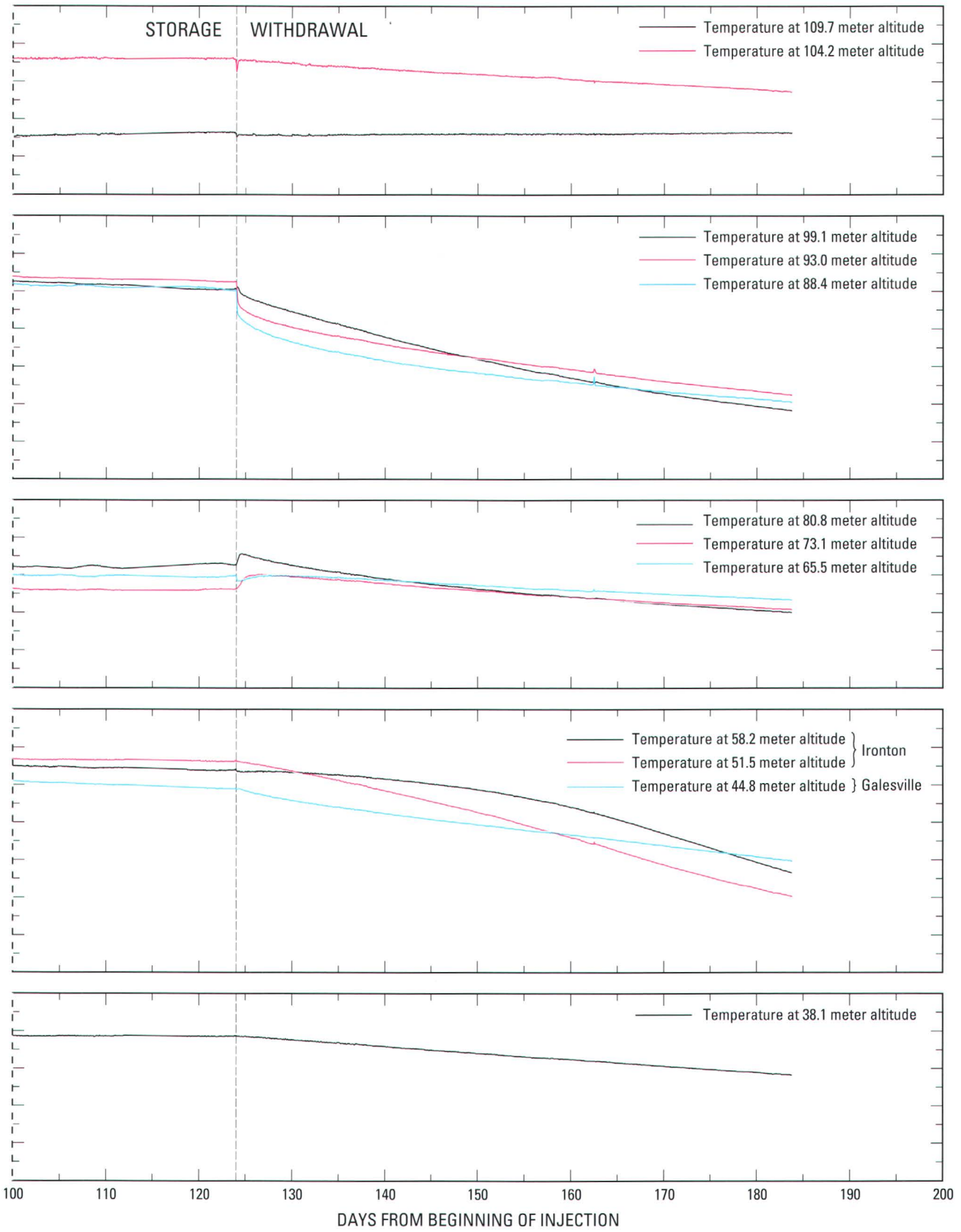

long-term test cycle 2, October 1986 through April 1987.

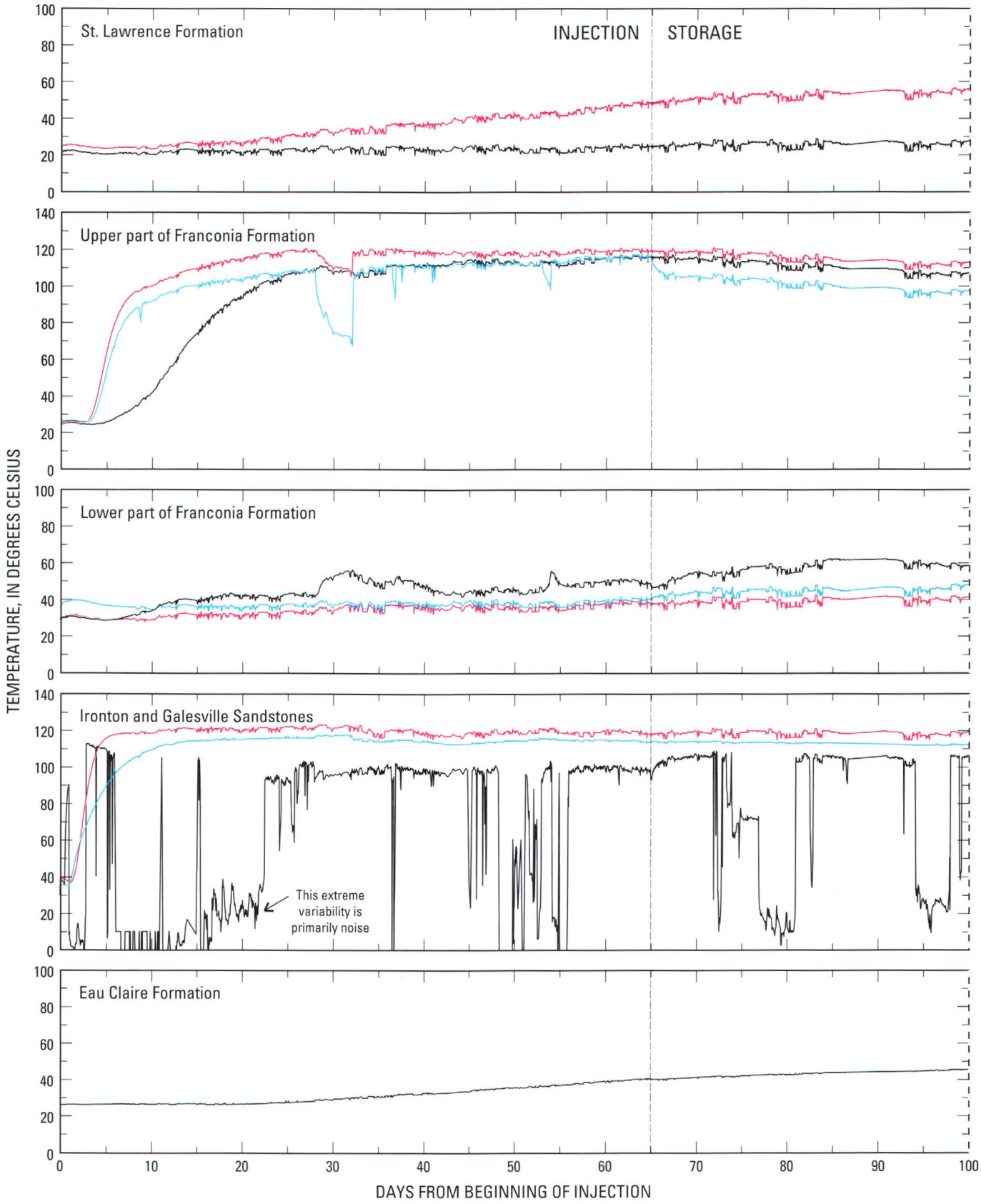

Figure 14. Temperatures in observation well AS1 during

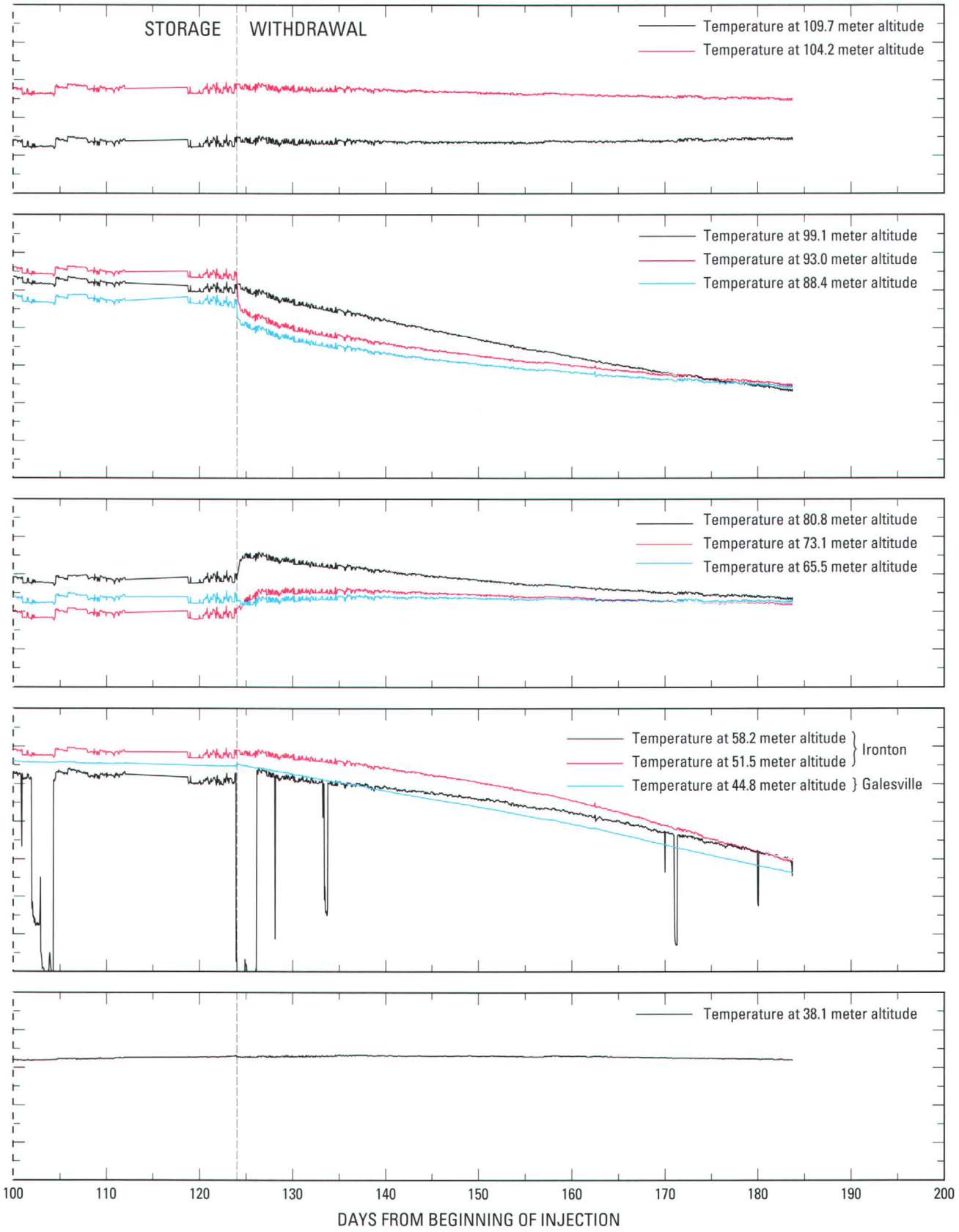

long-term test cycle 2, October 1986 through April 1987.

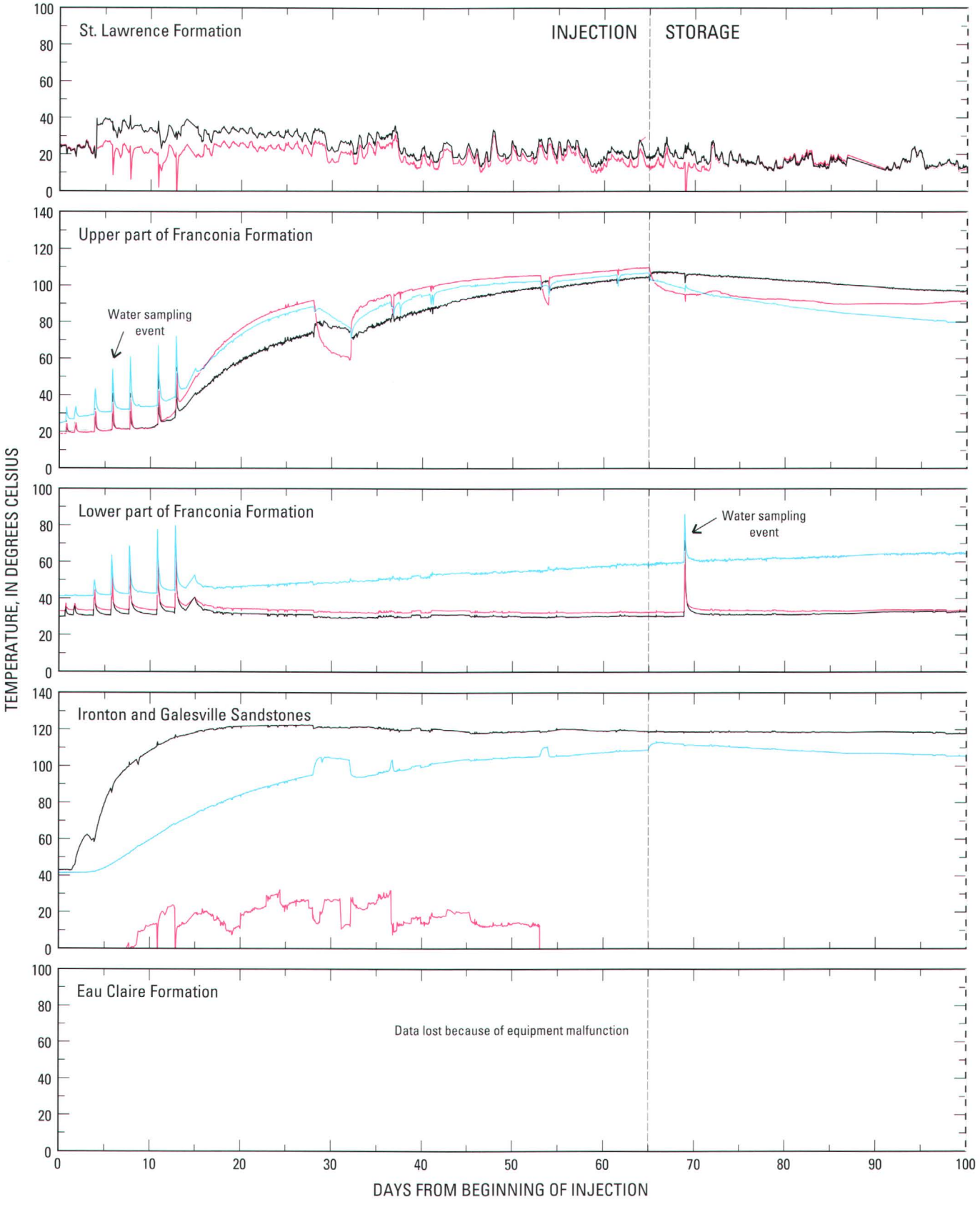

Figure 15. Temperatures in observation well AM2 during

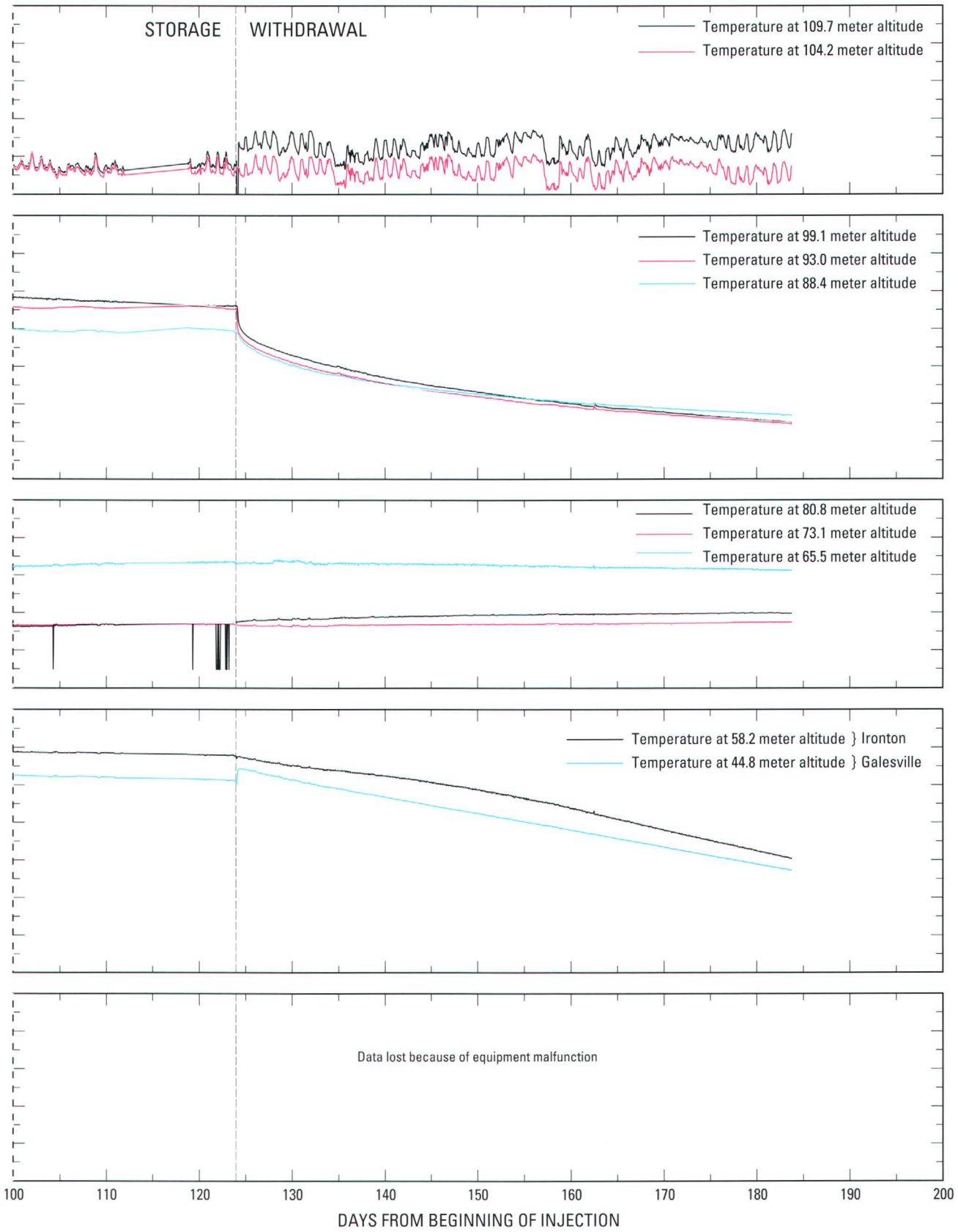

long-term test cycle 2, October 1986 through April 1987.

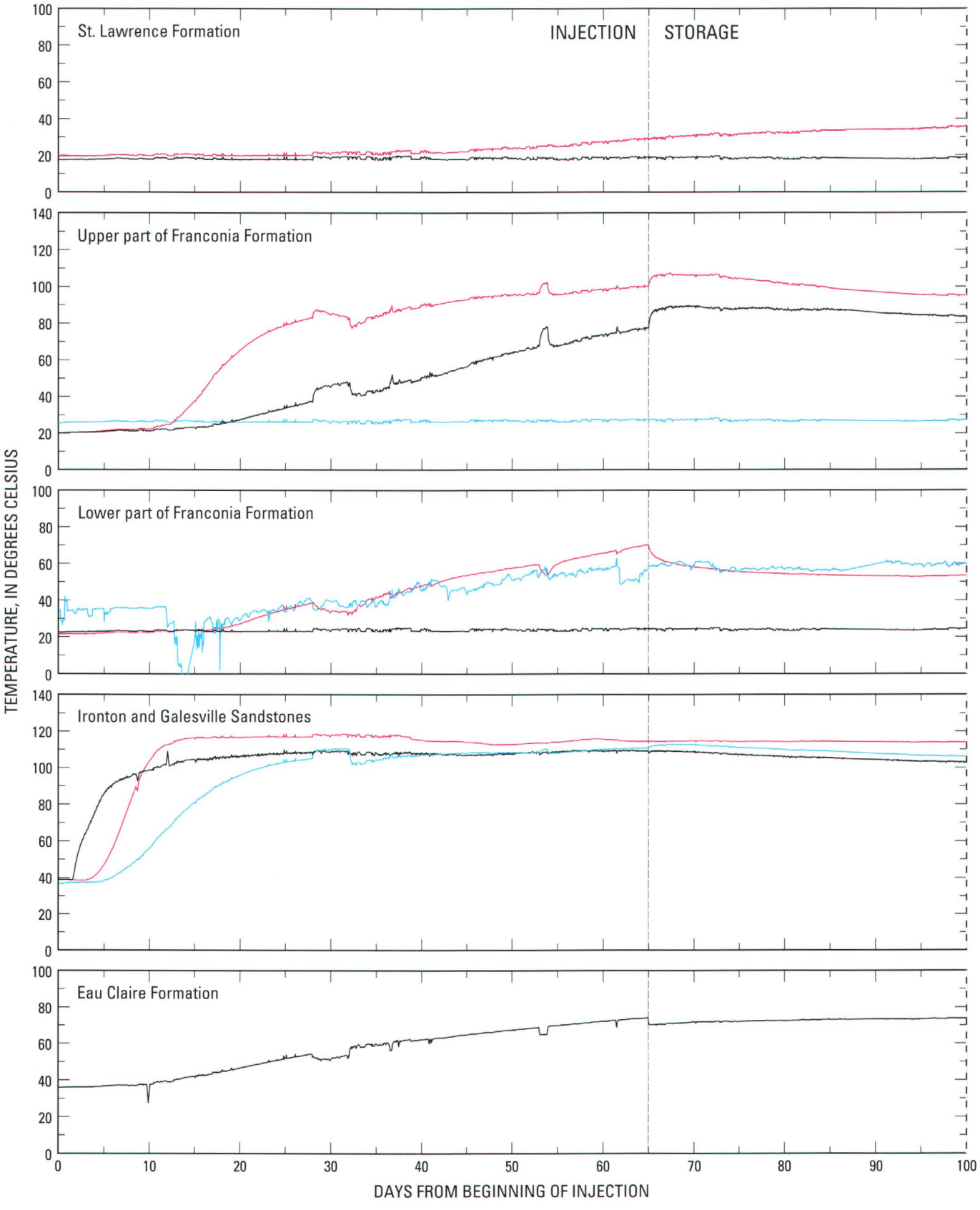

Figure 16. Temperatures in observation well AM3 during

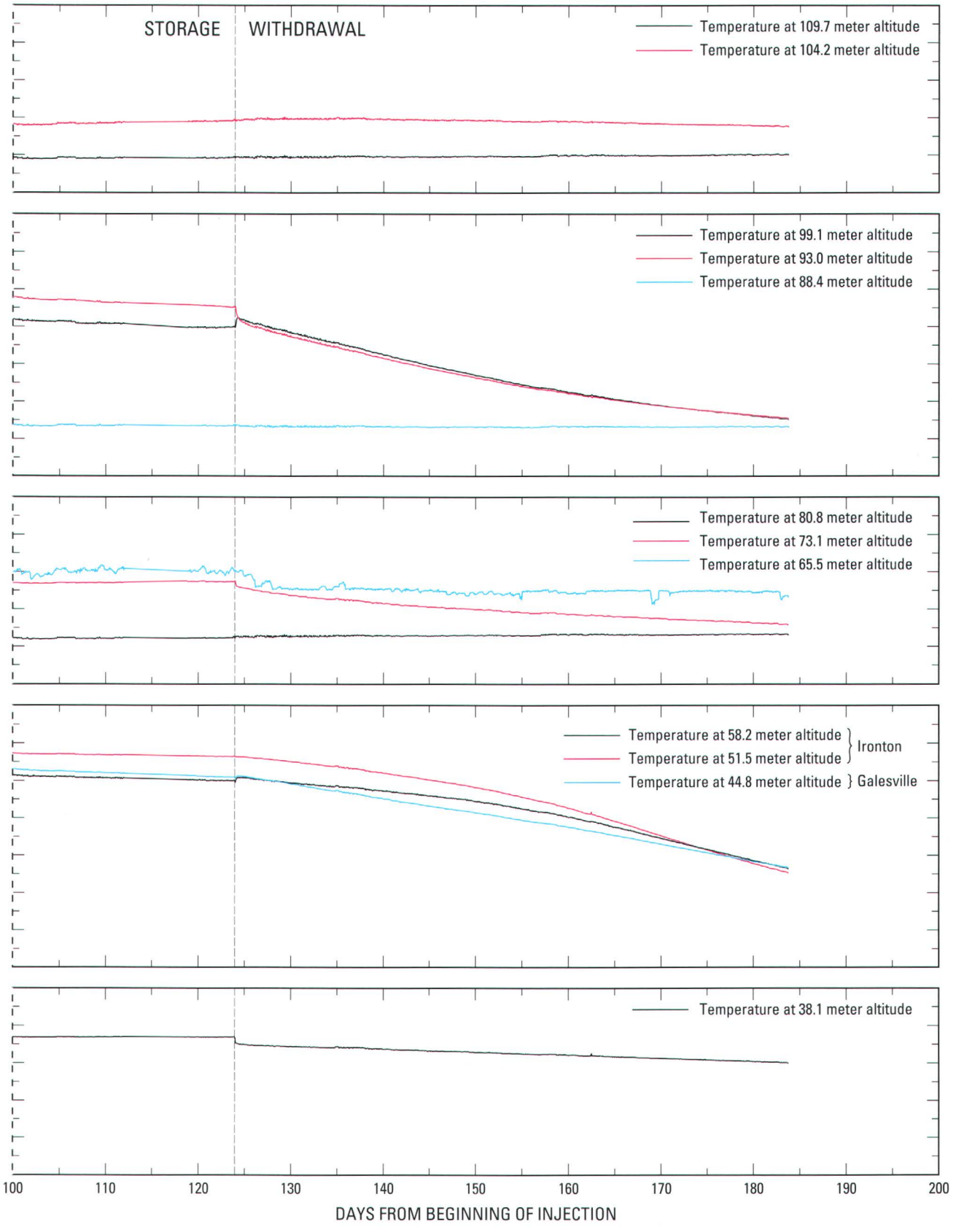

long-term test cycle 2, October 1986 through April 1987.

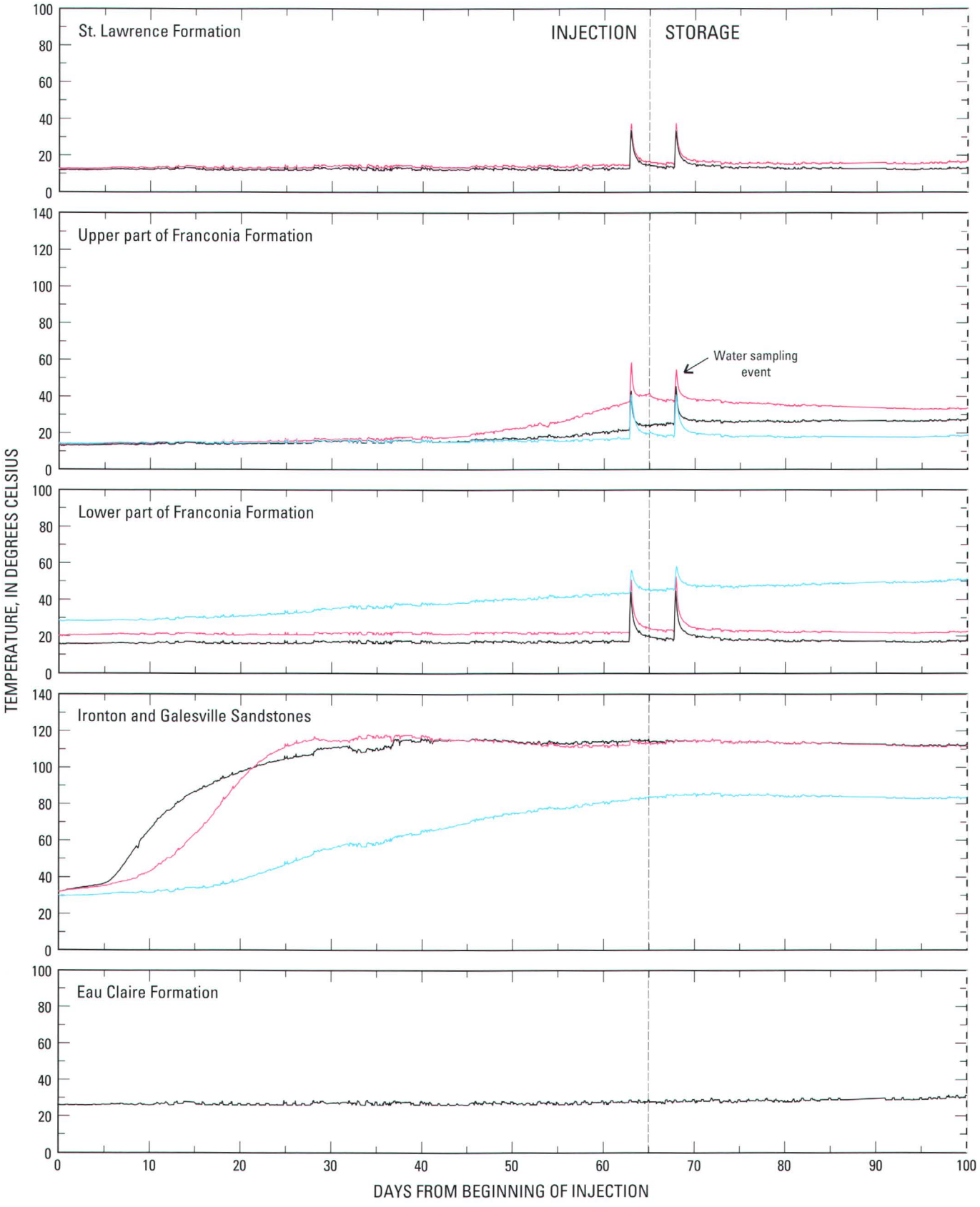

Figure 17. Temperatures in observation well AM4 during

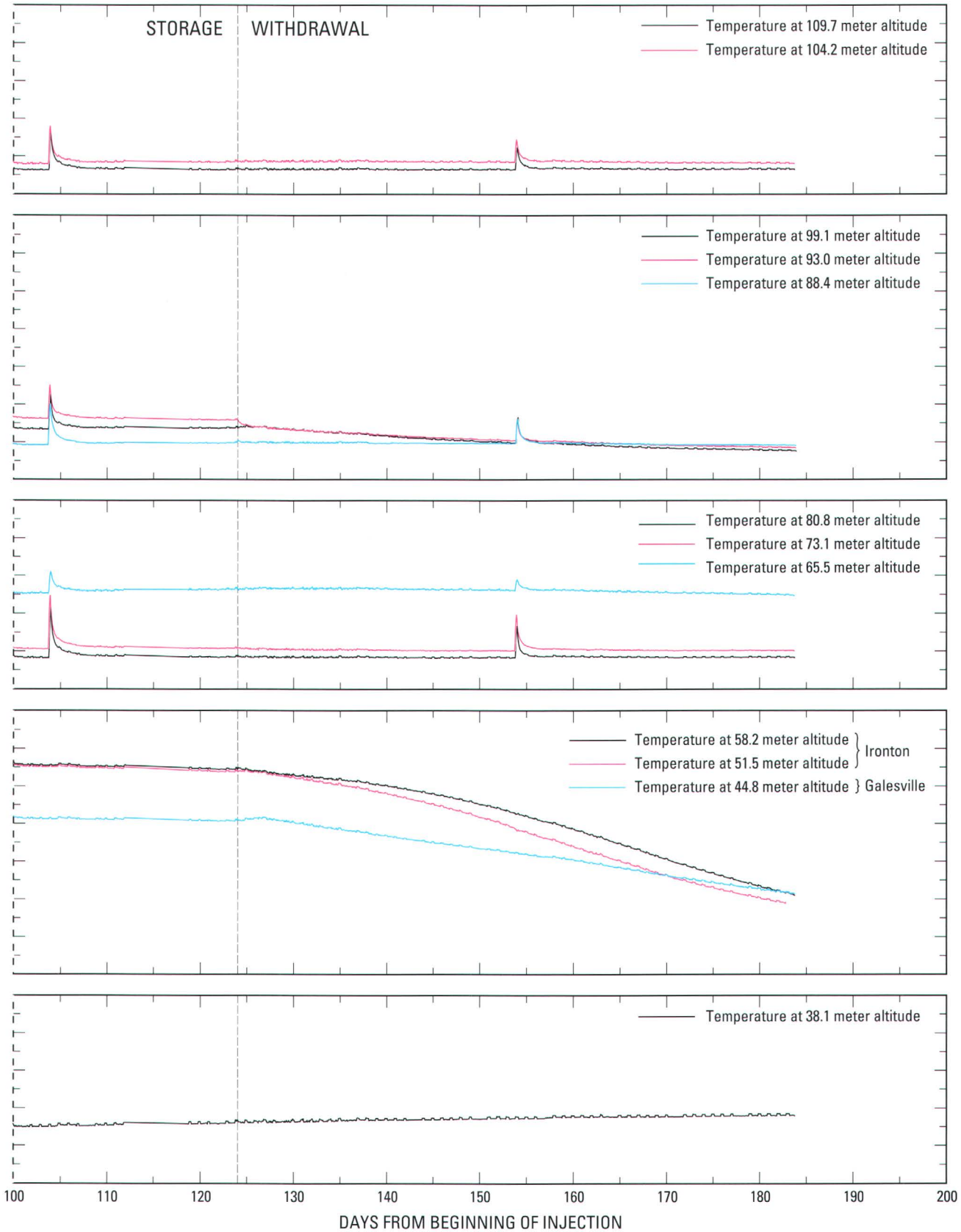

long-term test cycle 2, October 1986 through April 1987.

measured temperatures were fluctuating. The arrival of temperature fronts at the observation wells can be seen in the graphs for the observation wells. Figure 8, for example, shows the arrival of a temperature front in observation well AS1 less than 1 day into the injection phase of long-term test cycle 1 in the Ironton and Galesville Sandstones part of the aquifer. A temperature front arrived in the upper part of the Franconia Formation in observation well AS1 after about 3.5 days (fig. 8).

For the Ironton and Galesville Sandstones, the earliest arrival times for the temperature front in all wells for both cycles typically were at the 58.2-m altitude in the upper part of the Ironton Sandstone (figs. 7–11 and 13–17; table 2). The second measured arrival times typically were at the 51.5-m altitude, although the second arrival time occurred at the 44.8-m altitude for well AS1 (fig. 8). The rate of temperature rise was greatest at the 52.8-m altitude. For observation AM4 during the second cycle (fig. 17), the temperature change initially was very slow; about 4 days into the cycle the rate of temperature change suddenly increased. The initial arrival may have been residual heat from the previous cycle; the increase in rate may

Table 2. Temperature front arrival time at measurement points in the upper part of the Franconia Formation and in the Ironton and Galesville Sandstones for long term test cycles I and 2

[m, meters; --, no data or temperature front not detected; do., ditto]

Well number and distance from injection well	Stratigraphic unit	Altitude of measurement point (meters above sea level)	Time of temperature front arrival (days since start of injection)	
			Cycle 1	Cycle 2
AM1	Upper part of the Franconia Form.	99.1	3.1	1.7
7 m	do.	93.0	3.1	1.7
	do.	88.4	4.7	1.7
	Ironton and Galesville Sandstones	58.2	0.1	0.2
	do.	51.5	0.1	0.8
	do.	44.8	1.6	2.7
AS1	Upper part of the Franconia Form.	99.1	5.0	3.5
7 m	do.	93.0	3.9	3.0
	do.	88.4	3.9	3.0
	Ironton and Galesville Sandstones	58.2	0.6	0.4
	do.	51.5	1.5	1.2
	do.	44.8	1.3	1.0
AM2	Upper part of the Franconia Form.	99.1	9.5	10.0
14 m	do.	93.0	9.5	10.0
	do.	88.4	4.5	2.0
	Ironton and Galesville Sandstones	58.2	3.6	1.5
	do.	51.5	--	--
	do.	44.8	4.8	4.0
AM3	Upper part of the Franconia Form.	99.1	12.0	10.0
14 m	do.	93.0	11.3	8.7
	do.	88.4	--	--
	Ironton and Galesville Sandstones	58.2	3.2	1.5
	do.	51.5	5.0	3.2
	do.	44.8	5.8	4.4
AM4	Upper part of the Franconia Form.	99.1	50.0	45.0
30 m	do.	93.0	40.0	35.0
	do.	88.4	55.0	50.0
	Ironton and Galesville Sandstones	58.2	7.0	4.5
	do.	51.5	8.0	8.5
	do.	44.8	12.0	12.5

have been the actual arrival from the second cycle. Multiple cycles somewhat complicate data interpretation.

For the upper part of the Franconia, temperature front arrival times were considerably slower than in the Ironton and Galesville Sandstones (figs. 7–11 and 13–17; table 2). This delay is not surprising because the permeability of the upper part of the Franconia Formation is about one-half that of the Ironton and Galesville Sandstones. The earliest arrival times for the temperature front at observation well AM1 were at the 93.0-m and the 99.1-m altitudes during the first long-term test cycle (fig. 7), and at all three thermocouples (88.4-m, 93.0-m, 99.1-m) during the second long-term test cycle (fig. 13). The temperature front reached observation well AS1 in the upper part of the Franconia Formation first at the 93.0-m and 88.4-m, and last at the 99.1-m altitudes (figs. 8 and 14). The first arrivals at well AM2 were at the 88.4-m altitude (figs. 9 and 15). The first arrivals at wells AM3 (figs. 10 and 16) and AM4 (figs. 11 and 17) were at the 93.0-m altitude.The initial arrival may have been residual heat from the previous cycle; the increase in rate may have been the actual arrival from the second cycle.

The highest temperatures measured during both cycles in every observation well were at either the 51.5 or 58.2 m altitudes, corresponding to the Ironton Sandstone, which is the most permeable part of the Franconia-Ironton-Galesville aquifer (Walton and others, 1991; Miller and Delin, 1993). The Ironton Sandstone part of the aquifer is approximately four times as permeable as the Galesville Sandstone part of the aquifer, represented by the 44.8-m thermocouple. Highest temperatures measured at the 44.8, 51.5, and 58.2-m thermocouples were measured during the injection phase. At all observation wells, the maximum temperatures in the Ironton and Galesville Sandstones were reached before the end of the injection phase, probably due to the temperature of the injected water being lower toward the end of the injection phase (figs. 6 and 12). After reaching their maximums, temperatures in the Ironton and Galesville Sandstones at observation wells AM1, AS1, AM2, and AM3 decreased similar to the trend of the injected-water temperatures.

The highest temperatures in the upper part of the Franconia Formation at observation wells AM1, AS1, AM2, and AM3 during the second cycle were only a few degrees lower than those measured in the Ironton and Galesville Sandstones. However, the highest temperature was reached at the end of the injection phase. Similar observations were made for the first cycle except at wells AS1 and AM1. For well AM4, a high temperature of between 40 and 50°C was reached at the end of the injection phases of both test cycles.

Temperatures measured at several thermocouples changed immediately at the end of injection periods and at the beginning of withdrawal periods. These temperature changes of generally less than 5°C, some increases and some decreases, may be attributed to the pressure changes caused by interruptions or startups. The changes caused water in the piezometer tubes adjacent to the thermocouples to move past the thermocouples, moving water of a different temperature to the level of the thermocouple.

Some of the temperature-versus-time graphs for observation wells AM2 (fig. 15) and AM4 (fig. 17) show the effect of sampling the wells during the test cycles. These sampling periods are evident as sharp vertical spikes in the graphs, such as those for the upper part of the Franconia Formation at AM2 during the first 13 days of cycle 2 (fig. 15). Water samples were obtained by pumping water from the observation wells at a rate of approximately 0.06 L/s. The effect is shown most frequently during the second long-term test cycle at well AM2 (fig. 15). The pumping caused the sampled water to flow past thermocouples at all overlying temperature measurement points. When the sampled water had a temperature greater (or less) than the temperature detected by the thermocouples, a sudden increase (or decrease) was measured. When sampling was completed, temperatures measured at the affected thermocouples returned to pre-sampling temperatures.

During storage periods, when water was not added to or removed from the storage zone around production well A, temperatures in the observation wells changed slowly. In most wells, temperature changes at the same altitudes were generally in the same direction, either decreasing or increasing, and of similar magnitude during both test cycles.

During storage periods, heat was conducted from the upper part of the Franconia Formation both into the St. Lawrence Formation and into the lower part of the Franconia Formation. Heat was also conducted from the Ironton and Galesville Sandstones both into the lower part of the Franconia Formation and into the Eau Claire Formation. Temperatures for the beginning of withdrawal periods generally were lower than the temperatures at the end of the injection periods at all

temperature measurement points opposite the screened intervals of production well A. The greatest drop in temperature was measured at the lowest thermocouple in the upper part of the Franconia Formation (88.4-m altitude) and the thermocouple in the Galesville Sandstone (44.8-m altitude). Thermally-induced convection during storage periods may have caused some of the measured temperature changes.

In addition to the heat conduction described above, heat was also transported down the well bore of production well A from the upper part of the Franconia Formation to the Ironton and Galesville Sandstones during storage periods. This heat transport occurred because production well A was open to both formations and because hydraulic heads decreased with depth, allowing ground water to flow down and out of the well bore during storage periods. Thus, heat was transported from the Franconia Formation to the Ironton and Galesville Sandstones because of the convective flow of heated water through the well bore of production well A.

Temperatures measured during withdrawal periods support the concept that transport of heat within the aquifer was a function of permeability; the maximum decrease [cooling] of aquifer temperature occurred in the Ironton and Galesville Sandstones. At the start of withdrawal periods, temperatures in the Ironton and Galesville Sandstones and in the upper part of the Franconia Formation were somewhat lower than at the beginning of storage periods. Temperatures measured in the lower part of the Franconia Formation and in the St. Lawrence Formation and Eau Claire Formation were somewhat higher than at the beginning of storage periods. During withdrawal periods, temperatures initially decreased rapidly in the upper part of the Franconia Formation, then decreased more slowly. During withdrawal periods, temperatures in the Ironton and Galesville Sandstones decreased slowly. Temperatures of the withdrawal water more closely resembled the temperatures in the Ironton and Galesville Sandstones than in the upper part of the Franconia Formation. Thus, the Ironton and Galesville Sandstones contributed a majority of the water and heat during withdrawal periods. The withdrawal plots (figs. 7–17) illustrate that, as expected, the injected heat was not fully recovered by the end of the withdrawal periods.

Water temperatures reached a maximum at production well A about 12 to 24 hours after withdrawal began (figs. 6 and 12), likely because the well was completed in two different units. Intra-aquifer [interformational] flow during storage periods, described earlier, resulted in a slight cooling of water in the well bore as it flowed from the upper part of the Franconia Formation into the Ironton and Galesville Sandstones. At the beginning of withdrawal periods, the water withdrawn from the Ironton and Galesville Sandstones was cooled further as it traveled up the well bore past the unscreened lower part of the Franconia Formation. The water also lost heat through conduction to the well bore and casing at the beginning of withdrawal periods that also caused an initial warming of the lower part of the Franconia Formation in the vicinity of the well bore. Consequently, thermal equilibrium at the wellhead, and thus the highest temperatures, were not reached until 12 to 24 hours into each withdrawal period (figs. 6 and 12).

Temperature Profiles

Temperature profiles as a function of depth at individual observations wells are useful in: (1) determining whether density-driven buoyancy flow of heated water occurs (Miller and Delin, 1994), (2) examining temperature variations in relation to hydraulic and thermal properties of the aquifer, and (3) determining possible long-term trends of vertical heat loss from the aquifer. Temperature profiles are presented for the beginning and the end of each injection period, and for the end of each storage and recovery period for each cycle at each observation well (figs. 18 through 22). The temperature-measurement altitudes for each of the observation wells are shown in figure 4.

The temperature profiles were constructed by connecting the successive temperature-measurement values with straight lines. Where thermocouples failed, successive operating temperature-measurement values were connected with straight lines. This linear interpolation may not accurately represent temperatures between the temperature-measurement points, especially where temperatures are interpolated across a major hydraulic or thermal boundary such as near confining layers or the unscreened lower part of the Franconia Formation. Contrasts in temperatures across major hydraulic boundaries were large (about 20 to 40°C) following injection. The contrast in the advective heat-transport rate in the most permeable part of the aquifer and the conductive heat-transport rate in the least permeable parts of the aquifer and in the confining layers was noticeable at all wells. The contrast in temperatures across major hydraulic boundaries is best

illustrated by the thermal separation, both in time and space, measured at well AM4, the most distant well from production well A (figs. 11, 17, and 22). Although detail is lacking for temperature variation at the hydraulic and thermal boundaries, the linear-interpolation method did not seriously hinder use of the temperature profiles in describing the energy-transfer processes within the aquifer and confining units.

The shape of the temperature profiles in figures 18 through 22 generally reflects the permeability distribution described by Miller and Delin (1993) for the Franconia-Ironton-Galesville aquifer. Highest temperatures were measured in the Ironton and Galesville Sandstones and in the upper part of the Franconia Formation, the most permeable parts of the aquifer. Lowest temperatures were measured in the lower part of the Franconia Formation, the least permeable part of the aquifer. Maximum temperatures in the Ironton and Galesville Sandstones and in the upper part of the Franconia Formation at radial distances of 7 m and 14 m from production well A, as expected, were similar to the injected water temperatures of 108.5°C (cycle 1) and 117.7°C (cycle 2) (figs. 18 through 22). The lowest temperatures were measured in the lower part of the Franconia Formation, the St. Lawrence Formation, and in the Eau Claire Formation, which are confining units. By the end of the withdrawal periods, temperatures in all formations were within about 15°C of each other.

The convection of ground water created by differences in density between the ambient-temperature aquifer water and the warmer injected water is termed buoyancy flow (Hellstrom and others, 1979). Buoyancy flow causes thermal stratification and tilting of the thermal front (Miller and Delin, 1994). If buoyancy flow occurred it would be most readily observed near the top of an aquifer at the end of storage periods.

The effects of buoyancy flow were not readily noticeable in the temperature profiles at the test facility (figs. 18 through 22). The effects of buoyancy flow were most noticeable in the Ironton and Galesville Sandstones in observation well AM4 at the end of injection and storage periods for cycle 2 (fig. 22). The measured buoyancy flow was small in comparison to the buoyancy flow as described by the sensitivity analysis for the Franconia-Ironton-Galesville aquifer (Miller and Delin, 1993). Although the magnitude of buoyancy flow was small, it was likely realistic for an operational thermal-energy storage system and, perhaps, accurately represents the potential long-term effects of buoyancy flow for the Franconia-Ironton-Galesville aquifer at the end of injection and storage periods (fig. 22). The general lack of noticeable buoyancy flow in the test results probably was due to (1) an insufficient density of temperature-measurement locations, and (2) vertical changes in hydraulic properties caused by the presence of generally continuous, thin, horizontally bedded silt, shale, and clay stringers within the Franconia-Ironton-Galesville aquifer (Walton and others, 1991; Miller and Delin, 1994). These stringers could have reduced the effects of buoyancy flow by acting as barriers to convective flow induced by density differences in the water.

Earlier model-sensitivity analyses (Miller and Delin, 1993) indicated that the decreases in temperature within the upper part of the Franconia Formation near production well A could be due to interformation flow within the well bore of production well A. Similar decreases were observed during the storage periods of cycles 1 and 2 (figs. 18 through 22). Temperatures in the Ironton and Galesville Sandstones and the upper part of the Franconia Formation decreased at most observation points in all observation wells. The decrease in temperature in the upper part of the Franconia Formation at the observation wells likely resulted from both conduction of heat to the St. Lawrence Formation and the lower part of the Franconia Formation and from interformation flow through production well A. The decrease in temperature in the Ironton and Galesville Sandstones likely resulted from conduction of heat to the Eau Claire Formation and to the lower part of the Franconia Formation.

The above-described interformation flow, which was confirmed by use of a flow meter, resulted from a natural downward vertical gradient between the upper part of the Franconia Formation and the Ironton and Galesville Sandstones during periods of storage. This interformation flow caused advective flow of water in the upper part of the Franconia Formation past the observation wells toward production well A. Water from the upper part of the Franconia Formation was cooled as it traveled down production well A past the cooler, unscreened lower part of the Franconia Formation. This cooled water mixed with warmer water in the Ironton and Galesville Sandstones and maintained a positive advective flow outward into the sandstones. This flow of water into the Ironton and Galesville Sandstones tended to increase, or maintain,

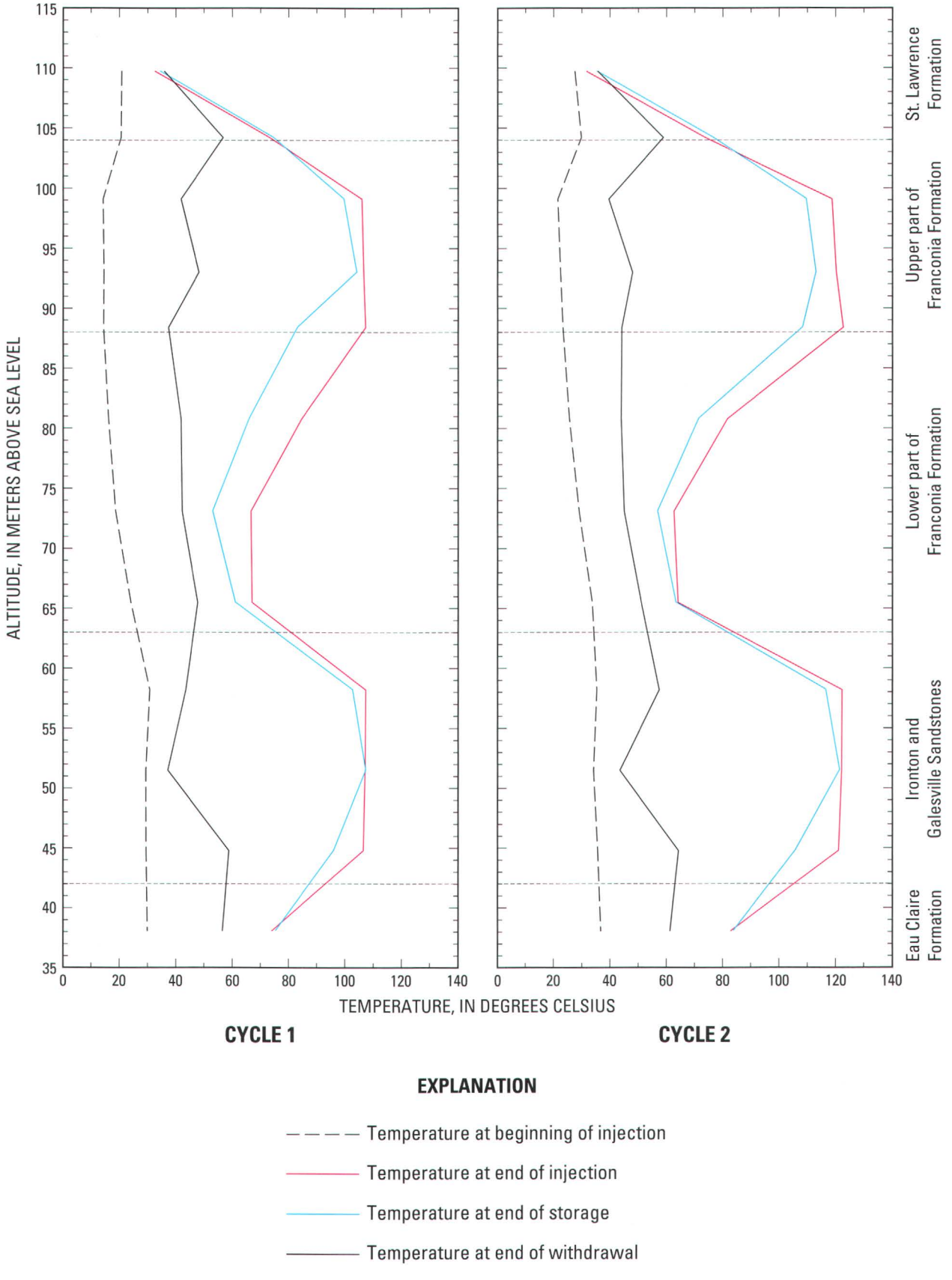

Figure 18. Temperatures measured in observation well AM1 at the beginning of injection and at the end of injection, storage, and withdrawal for long-term test cycles 1 and 2.

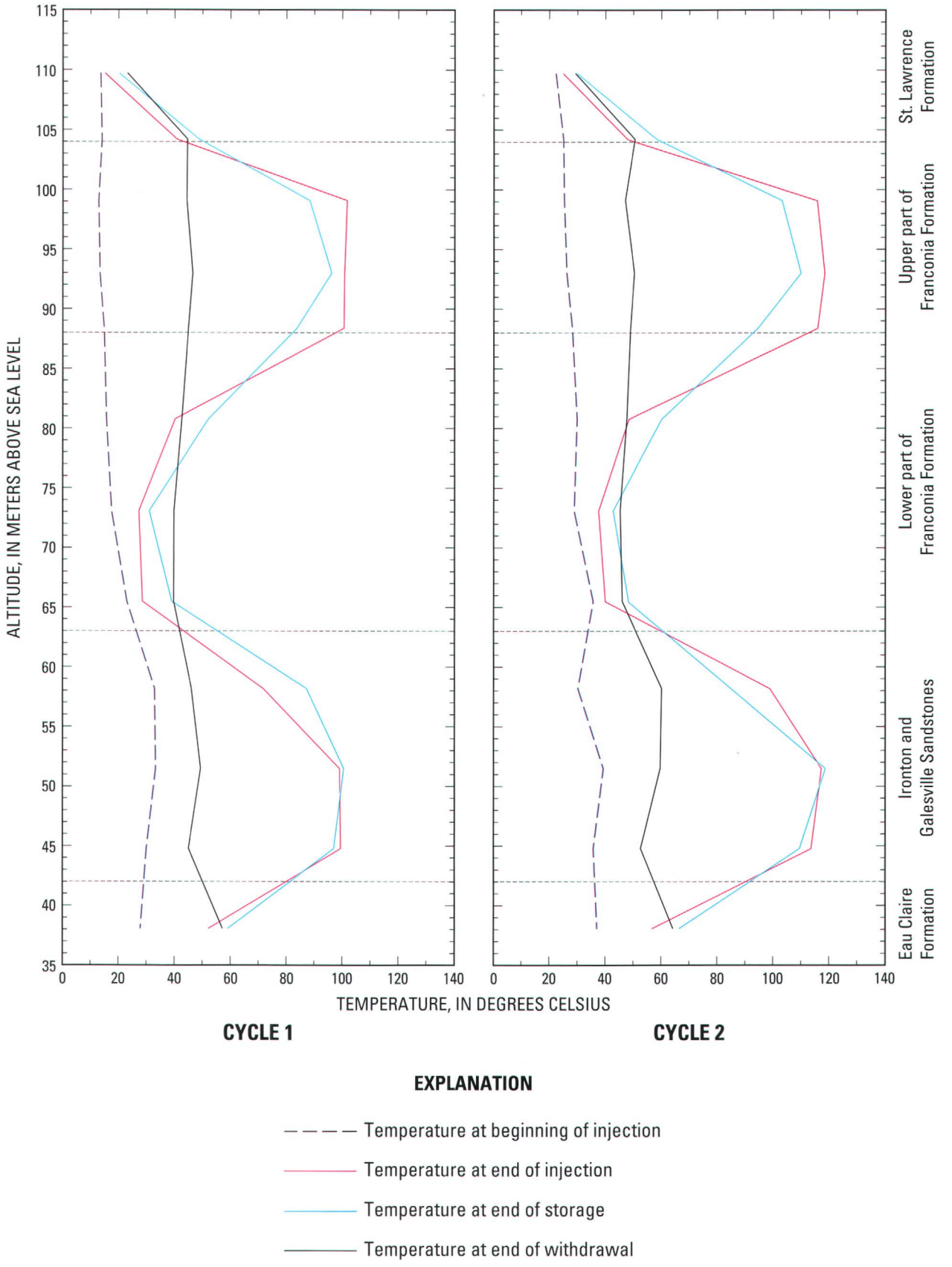

Figure 19. Temperatures measured in observation well AS1 at the beginning of injection and at the end of injection, storage, and withdrawal for long-term test cycles 1 and 2.

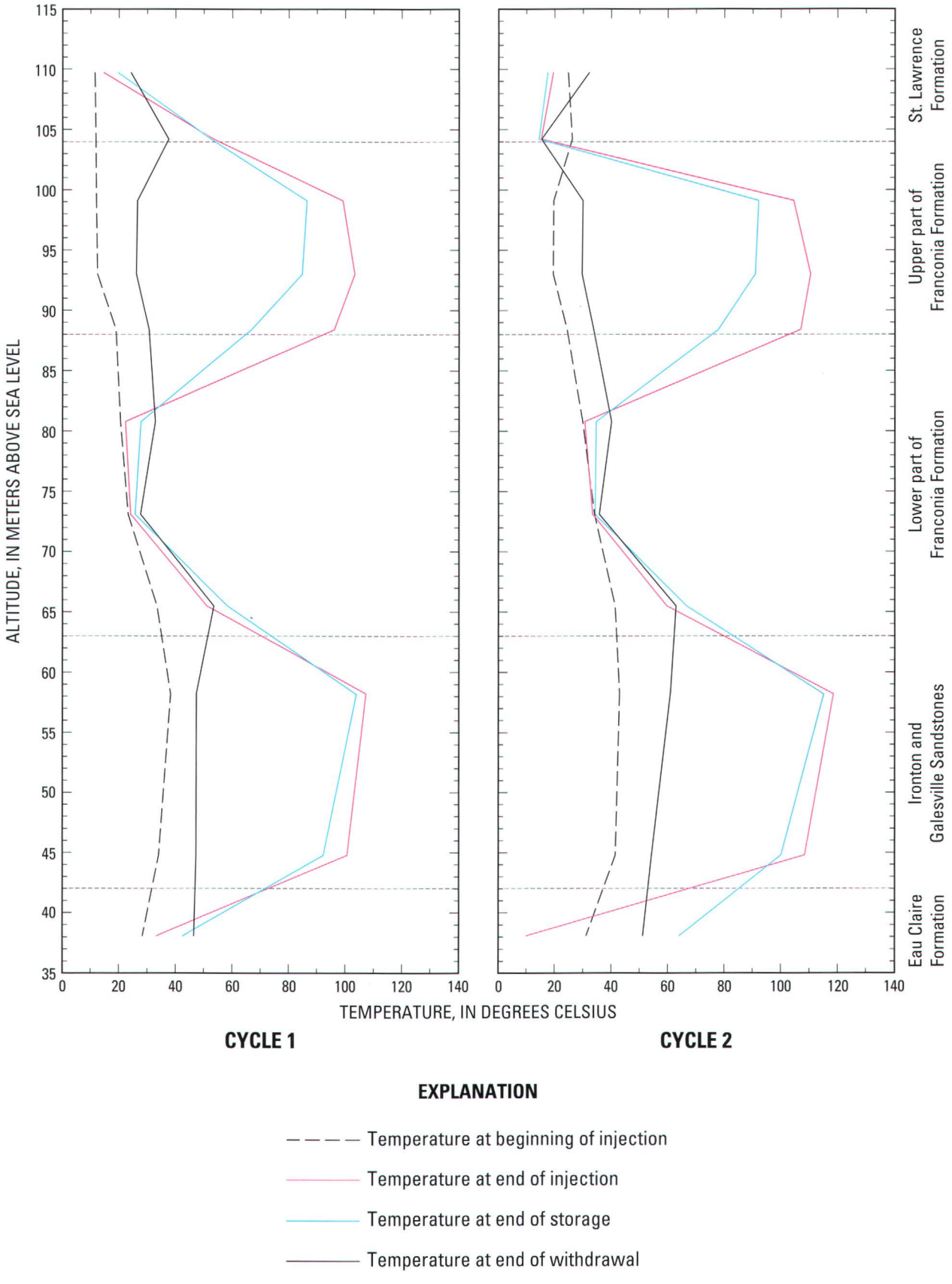

Figure 20. Temperatures measured in observation well AM2 at the beginning of injection and at the end of injection, storage, and withdrawal for long-term test cycles 1 and 2.

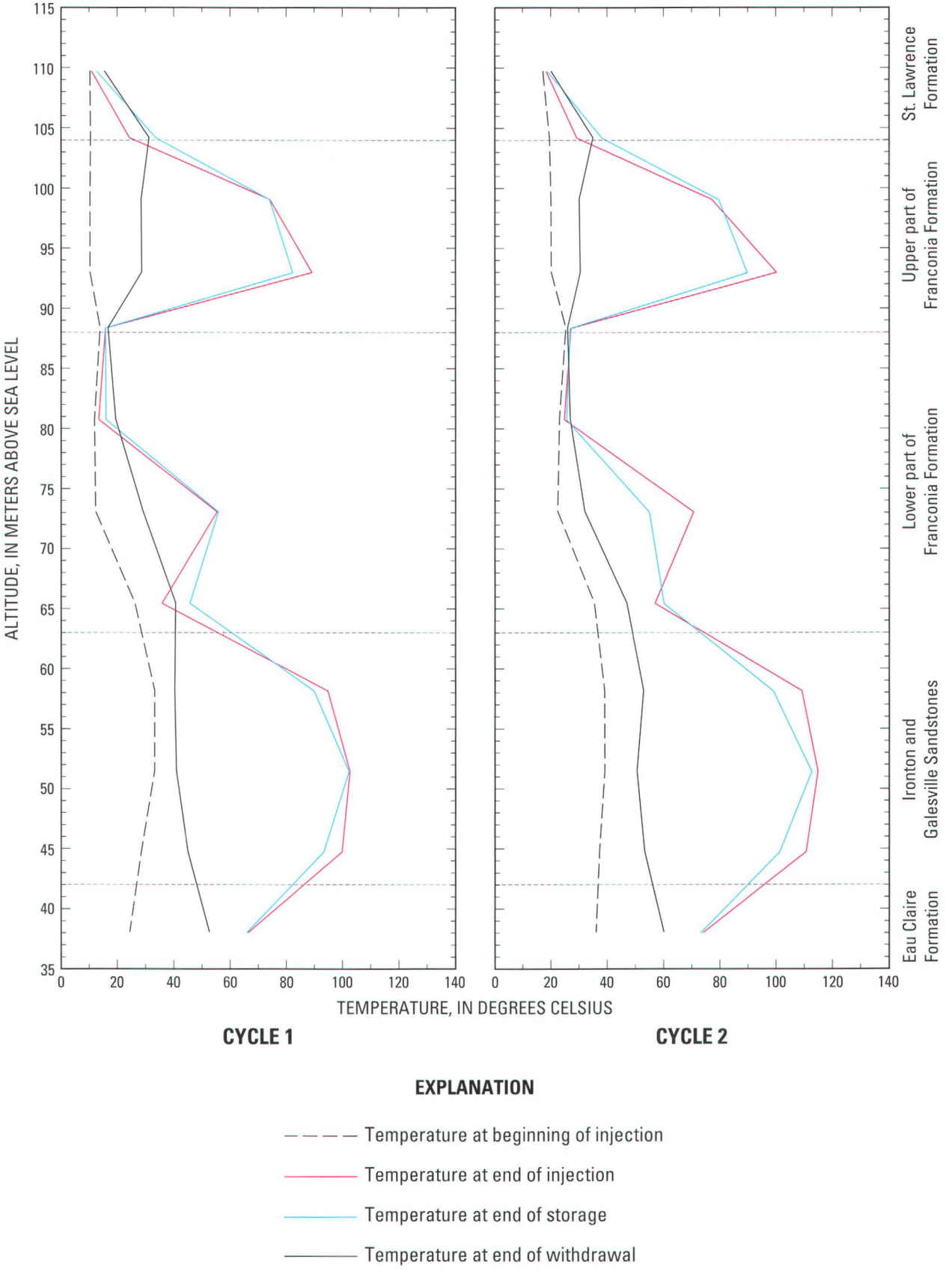

Figure 21. Temperatures measured in observation well AM3 at the beginning of injection and at the end of injection, storage, and withdrawal for long-term test cycles 1 and 2.

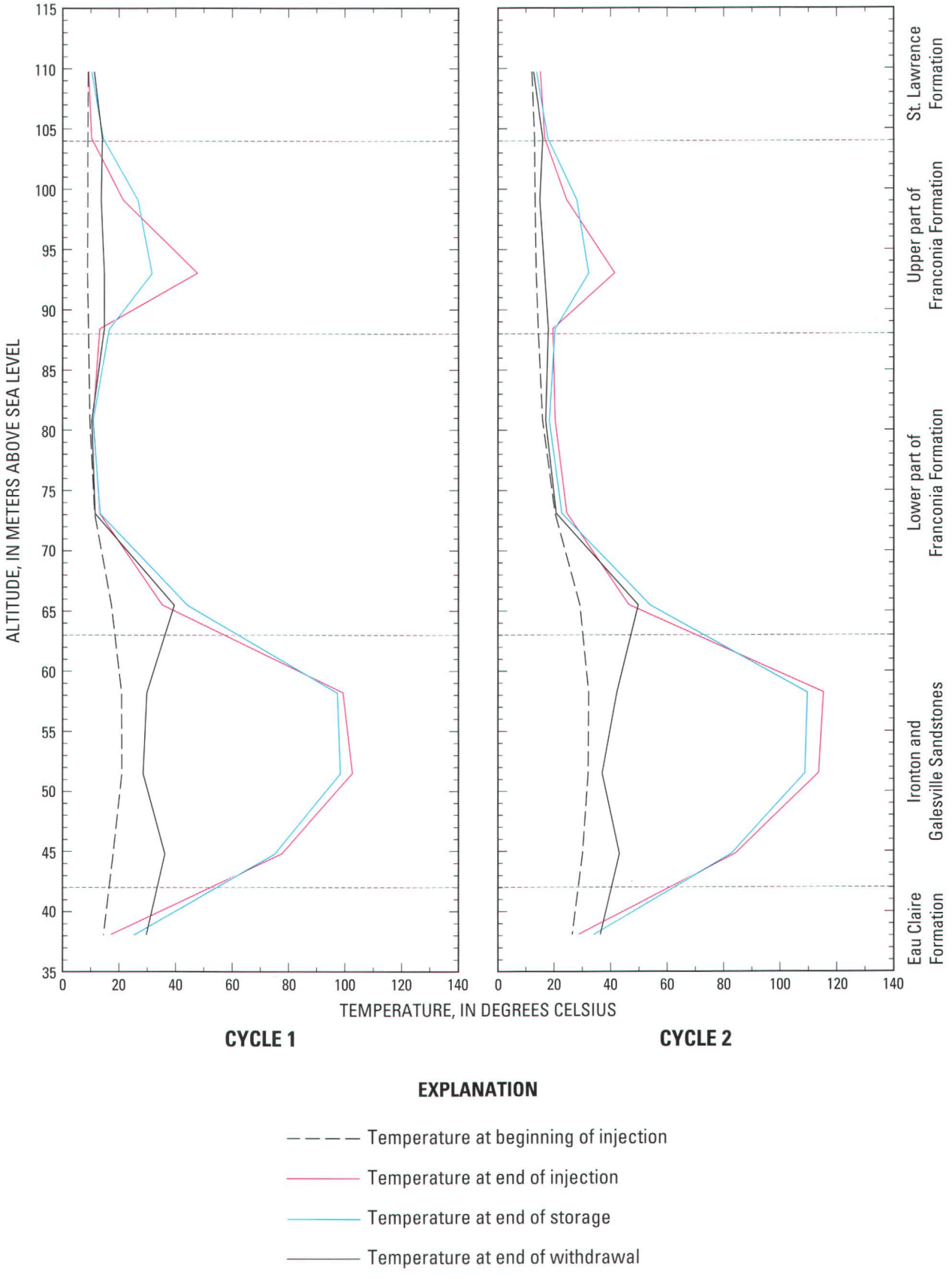

Figure 22. Temperatures measured in observation well AM4 at the beginning of injection and at the end of injection, storage, and withdrawal for long-term test cycles 1 and 2.

the temperatures measured at the observation wells completed in these formations.

Discussion of Thermal Data

Temperatures should have been similar at the same depths and radial distances from production well A if the hydraulic and thermal properties were similar in all directions. Although observation wells AM2 and AM3 were both 14 m from production well A at land surface (fig. 2), the temperatures at well AM2 were noticeably greater than temperatures at well AM3 (figs. 9, 10, 15, and 16). Although temperatures in the Ironton and Galesville Sandstones were similar in both wells, temperatures in the upper part of the Franconia Formation were 10°C to 75°C less in well AM3 than in well AM2. The measured temperature differences likely resulted from (1) the bottom of observation well AM2 being about 16 m from production well A and the bottom of observation well AM3 being about 19 m from production well A, and (2) anisotropy of the aquifer. Observation well AM2 was aligned more closely with the axis of maximum transmissivity than was observation well AM3 (Miller, 1984). Increased ground-water flow and heat transport likely occurred in association with the axis of maximum transmissivity, therefore resulting in higher temperatures at well AM2 than at well AM3.

Although observation wells AM1 and AS1 were both 7 m from production well A at land surface (fig. 2), arrival times for well AM1 were earlier than for well AS1. Earlier arrival times at well AM1 were probably due to the bottom of well AS1 being about 7 m farther from production well A (fig. 5).

Interpretation of the temperature graphs indicates that significant heat loss occurred through conduction from the injection zones to the overlying St. Lawrence confining unit (altitude 109.7 m), the underlying Eau Claire confining unit (altitude 38.1 m), and the unscreened lower part of the Franconia Formation (altitudes 8 to 65.5 m). Heat-conduction losses were greatest to the lower part of the Franconia Formation and the Eau Claire confining unit. Some of the temperature increases measured in well AM1 may have been due to horizontal heat convection, because the screened interval of production well A extended into the top 1.5 m of the Eau Claire Formation (Miller and Delin, 1993). Although observation wells AM1 and AS1 were both 7 m from production well A at land surface, heat-conduction losses were greater for well AM1. These greater heat losses probably were due to the bottom of well AM1 being 7 m closer to production well A than the bottom of well AS1 (fig. 5). Because water temperatures were greater at well AM1, greater heat-conduction losses to the Eau Claire confining unit probably occurred at that well.

Time-lag heat conduction was not as apparent during the long-term test cycles as it was in the short-term test cycles (Miller and Delin, 1994). The relatively long injection periods with few interruptions likely limited time-lag heat conduction during the long-term test cycles.

Temperatures in the Ironton and Galesville Sandstones generally followed the trend of the injected water temperatures. Injected water temperatures were highest during the early part of the injection periods. Therefore, maximum temperatures occurred early in the injection periods in the Ironton and Galesville Sandstones at wells 7 and 14 m from production well A. Conversely, maximum temperatures occurred at the end of the injection periods in the upper part of the Franconia Formation at all observation wells, and in the Ironton and Galesville Sandstones at well AM4, located 30.5 m from production well A. Results of the long-term test cycles suggest that aquifer clogging either did not occur or was insignificant.

A significant amount of heat remained both in the aquifer and in the confining units when the long-term test cycles ended. Temperatures at the end of the first long-term cycle averaged about 40°C at the upper part of the Franconia Formation and about 45°C at the Ironton and Galesville Sandstones in observation wells, similar to temperatures of water withdrawn at the end of storage. Temperatures in the immediately overlying and underlying confining units were greater than those in the permeable part of the aquifer. A similar picture emerged at the end of the second long-term cycle, at somewhat higher temperatures. About 62 percent of the heat stored in the aquifer was recovered during each of the two long-term cycles (table 3).

NONISOTHERMAL MODELING OF LONG-TERM TEST CYCLES 1 AND 2

A three-dimensional, anisotropic, nonisothermal, ground-water-flow and thermal-energy-transport model was used to simulate the two long-term test cycles. The model is similar to the three-dimensional, isothermal ground-water-flow model described by Miller and Delin (1993). Miller and Voss (1986) describe discretization of the model and the sensitivity

of the lateral boundary conditions for various rates of heated-water injection.

The finite-difference, ground-water-flow, and thermal-energy-transport model used in this study was developed for waste-injection problems (Intercomp Resources Development and Engineering, 1976) and will be referred to in this report as the Survey Waste Injection Program (SWIP) code. The SWIP code can be used to simulate ground-water flow and heat and solute transport in a liquid-saturated porous medium; it contains both reservoir and well-bore modeling capabilities. The major model assumptions are as follows:

1. Ground-water flow is laminar (Darcian), three dimensional, and transient.
2. Fluid density is a function of pressure, temperature, and concentration.
3. Fluid viscosity is a function of temperature and concentration.
4. The injected fluid is miscible with the in-place fluids.
5. Aquifer properties vary with location.
6. Hydrodynamic dispersion is a function of fluid velocity.
7. The energy equation can be described as: enthalpy in minus enthalpy out equals the change in internal energy of the system.
8. Boundary conditions allow natural water movement in the aquifer and heat losses to adjacent formations.
9. Thermal equilibrium exists within the simulated area.

The basic equation describing single-phase flow in a porous medium is derived by combining the continuity equation and Darcy equation for three-dimensional flow (Intercomp Resources Development and Engineering, 1976, p. 3.4):

$$\nabla \bullet \left[\frac{\rho k}{\mu}(\nabla p - \rho g \nabla z)\right] - q' = \frac{\partial}{\partial t}(\phi\rho) \qquad (1)$$

where

ρ = fluid density [M/L^3] (kg/m^3),
μ = fluid viscosity [M/(L-T)] (Pa-s),
k = intrinsic permeability [L^2] (m^2),
g = gravitational acceleration [L/T^2] (m/s^2),
z = spatial dimension in direction of gravity [L] (m),
p = pressure [M/(L-T^2)] (Pa),
q'= mass rate of flow per unit volume from sources or sinks [M/(T-L^3)] (kg/m^3-s),
t = time [T] (s),
ϕ = porosity [dimensionless], and
∇ = gradient (for an axially symmetric cylindrical coordinate system, ∇ is

$$\frac{\partial}{\partial r} + \frac{1}{r}\frac{\partial}{\partial \theta} + \frac{\partial}{\partial z}$$

where r is the radial dimension).

The energy-balance equation describing the transport of thermal energy in a ground-water system (Intercomp Resources Development and Engineering, 1976, p.3.4)

$$\nabla \bullet \left[\frac{\rho k}{\mu} H(\nabla p - \rho g \nabla z)\right] + \nabla \bullet K \bullet \nabla T \qquad (2)$$
$$- q_L - q'H = \frac{\partial}{\partial t}[\phi\rho U + (1-\phi)(\rho C_p)_R T]$$

where

H = enthalpy per unit mass of fluid [E/M] (J/kg),
K = hydrodynamic thermal dispersion plus convection [E/(T- L-t)] (W/m-°C),
T = temperature [t] (°C),
q_L = heat loss across boundaries [E/T] (W),
U = internal energy per unit mass of fluid [E/M](J/kg),
$(\rho C_p)_R$ = heat capacity of aquifer matrix [E/L^3-T] (J/m^3-°C), and
Cp = specific heat of aquifer matrix [E/M-T] (J/kg-°C).
(All other terms are previously defined.)

Equations 1 and 2 are a nonlinear system of coupled partial-differential equations that are solved numerically by discretizing the aquifer into three dimensions (or two dimensions for radial flow) and developing finite-difference approximations. Finite-difference equations (Intercomp Resources Development and Engineering, 1976, p. 3.5) whose solutions closely approximate the solutions of equations 1 and 2 are, for the basic flow equation:

Table 3. Comparison of model-computed thermal efficiencies of the aquifer and final withdrawal-water temperatures at production well A with corresponding calculated and measured values for long-term test cycles 1 and 2

Long-term test-cycle number	Thermal efficiency of aquifer (percent)		Final withdrawal-water temperature, (degrees Celsius)	
	Calculated	Model computed	Measured	Model computed
1	62	61	45.6	45.6
2	62	62	55.4	59.5

$$\Delta[T_w(\Delta p - \rho g \Delta z)] - q = \frac{V}{\Delta t}\delta(\phi\rho) \quad (3)$$

and for the energy equation:

$$\Delta[T_w H(\Delta p - \rho g \Delta z)] + \Delta(T_c \Delta T) - q_L \quad (4)$$

$$-(q'H) = \frac{V}{\Delta t}\delta[\phi\rho U + (1-\phi)(\rho C_p)_R T]$$

where

q = mass rate of production or injection of liquid for a grid block units [L^3/t] (m^3/s),

V = volume of the grid block [L^3] (m^3)

$$T_w = \frac{kA\rho}{\mu l} \quad (5)$$

$$T_c = \frac{KA}{l} \quad (6)$$

A = the area perpendicular to flow (that is, $\Delta x\Delta y$, $\Delta x\Delta z$, or $\Delta y\Delta z$) [L^2] (m^2),

l = the distance between grid block centers [L] (m), and the temperature of the aquifer water (T_w) and the aquifer matrix (T_c) are defined as

(All other terms are previously defined.)

The finite-difference operators are defined as:

$$\Delta(T_w \Delta p) = \Delta_x(T_w \Delta_x p) + \Delta_y(T_w \Delta_y p) + \Delta_z(T_w \Delta_z p) \quad (7)$$

with the terms:

$$\Delta_x(T_w \Delta_x p) = T_{w,\,i+0.5,\,j,\,k}[p^{n+1}_{i+1,\,j,\,k} - p^{n+1}_{i,\,j,\,k}] - T_{w,\,i-0.5,\,j,\,k}[p^{n+1}_{i,\,j,\,k} - p^{n+1}_{i-1,\,j,\,k}] \quad (8)$$

and

$$\delta\kappa = \kappa^{n+1} - \kappa^n \quad , \quad (9)$$

where

x, y, z = cartesian-space coordinates,

i, j, k = grid-block indices,

n = time level, t_n,

(All other terms are previously defined.)

Finally, the thermal-conductance term, K, in equation 6 may be further defined as (Intercomp Resources Development and Engineering, 1976, p. 3.7):

$$K = \phi\left(\frac{\alpha u}{\phi}\right)(\rho C_p)_w + K_m \quad (10)$$

where

α = thermal dispersivity [L] (m),

ϕ = porosity [dimensionless],

u = volumetric flux (Darcy velocity) [L/T] (m/s),

$(\rho C_p)_w$ = heat capacity of water [E/(L^3-T)] (J/m^3-°C), and

K_m = molecular heat conductivity of porous media [E/(T-L-t)] (W/m-°C).

Simulation of Model Anisotropy

Analysis of aquifer-test data (Miller, 1984; Miller and Delin, 1993) indicates that the Ironton and Galesville Sandstones and the upper part of the Franconia Formation are areally anisotropic and that the angle between the major axis of transmissivity and the axis between production wells A and B is approximately 30 degrees. Although the anisotropy may be considered small (less than 3:1), its effect on the movement and direction of heat flow for the hydrologic conditions at the ATES site is not known. Use of a radial-flow equation would neglect the effect of anisotropy. The potential errors introduced in the radial-flow assumptions are discussed by Miller and Delin (1993) in the section of that report describing the radial-flow model. On the basis of their discussion, a three-dimensional model was constructed to represent anisotropic conditions and to simulate the ATES short-term test cycles (Miller and Delin 1994). This model was modified for simulation of the long-term test cycles and to accommodate movement of the thermal front past observation well AM4.

Discretization of Aquifer System

The area that can be modeled around the ATES doublet-well system is limited by (1) the constraint on the finite-difference grid spacings required by the model-solution techniques, (2) the lack of alignment of the axis of aquifer anisotropy and the axis on which the doublet wells are located, and (3) running the model for large three-dimensional problems exceeded allocated resources available at that time. Miller and Voss (1986) describe the construction of the finite-difference grid for the doublet-well system at the ATES site. Flow-net analysis (Miller and Voss, 1986) makes it possible to reduce the modeled area and to simulate flow only in the area around production well A, the flow region where energy transport is of greatest concern (figs. 23 and 24). The equipotentials and streamlines illustrated in figures 23 and 24 are the steady-state solutions to two-dimensional, isothermal flow in a homogeneous, confined, infinite, anisotropic aquifer that has no regional hydraulic gradient (Miller and Voss, 1986). Flow outside this modeled region is represented by a

specified flux at model boundaries, as determined by flow-net analysis.

The finite-difference grid for the ATES-site model was oriented such that the axis of maximum transmissivity was aligned with the horizontal-coordinate direction (figs. 23 and 24). The origin of the field-coordinate system shown in figures 23 and 24 was arbitrarily chosen to be halfway between production wells A and B. A variably-spaced grid was designed because of restrictions on grid size for solution accuracy and stability inherent to the difference approximation used in the SWIP code (Intercomp Resources Development and Engineering, 1976). Cell sizes range from 0.3 m on a side at production well A to a maximum of 10.0 m on a side at the periphery of the model. The grid had 6 layers with 806 cells per layer. Vertical grid spacings were selected to correspond with the four hydraulic zones in the Franconia-Ironton-Galesville aquifer and with the overlying and underlying confining units (table 4). The lateral boundaries of the model correspond to the 4.5-m equipotential for the Ironton and Galesville Sandstones (fig. 23) and for the upper part of the Franconia Formation (fig. 24).

Boundary and Initial Conditions

Flux rates were specified at the model boundaries such that the boundaries accurately represented groundwater flow and heat transport between the modeled area and the area outside the simulated region. The correct boundary fluxes were determined by analysis of the flow net for steady-state conditions (Miller and Voss, 1986; Miller and Delin, 1993). The total flow crossing an equipotential (fig. 23 and 24) is equal to the injection rate and is thus known. In addition, an equal amount of flow is represented by each streamtube. Therefore, if quasi-steady-state flow is assumed, the distribution of fluxes along an equipotential is known for any injection rate. The locations of lateral-flux boundaries in the model are illustrated in figures 23 and 24. More detailed descriptions of the methods used to calculate the boundary fluxes for the model are provided by Miller and Voss (1986), and Miller and Delin (1993 and 1994).

The following is a brief description of the thermal properties of the aquifer used as variables in the nonisothermal model. Heat capacity is the amount of heat required to raise the temperature of a material a specified amount. It is the product of density and specific heat and is a measure of the ability of a material to store heat. Values of 1.81×10^6 and 3.89×10^3 J/m^3-°C were used for heat capacity of rock and water, respectively (table 5). The value of rock heat capacity represents sandstones similar to those in the Franconia-Ironton-Galesville aquifer. These values were based on data from Sommerton and others (1965), Clark (1966), Helgeson and others (1978), and Robie and others (1978). The values were calculated by use of methods described by Martin and Dew (1965).

The constant of proportionality between the heat flux and the temperature gradient is termed thermal conductivity. It is the quantity of heat transmitted in unit time through a unit cross-sectional area under a unit temperature gradient. For purposes of data analysis, thermal conductivity was assumed to be isotropic in the aquifer system. Values of thermal conductivity (table 5) were obtained from Clark (1966).

Thermal diffusivity is defined as the transport of energy by conduction due to the exchange of kinetic energy between molecules. Molecular diffusion is independent of fluid velocities and is usually constant in saturated porous media. The value of 1.56×10^6 m^2/s (table 5) used for thermal diffusivity is representative of sandstones in the Franconia-Ironton-Galesville aquifer (Kappelmeyer and Haenel, 1974).Thermal dispersion, resulting from fluctuations of velocity and temperature in the pore space, is similar to the more common term of mechanical hydrodynamic dispersion used in solute mass-transport problems. Hydrodynamic dispersion is the name for a group of mixing mechanisms that cause the spreading of a solute in a flow system (Bear, 1972). Values of dispersivity are dependent on the scale of model discretization. The values shown in table 5 were determined through calibration of the model.

Model Calibration

The model was calibrated to nonisothermal conditions to ensure that the hydraulic and thermal properties selected were reasonable for simulation of heat transport in the flow system. The relative importance of each property was evaluated during preliminary model analyses (Miller and Delin, 1993). Model sensitivity to changes in the hydraulic properties of hydraulic conductivity, porosity, and vertical anisotropy, plus model sensitivity to changes in the thermal properties of thermal conductivity of rock, heat capacity of rock, and thermal dispersivity, were tested during preliminary model analyses (Miller and Delin, 1993). Based on results of these analyses, the model was most sensitive to changes in thermal dispersivity. The longitudinal thermal dispersivity was varied from 1 to 6 m during the long-term nonisothermal model

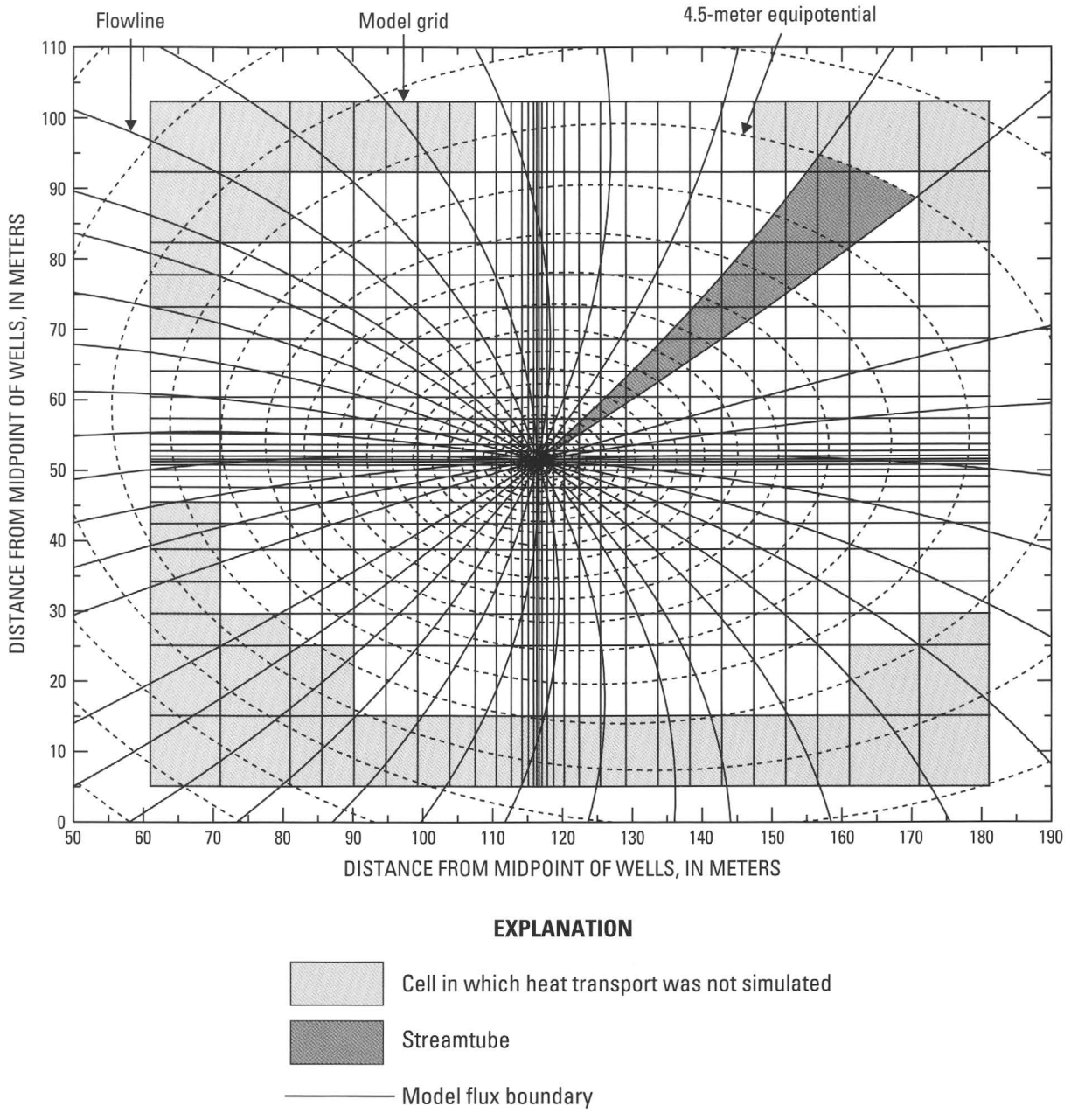

Figure 23. Model grid and flow net for the Ironton and Galesville Sandstones near production well A for the long-term test cycles.

calibration and a value of 3.33 m most accurately duplicated the measured data (table 5). Field data have shown that transverse dispersivity usually is 0.1 to 0.3 times the longitudinal dispersivity (Freeze and Cherry, 1979, p. 396). Therefore, the transverse thermal dispersivity was varied from 0.1 to 0.6 m during the long-term nonisothermal model calibration and a value of 0.33 m most accurately duplicated the measured data (table 5). The final thermal and hydraulic properties simulated in the model are listed in tables 5 and 6, respectively. Model accuracy perhaps could be improved by adjusting this long-term model following a rigorous sensitivity analysis; however, this was not deemed necessary based on the preliminary sensitivity analyses. The model necessarily is a simplification of the flow system, and accuracy of the model results is limited by the accuracy of the hydraulic and thermal input data on which the computations are based. In addition, different combinations of input data could

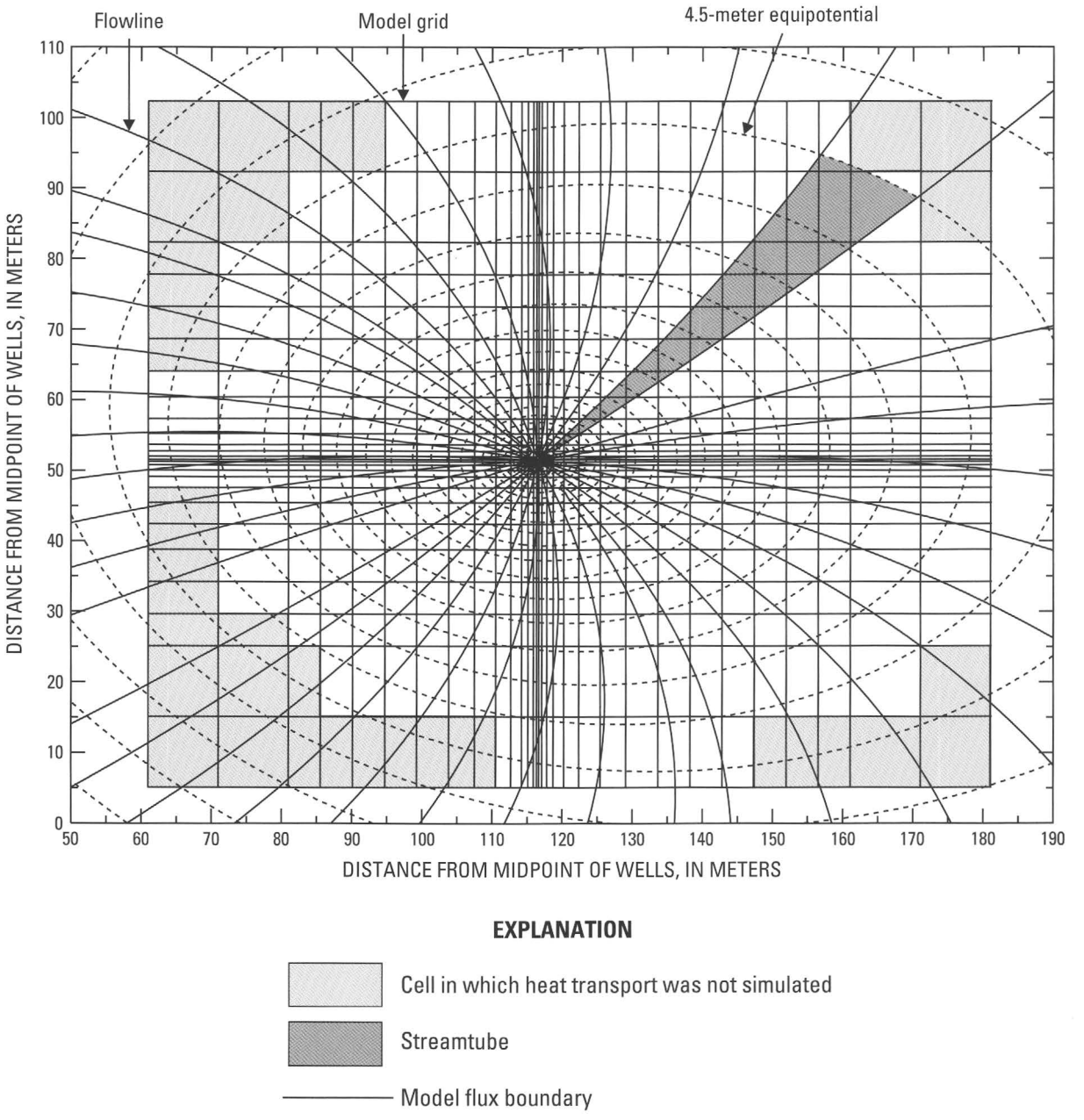

Figure 24. Model grid and flow net for the upper part of the Franconia Formation near production well A for the long-term test cycles.

conceivably yield the same results, particularly because only two variables were adjusted during calibration.

The injection, storage, and withdrawal phases of the two long-term test cycles were simulated from the beginning of the first long-term test cycle to the end of the second long-term test cycle. Temperatures measured at observation wells in the aquifer at the start of the first long-term test cycle were used as initial temperatures for the simulation. Modeling the entire period of the two long-term test cycles allowed residual heat left in the aquifer at the storage site to be taken into account for the second cycle. The simulated injection was divided into periods of injection, flow-rate change, and injection-temperature change during each cycle (table 7). Simulated flow rates during periods of withdrawal were similarly divided.

Calibration of the model to nonisothermal conditions consisted of comparing model-computed thermal

Table 4. Layer number, thickness, and corresponding stratigraphic/hydrogeologic unit for the three-dimensional model

Model layer	Thickness (meters)	Stratigraphic/hydrogeologic unit
1	7.6	St. Lawrence Formation (confining unit)
2	13.7	Upper part of the Franconia Formation (aquifer)
3	24.4	Lower part of the Franconia Formation (confining unit)
4	15.2	Ironton Sandstone (aquifer)
5	6.1	Galesville Sandstone (aquifer)
6	30.5	Eau Claire Formation (confining unit)

efficiencies and withdrawal-water temperatures to calculated and measured values (table 3). Thermal efficiency of the aquifer was computed by dividing the total energy injected into the aquifer system by the total energy withdrawn from the system. Calibration of the model also was achieved by comparing model-computed and average temperatures at the observation wells during the test cycles (figs. 25–36). The longitudinal and transverse dispersivities were varied during nonisothermal model calibration on the basis of relative hydraulic conductivities of the aquifer in the longitudinal and transverse directions (Miller, 1984). The longitudinal dispersivity was varied from 1.0 to 30.0 m and the transverse dispersivity was varied from 0.1 to 3.0 m, similar to calibration of the model for the short-term cycles (Miller and Delin, 1994). Values of 3.33 and 0.33 m for longitudinal and transverse dispersivity, respectively, simulated aquifer thermal efficiencies, wellhead temperatures (table 5, and figs. 25 and 31), and average temperatures (figs. 26–30, and 32–36) close to measured values.

Model-computed temperatures were compared to measured temperatures at each of the observation wells for each period of injection, storage, and withdrawal for the two long-term test cycles. Actual temperature measurements were averaged for all measurement points (which were operating) within each hydrogeologic unit in an attempt to make measured and model-computed data comparable. Table 8 lists the measurement-point altitudes for which data were averaged to compare with the model's vertical layering. Thermocouples that failed completely for a cycle phase were omitted from the temperature averages for comparison with model-computed temperatures. A factor that was considered when comparing model-computed temperatures with measured data is the radial distance of measurement points from production well A. Because of the limitations of finite-difference modeling, the actual location of measurement points may not be exactly simulated in the model at the correct radial distance (fig. 5). As described earlier, depth-deviation surveys indicate that some of the observation wells deviate as much as 7 m horizontally for depths ranging through the model's vertical-simulation region. Model-computed temperatures for each monitoring point at the site were correlated with measured values taking into account results of the deviation survey.

Representation of variable pumping rates and injection temperatures must be considered when comparing model-computed and averaged temperatures. Variations in inputs are illustrated in figures 25 and 31, which show injection temperatures recorded at the wellhead and injection temperatures simulated with the model. During the long-term test cycles, the source-water temperature varied smoothly and the temperature of the injected water was controlled by the temperature controller, or varied as a response to

Table 5. Thermal properties used for simulation of the long-term test cycles 1 and 2

Thermal property	Value and unit of measure
Thermal conductivity, rock	= 2.20 watts per meter-degree Celsius
Thermal conductivity, aquifer water at 20 degrees Celsius	= 0.60 watts per meter-degree Celsius
Thermal diffusivity	= 1.56×10^{6} square meter-second
Heat capacity, rock	= 1.81×10^{6} joules per cubic meter-degree Celsius
Heat capacity, aquifer water	= 3.89×10^{3} joules per cubic meter-degree Celsius
Longitudinal dispersivity	= 3.33 meters
Transverse dispersivity	= 0.33 meters

Table 6. Hydraulic properties used for simulation of the long-term test cycles

Model layer	Hydraulic conductivity (meters per day)			K_x:K_y	Porosity (percent)
	K_x	K_y	K_z		
1	0.003	0.003	0.00003	1.00	26.8
2	2.89	1.71	.222	1.69	28.2
3	.03	.03	.0003	1.00	27.3
4	5.78	2.51	.380	2.30	25.2
5	1.45	.628	.095	2.30	25.6
6	.003	.003	.00003	1.00	31.6

the capacity of the heat exchanger (Hoyer and others, 1991a and 1991b).

Analysis of Simulations

A description of the differences between model-computed and averaged temperatures for long-term cycles 1 and 2 follows. Trends in the averaged temperatures will be discussed and related to model results to describe thermal processes that may explain the results. As described earlier, some thermocouples failed intermittently because of insulation wear at kinks in the wires or electronic noise in the data logger. These failures appear as small temperature fluctuations in figures 25–36 and are not discussed further.

The model accurately predicted thermal efficiencies of the aquifer to within about 1 percent of calculated values for the long-term test cycles (table 3). The model also accurately predicted the final withdrawal-water temperatures to within an average of about 3 percent of calculated values, or to within about 1°C for the first long-term test cycle and to within about 5°C for the second long-term test cycle (table 3).

Model-computed and measured temperatures at production well A compare closely (figs. 25 and 31). However, the model-computed temperatures are somewhat lower than measured temperatures throughout most of the withdrawal periods for both cycles (figs. 25 and 31). This deviation may be an indication that the model overestimated the down-well flow between the two screened intervals of production well A.

The model closely matched both the trends in the averaged temperature profiles and the temperatures at the end of injection and withdrawal periods for cycles 1 and 2. Overall, model-computed temperatures more closely matched averaged values for cycle 2 than for cycle 1. The close correspondence between model-computed and averaged temperatures for observation well AM1 may be related to its short distance from production well A, compared to the other observation wells. Trends of the model-computed temperatures for observation wells AS1 (figs. 27 and 33), AM2 (figs. 28 and 34), and AM3 (figs. 29 and 35) do not agree as well with averaged temperatures. The model did not duplicate the rapid rise in temperatures at all observation wells, and particularly in the Ironton and Galesville Sandstones that peaked about five days into both long-term tests. The model-computed and averaged temperatures differ by different amounts at different stages of the two cycles. For example, model-computed temperatures for observation well AM4 are too high for the upper part of the Franconia Formation, too low for the lower part of the Franconia Formation, and very close to measured values for the Ironton and Galesville Sandstones. The timing of the temperature changes for the Ironton and Galesville Sandstones is considerably behind the averaged temperature changes (figs. 30 and 36).

For the upper part of the Franconia Formation, model-computed temperatures during injection were generally higher than average measured temperatures except at AS1. Initial injection temperatures at wells AS1, AM1, and AM2 were also higher than measured values. By the end of injection, the model-computed temperatures were within 5°C of the averaged temperatures at all wells except AM3 for both cycles 1 and 2 and AM4 for cycle 2, which were within about 10°C of the averaged values. By the end of withdrawal, model-computed temperatures in the upper part of the Franconia Formation were within about 5°C of averaged temperatures at all wells except AM3, which was 30°C higher than averaged values. Model-computed temperatures at AM2 cycle 2 were higher than averaged temperatures at all times.

Table 7. Summary of long-term test cycles 1 and 2 simulation times, durations, flow rates, and temperatures

[--, not applicable]

	Simulation time (days)	Duration (days)	Flow rate (liters per second)	Temperature at wellhead (degrees Celsius)
		LONG-TERM TEST CYCLE 1		
Injection	0.0	1.6	284.0	234.0
	1.6	1.2	0	--
	2.8	6.9	282.7	235.0
	9.6	3.9	294.0	234.0
	13.6	5.4	296.0	234.0
	18.9	.9	0	--
	19.8	2.7	290.5	229.4
	22.5	.3	0	--
	22.8	2.7	286.6	238.3
	25.5	1.4	0	--
	26.8	9.8	286.6	233.8
	36.6	7.0	0	--
	43.6	3.4	287.8	230.5
	47.0	15.7	278.0	221.5
	62.7	7.3	280.0	220.0
	70.0	4.7	280.0	211.3
Storage	74.7	64.0	0	--
Withdrawal	138.7	1.1	297.2	156.0
	139.8	1	297.2	162.0
	140.8	2	297.2	169.0
	142.8	1	297.2	180.0
	143.8	3	296.1	185.0
	146.5	2	296.1	189.0
	148.8	4.1	296	190.0
	152.8	6.0	296	189.0
	158.8	1.1	293.3	181.0
	159.8	.8	0	170.0
	160.6	3.2	293.3	175.0
	163.8	5	291.8	177.0
	168.8	10	289.9	167.0
	178.8	5	289.9	149.0
	183.8	5	288.5	140.0
	188.8	5	288.3	132.0
	193.8	4	286.9	125.0
	197.8	0	0	120.0
		LONG-TERM TEST CYCLE 2		
Injection	685.8	8.3	291.7	244.6
	694.1	9.5	291.7	247.5
	713.7	4.1	0	--
	717.8	13.4	291.6	241.2
	731.1	8.5	291.6	243.9
	739.6	7.0	285.6	241.5
	746.6	3.1	285.6	237.3
Storage	749.7	58.2	0	--
Withdrawal	808.0	29.0	269.6	206.0
	837	10	269.6	187.0
	847	10	269.6	169.0
	857	10.2	269.6	153.0
	867.2	0	269.6	139.0

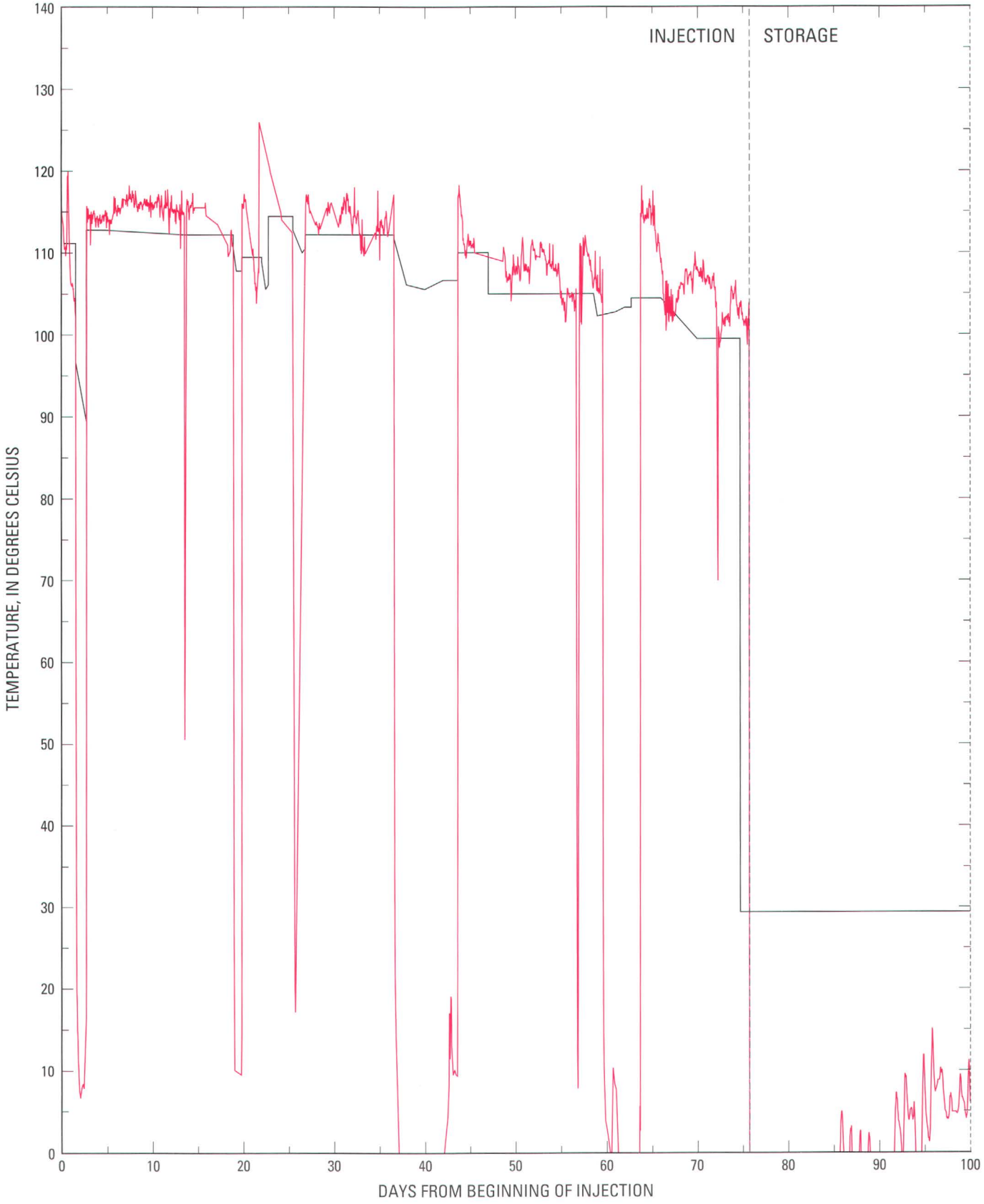

Figure 25. Model-computed and measured temperatures

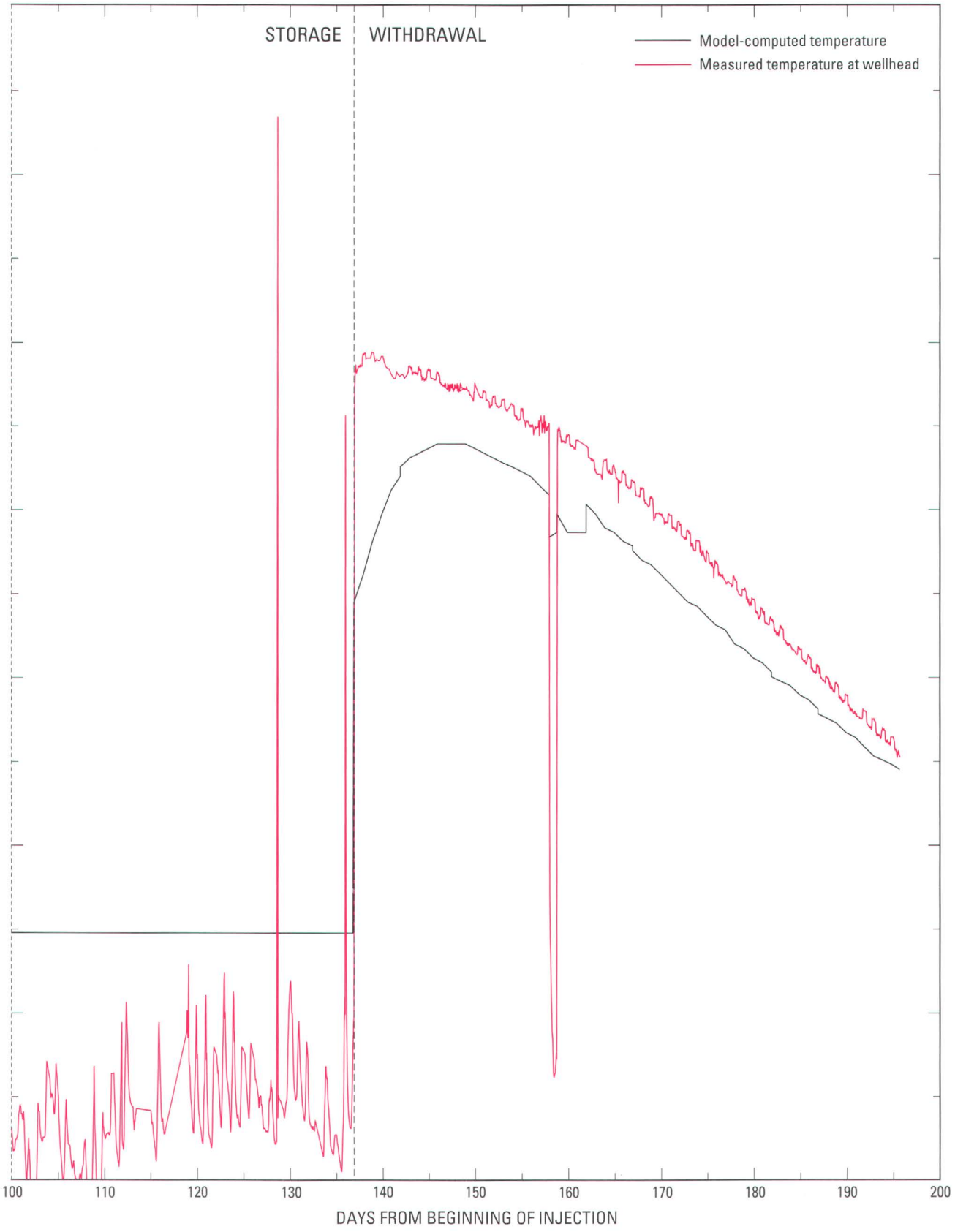

in production well A during long-term test cycle 1.

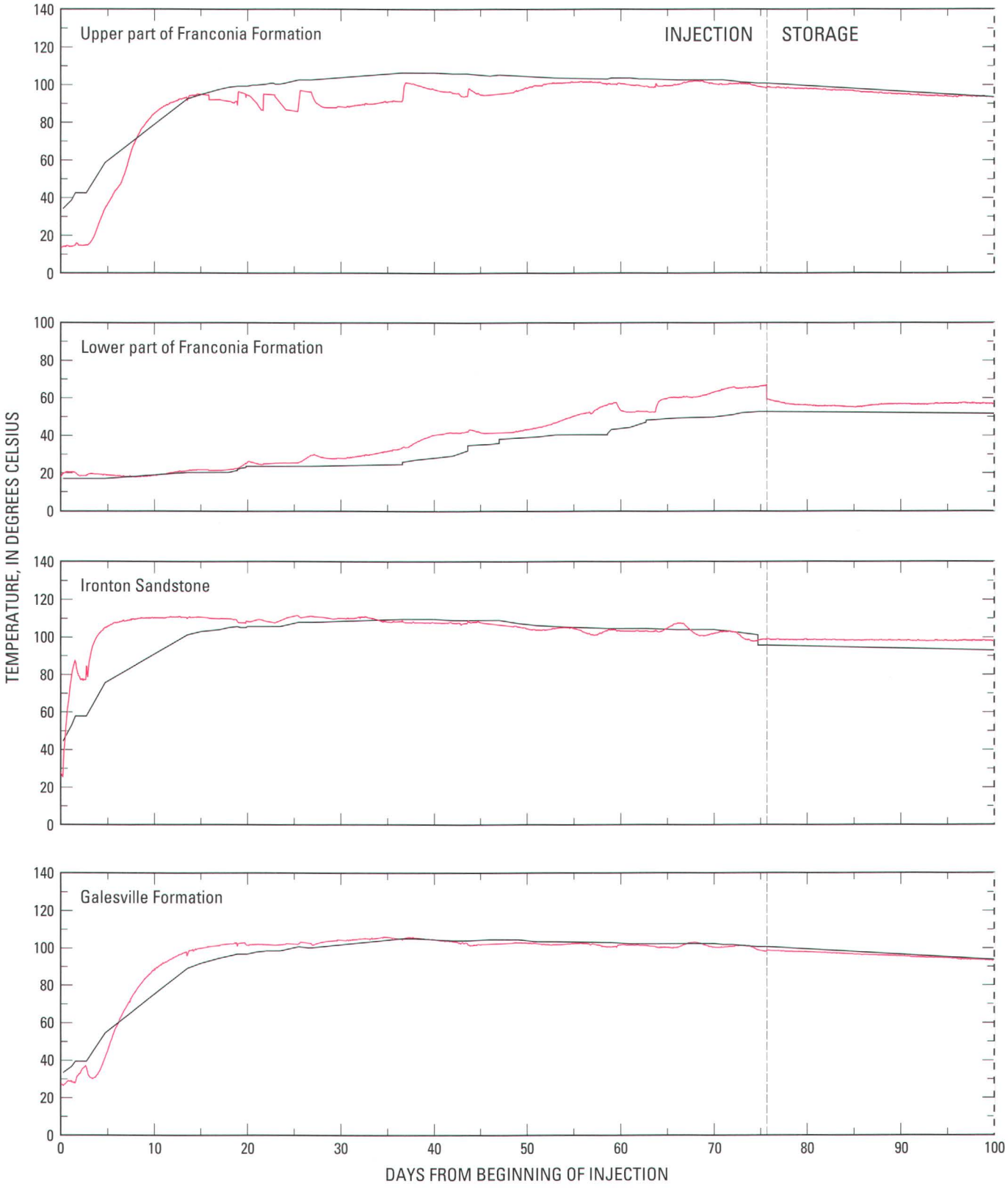

Figure 26. Model-computed and average measured temperatures

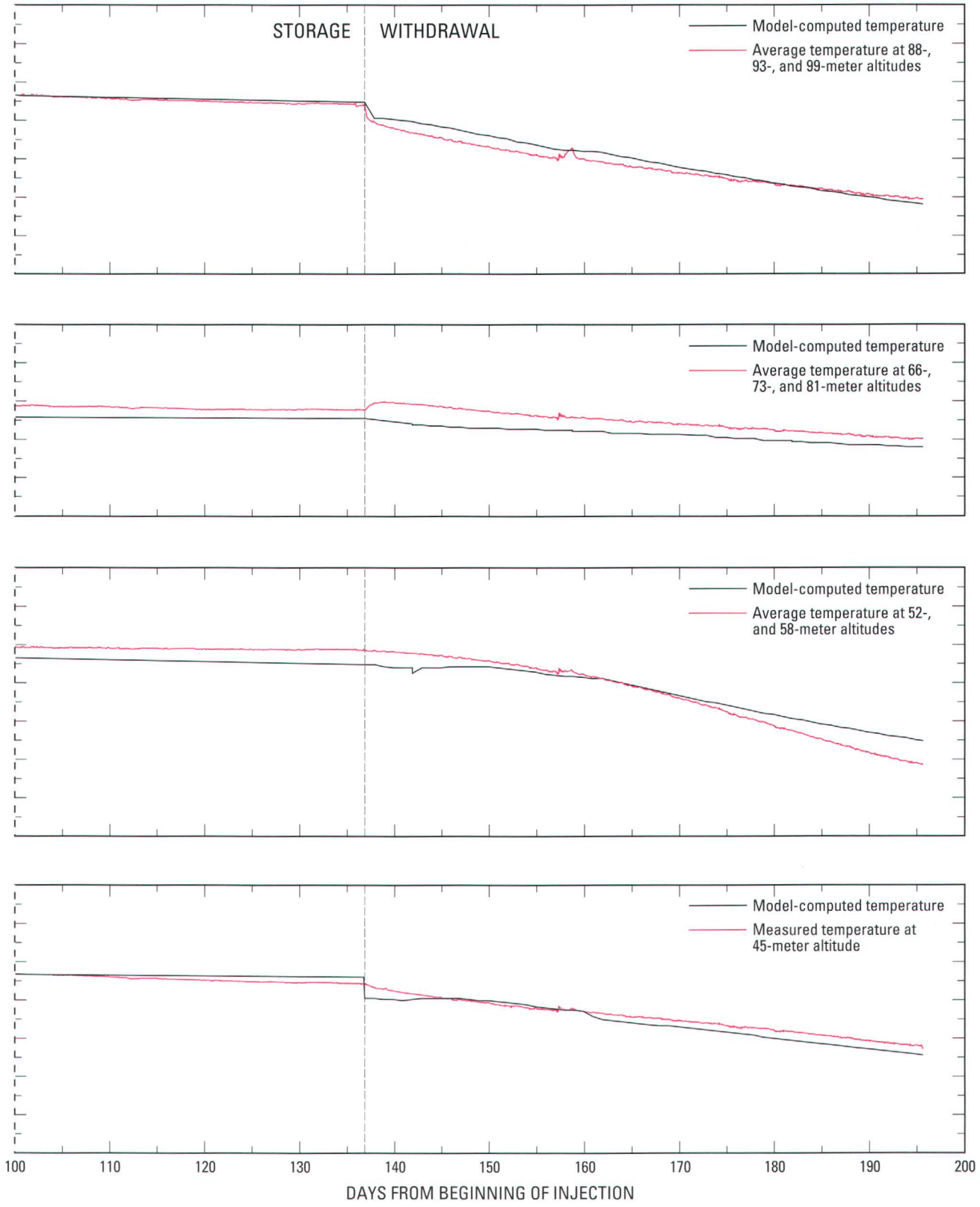

in observation well AM1 during long-term test cycle 1.

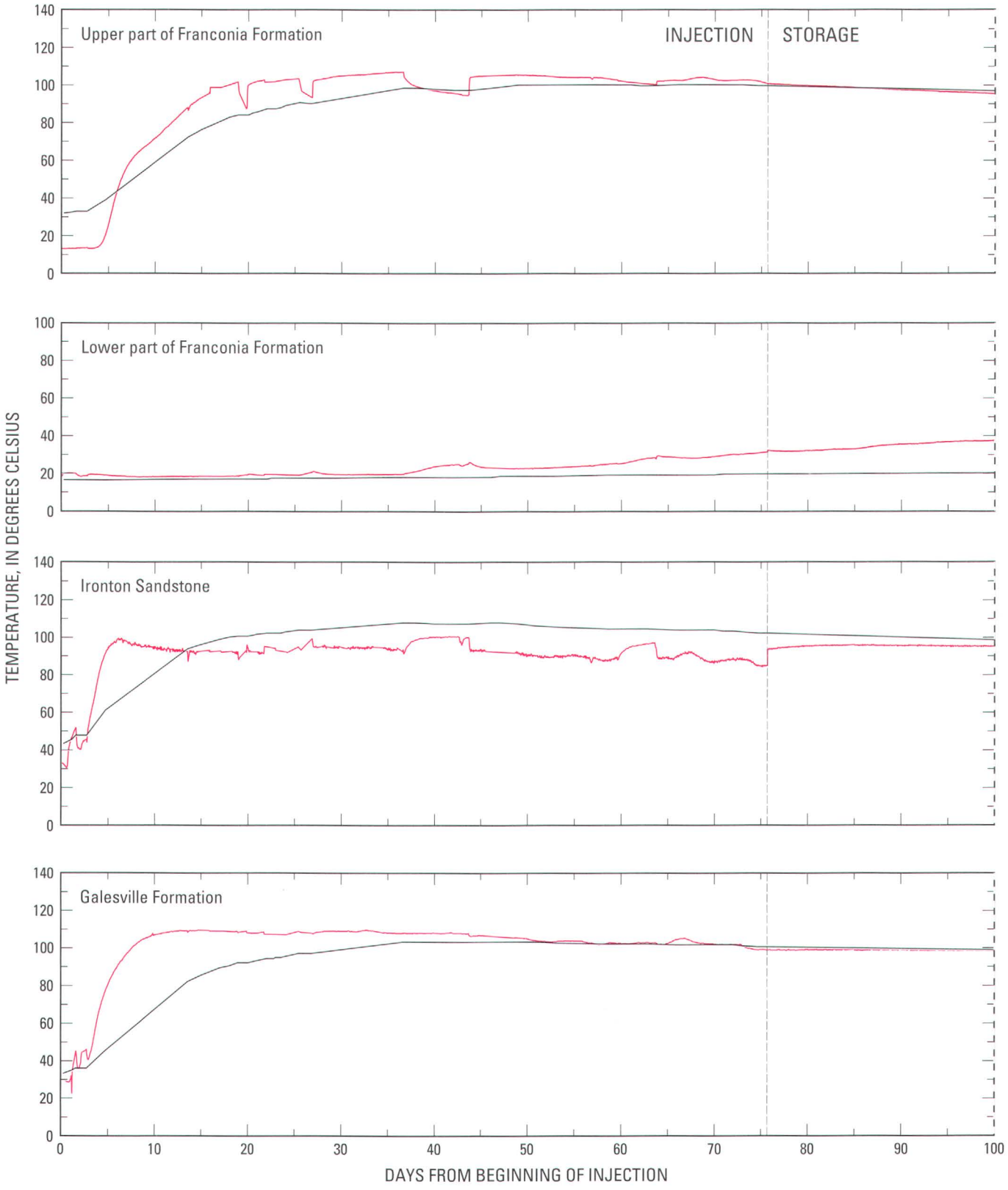

Figure 27. Model-computed and average measured temperatures

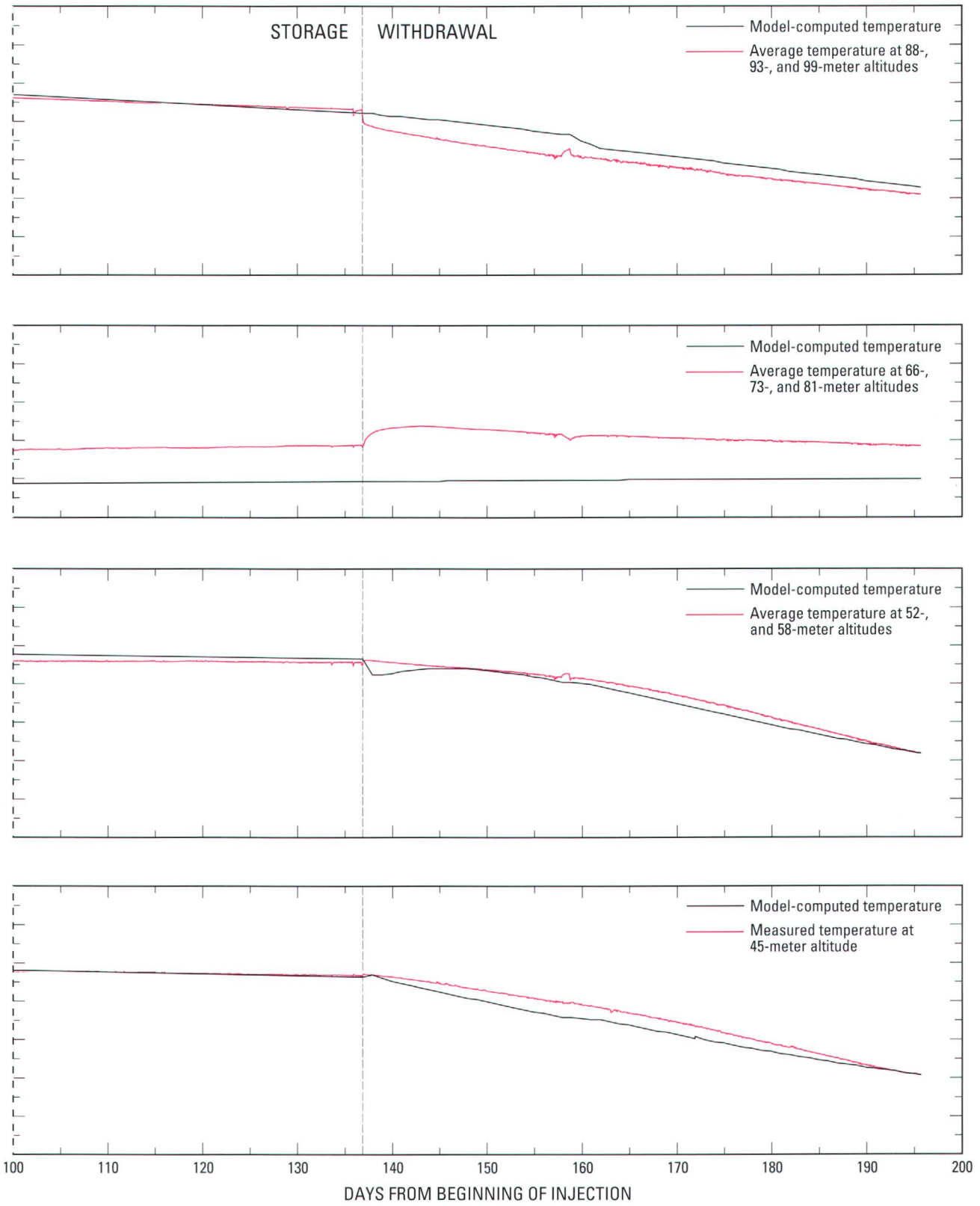

in observation well AS1 during long-term test cycle 1.

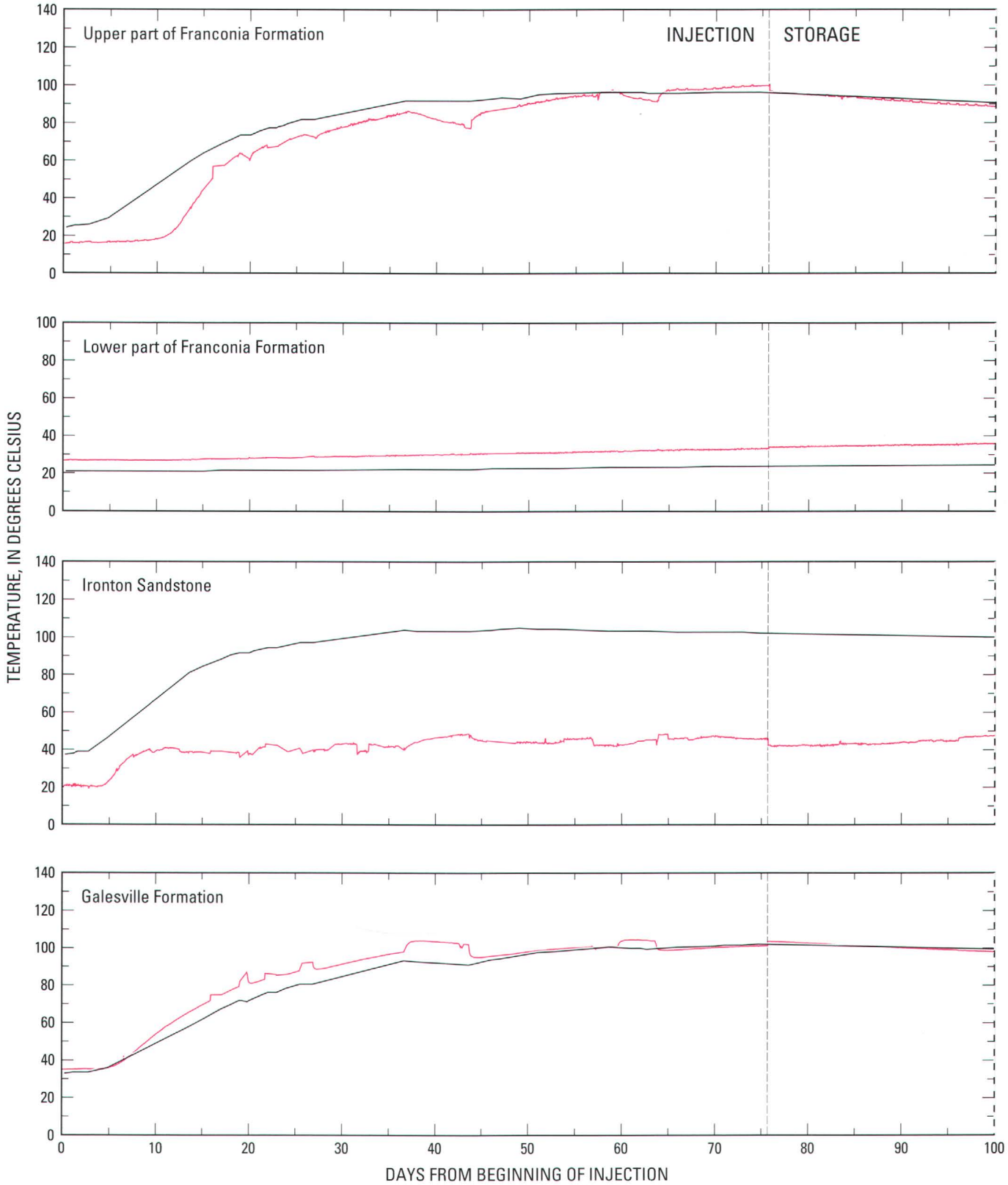

Figure 28. Model-computed and average measured temperatures

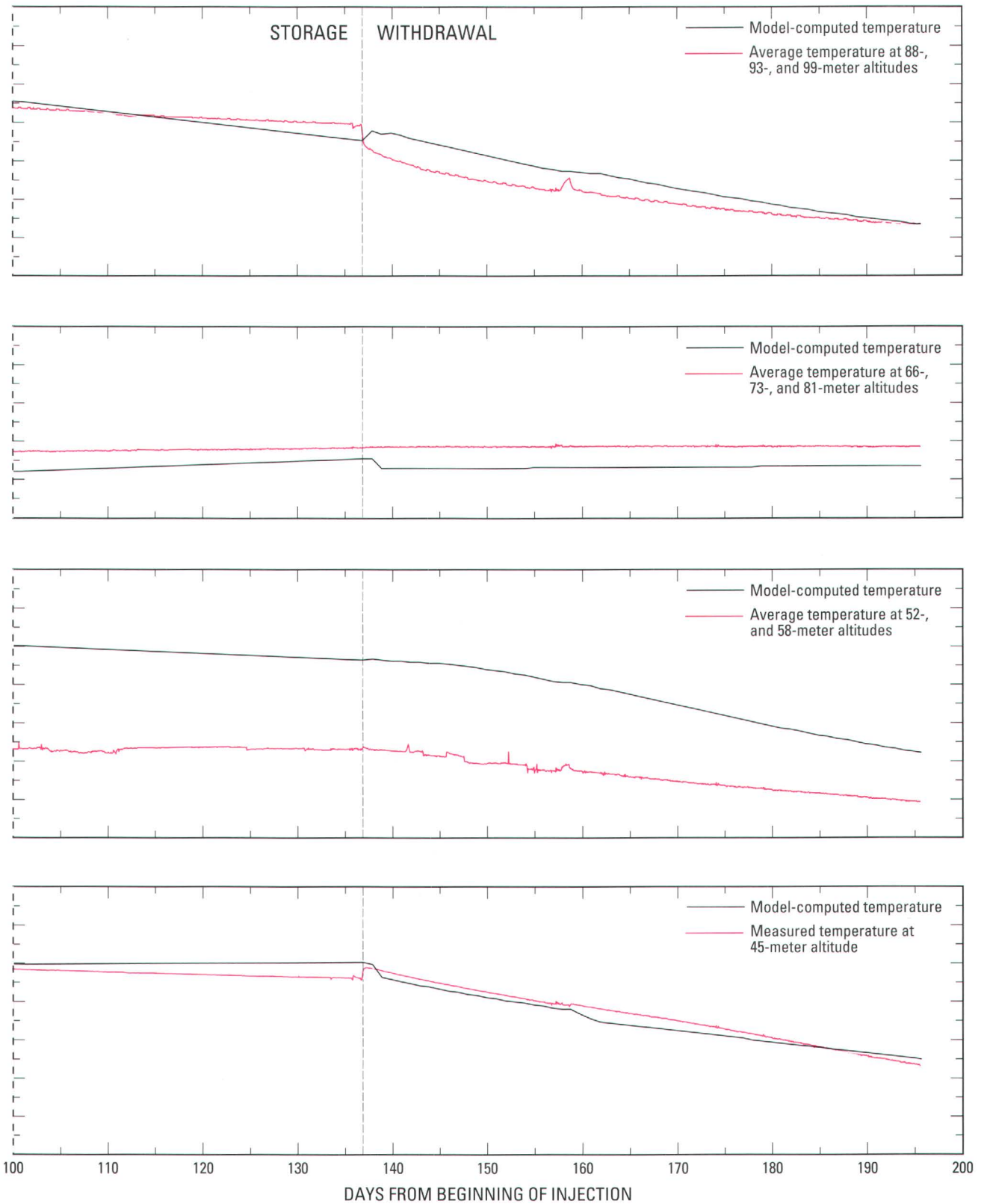

in observation well AM2 during long-term test cycle 1.

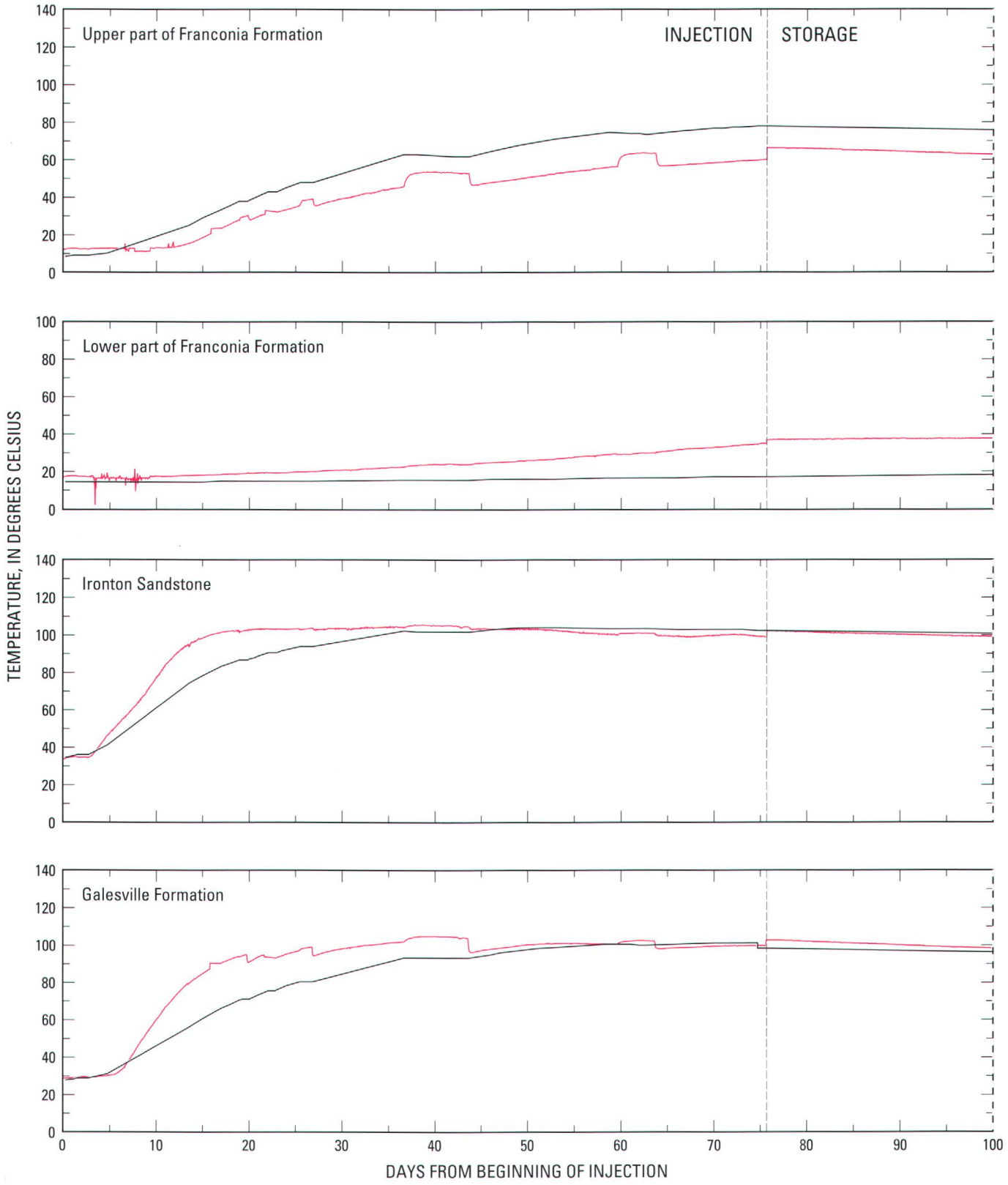

Figure 29. Model-computed and average measured temperatures

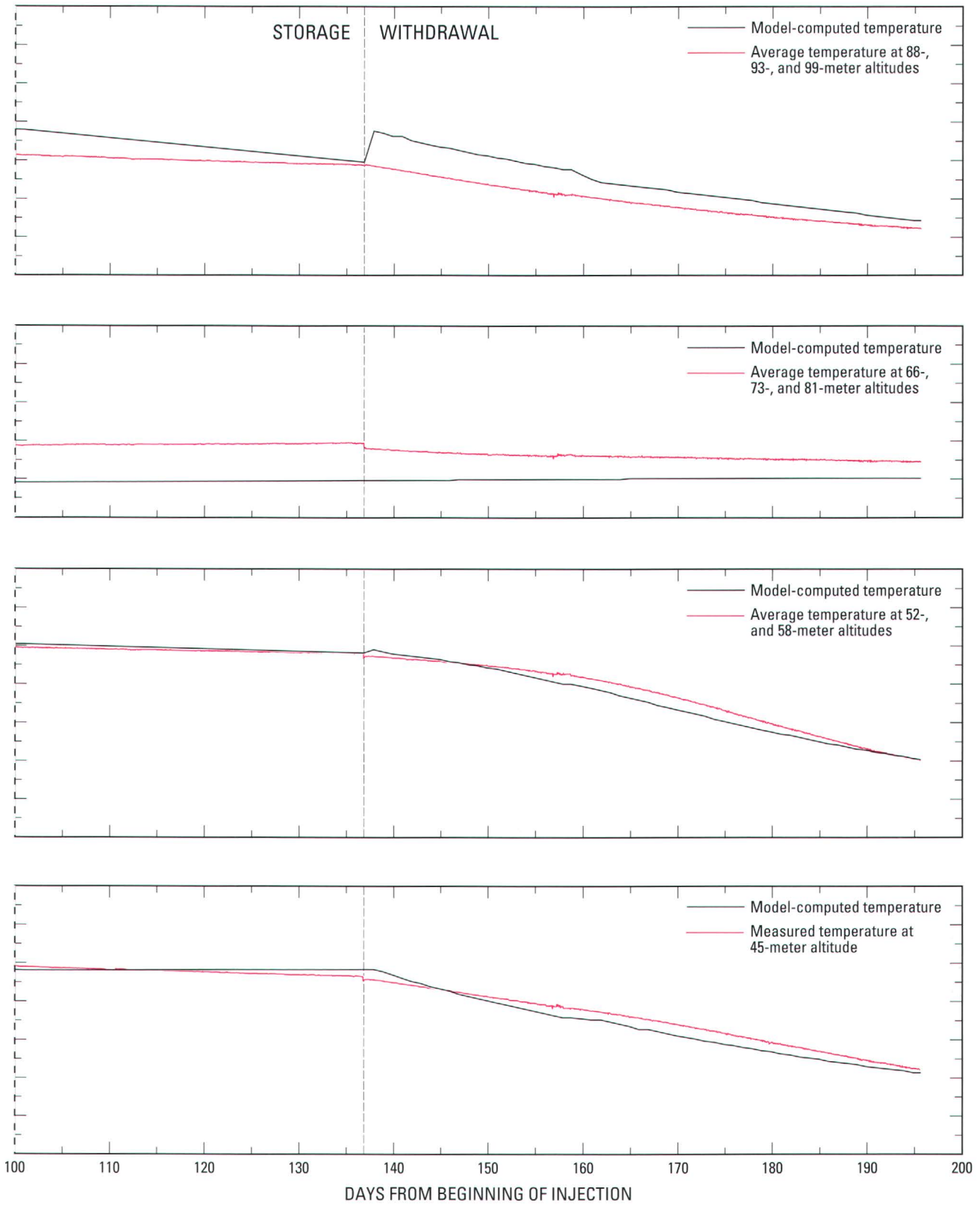

in observation well AM3 during long-term test cycle 1.

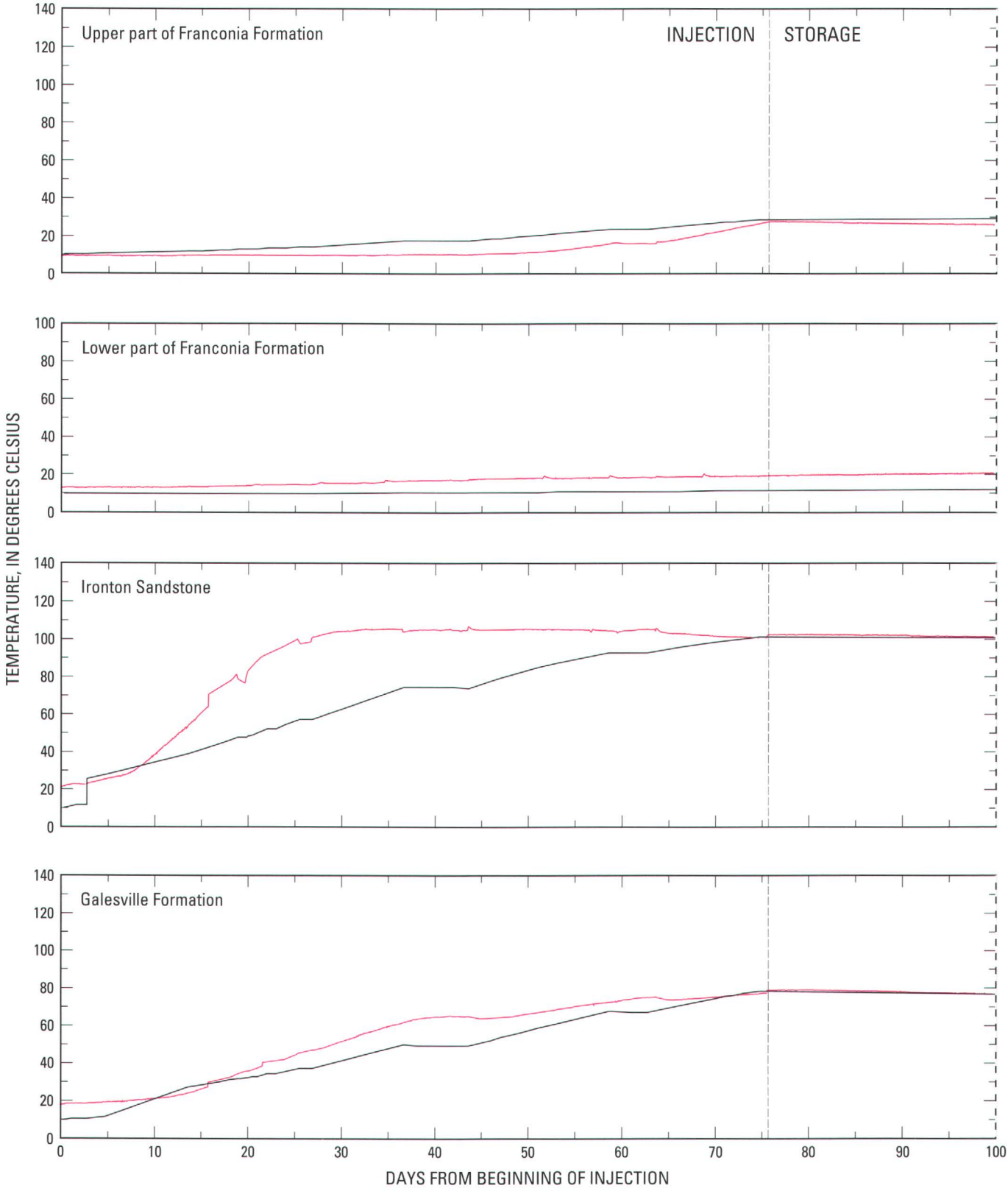

Figure 30. Model-computed and average measured temperatures

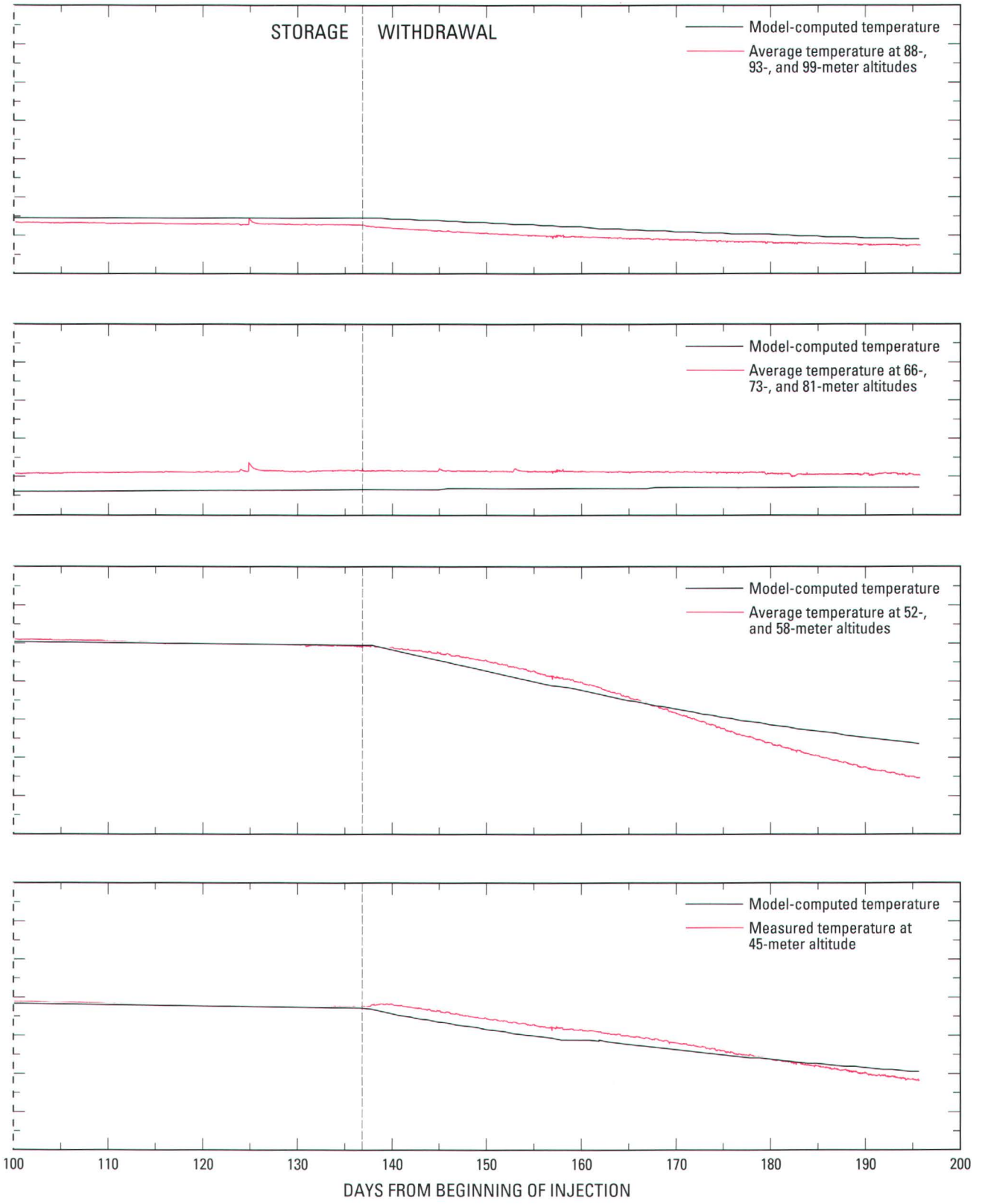

in observation well AM4 during long-term test cycle 1.

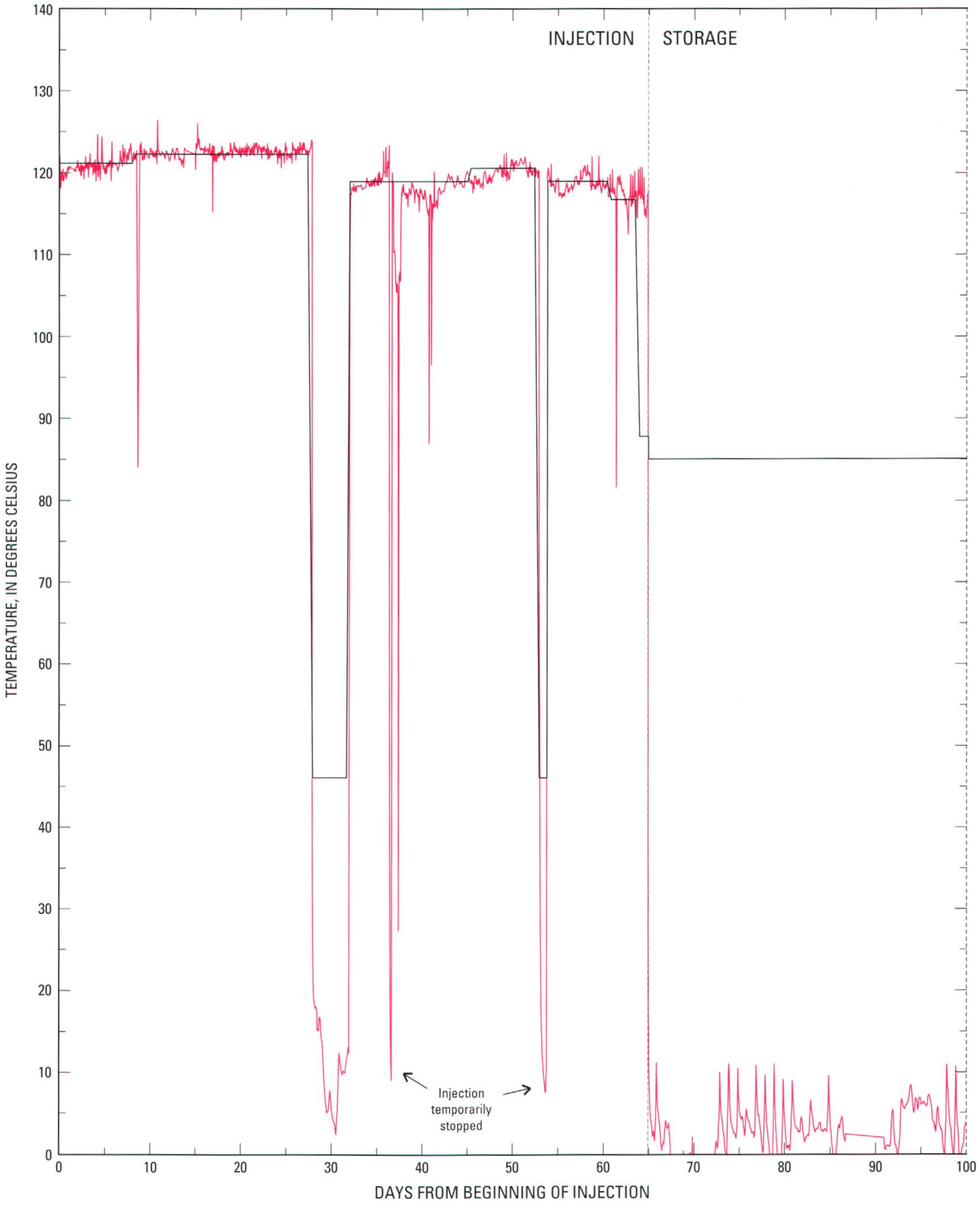

Figure 31. Model-computed and measured temperatures

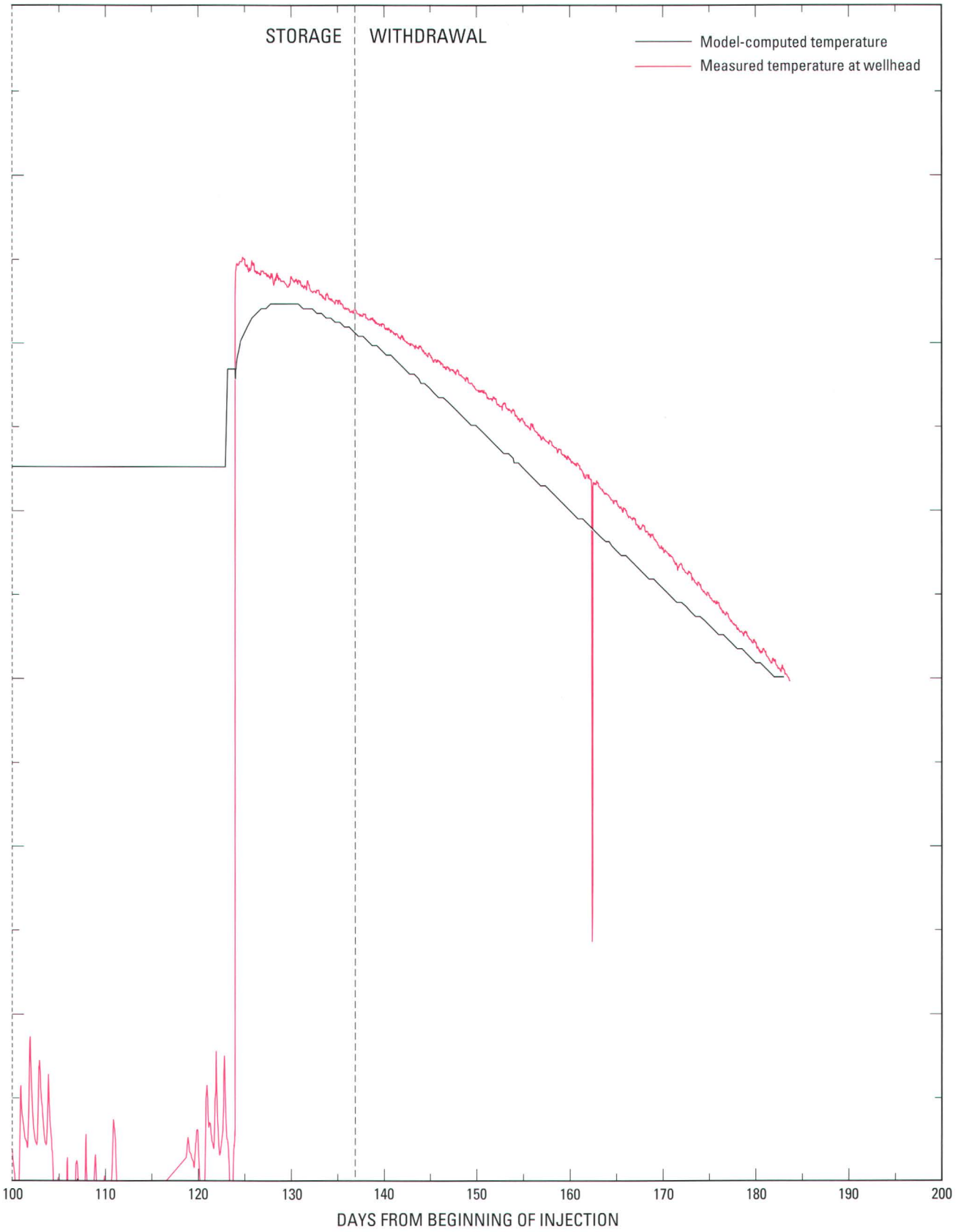

in production well A during long-term test cycle 2.

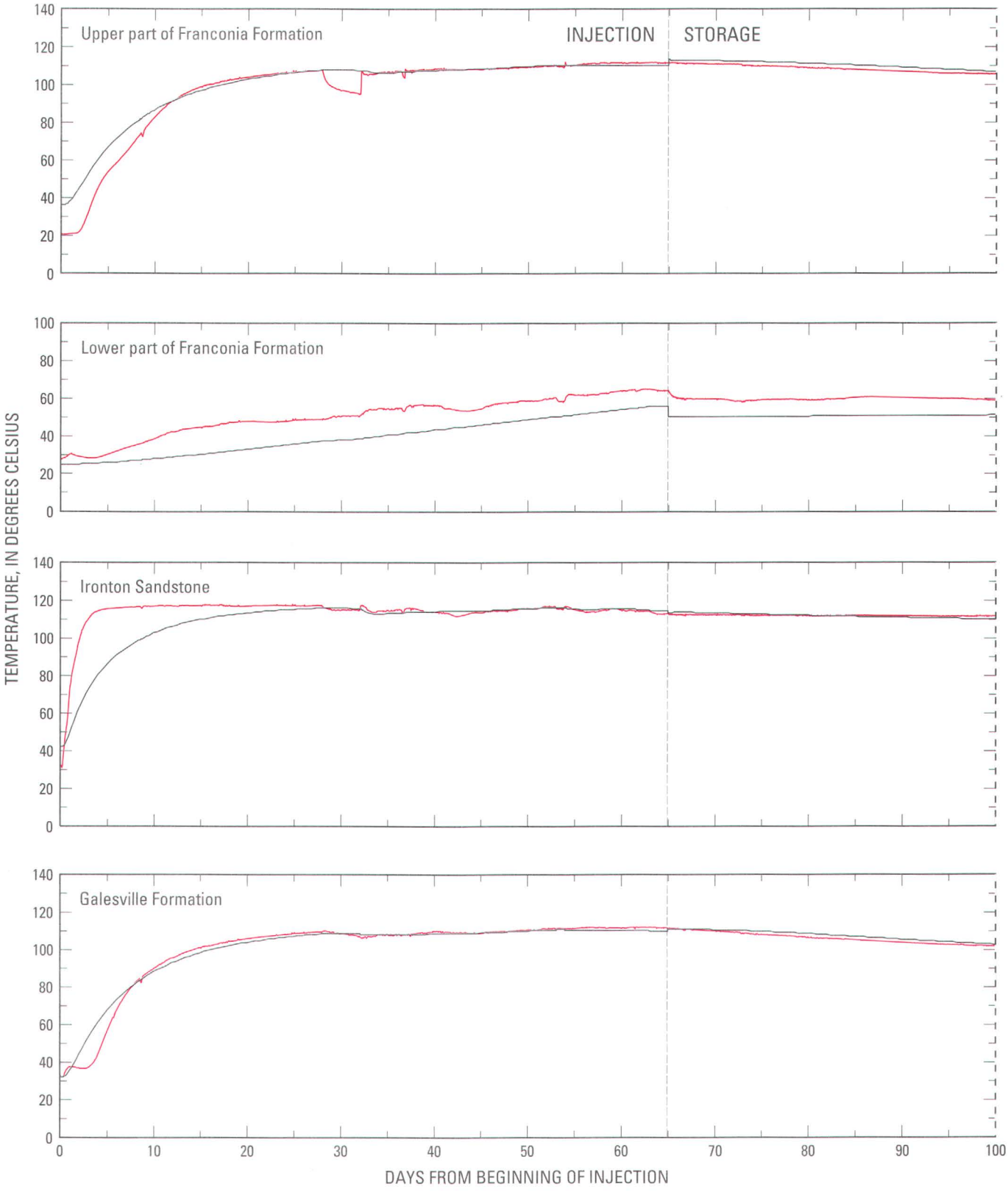

Figure 32. Model-computed and average measured temperatures

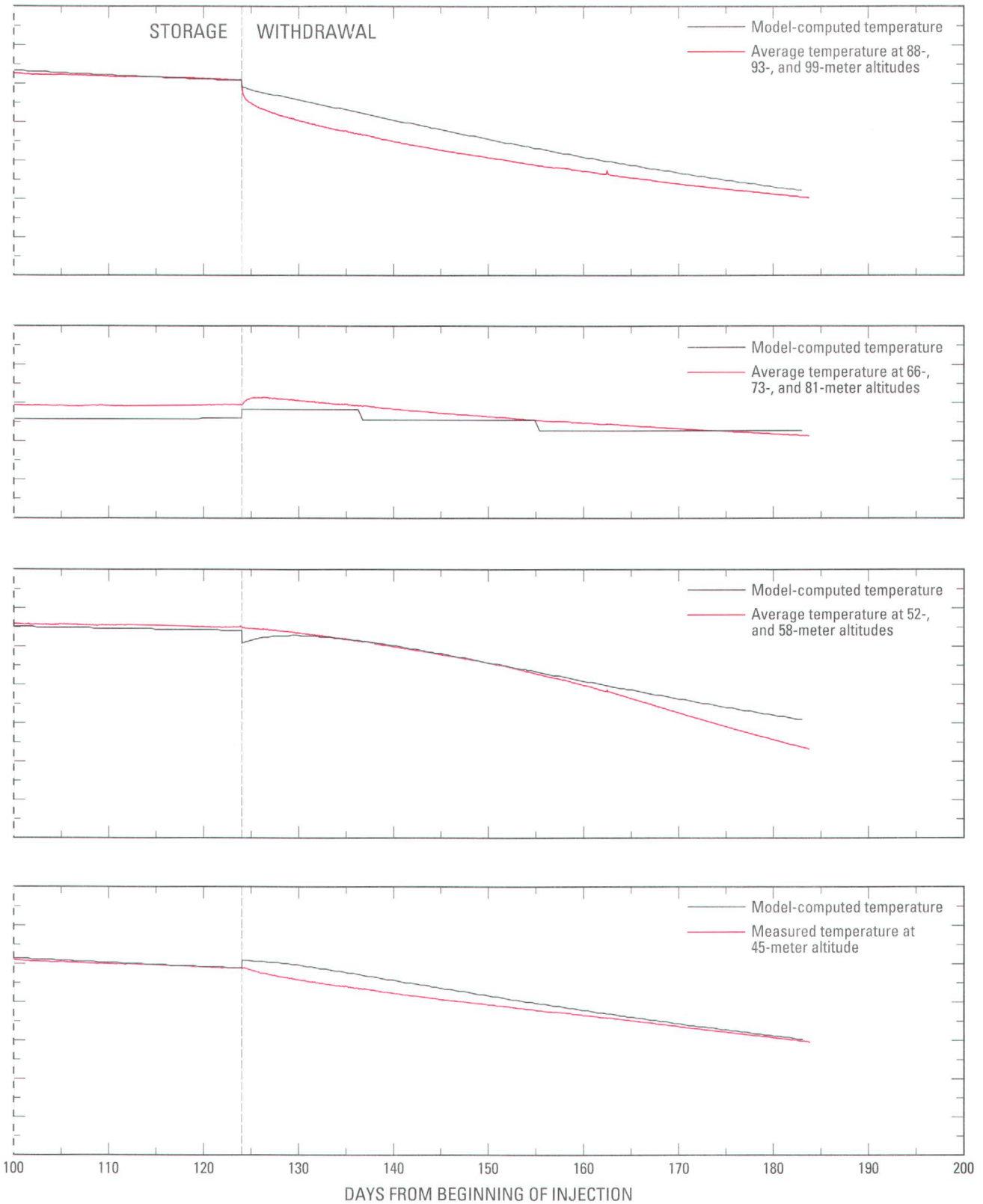

in observation well AM1 during long-term test cycle 2.

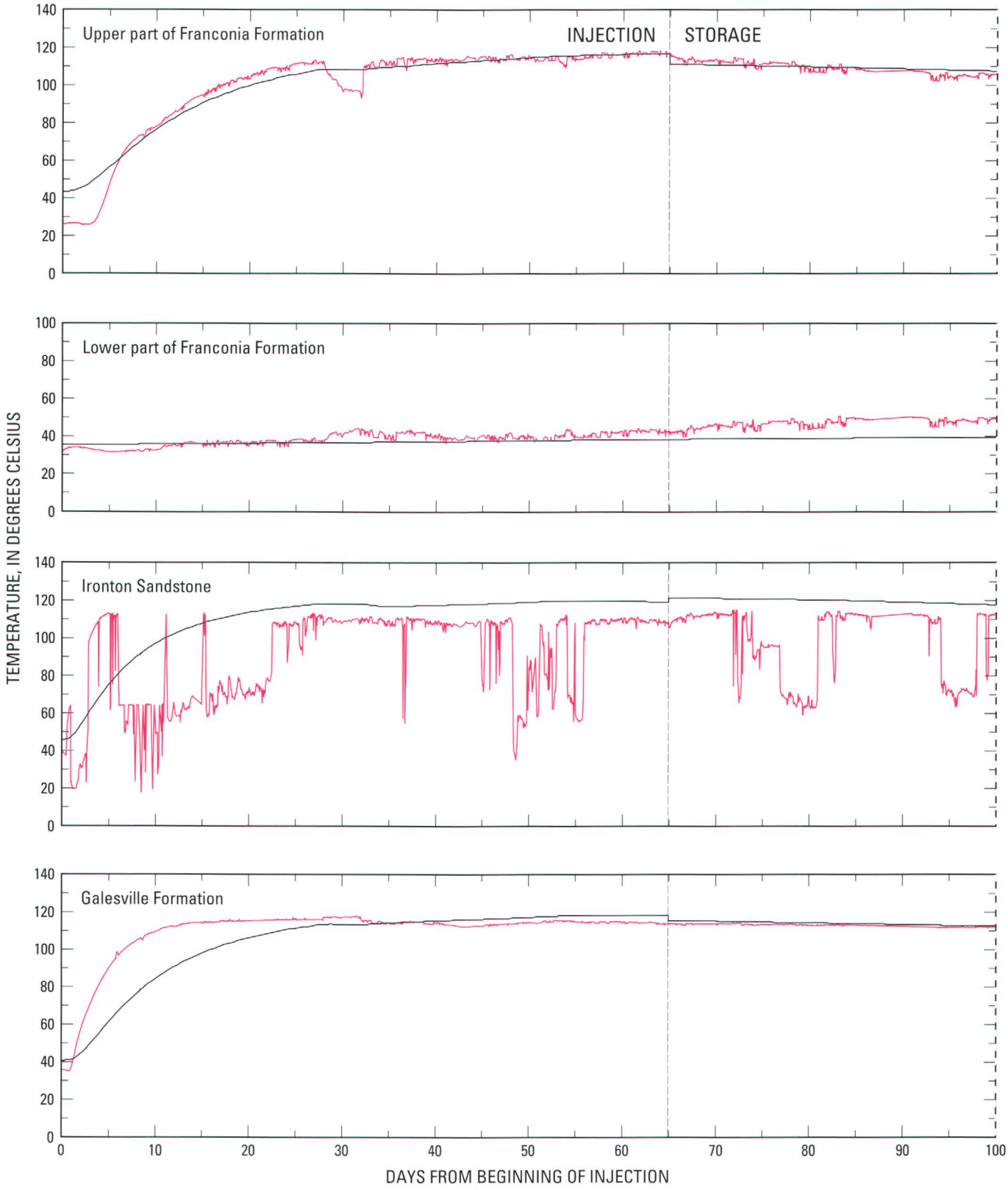

Figure 33. Model-computed and average measured temperatures

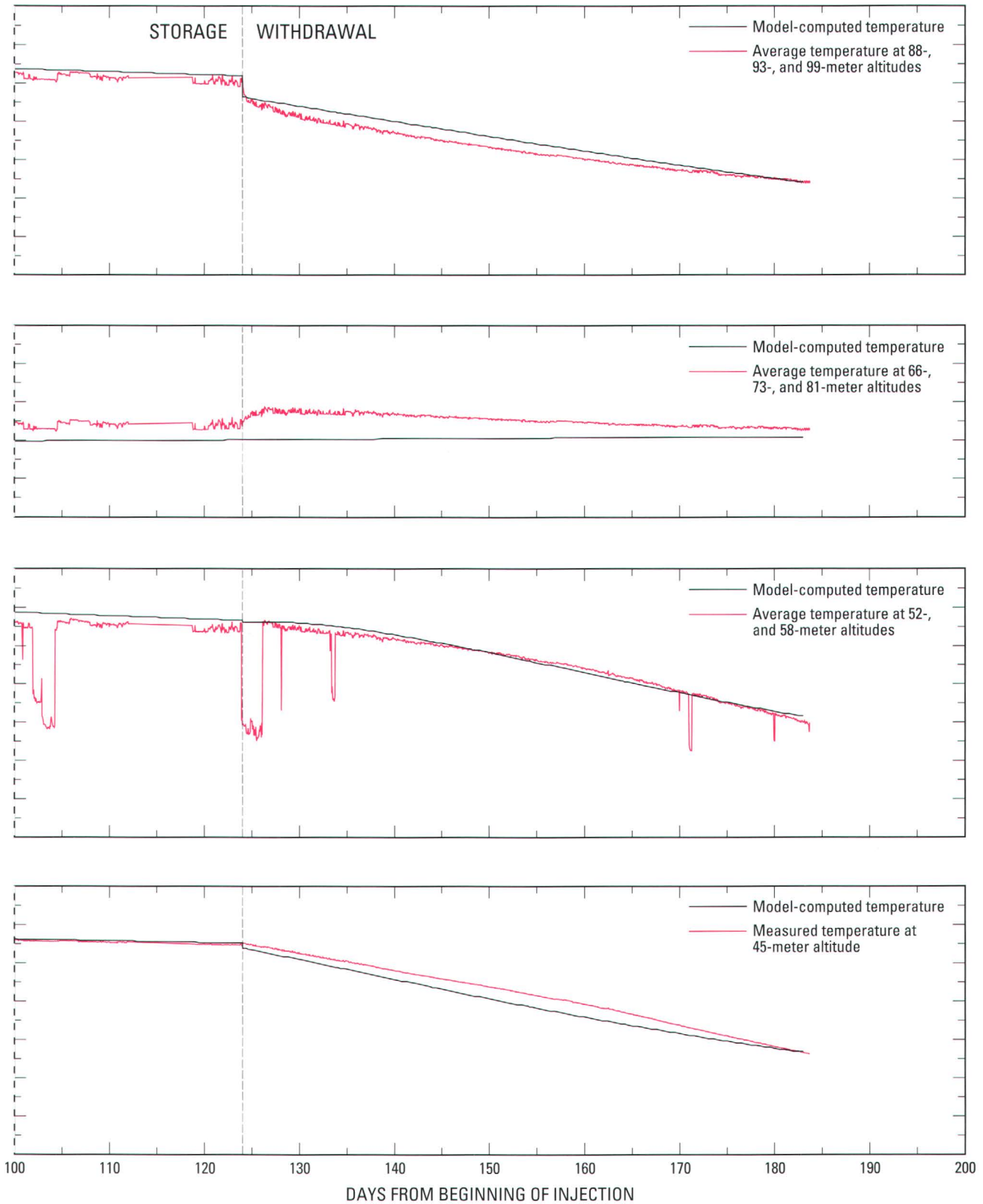

in observation well AS1 during long-term test cycle 2.

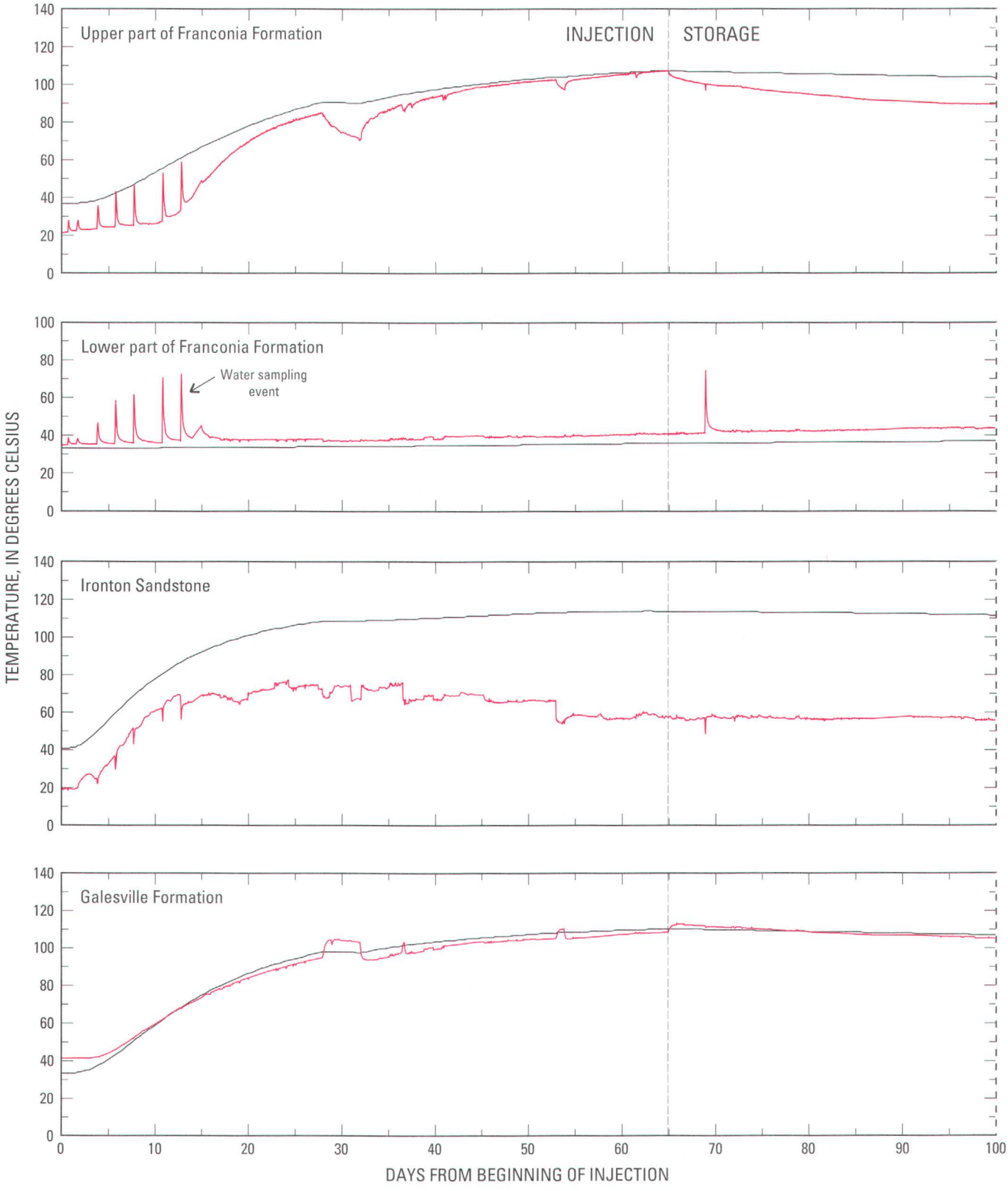

Figure 34. Model-computed and average measured temperatures

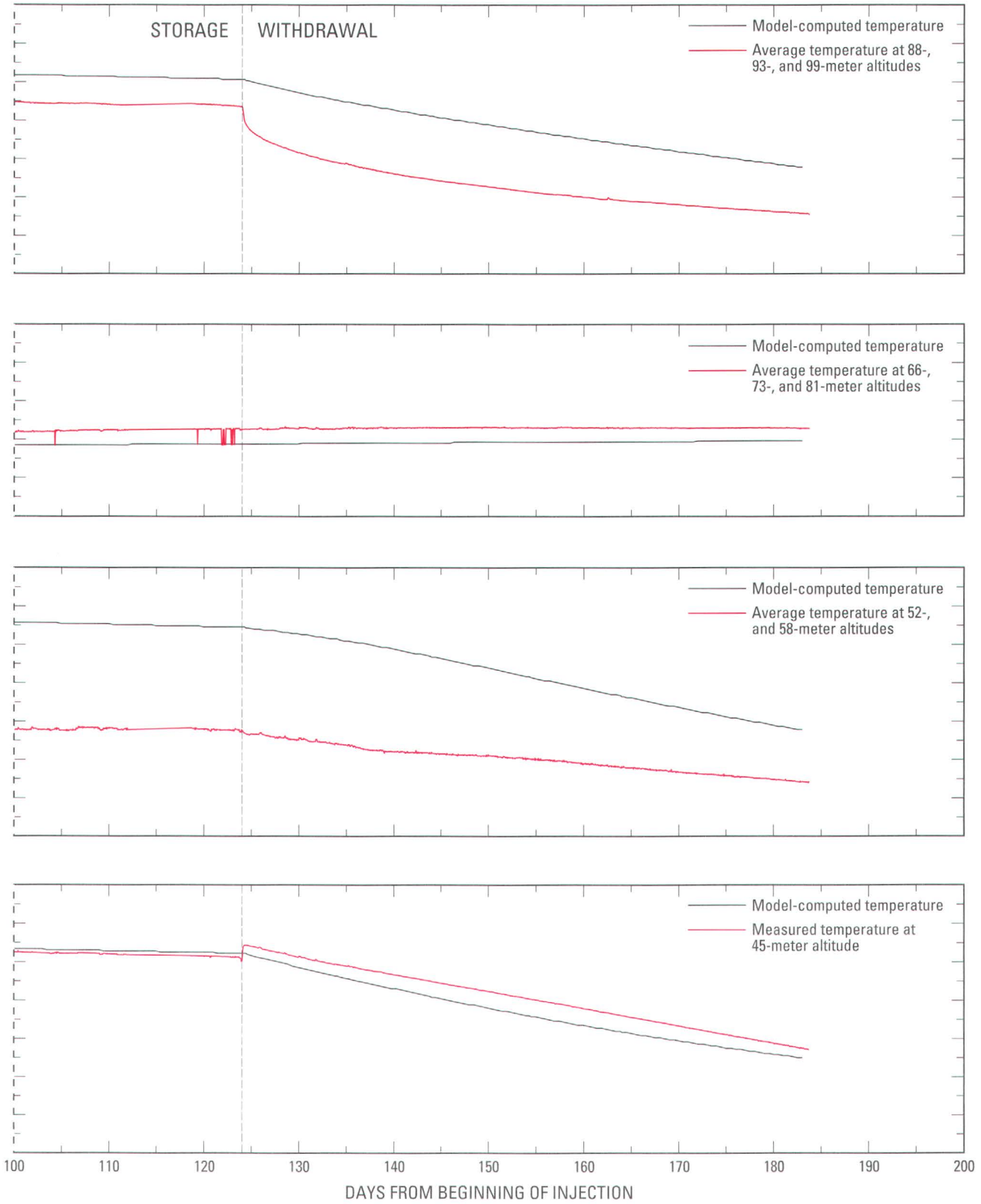

in observation well AM2 during long-term test cycle 2.

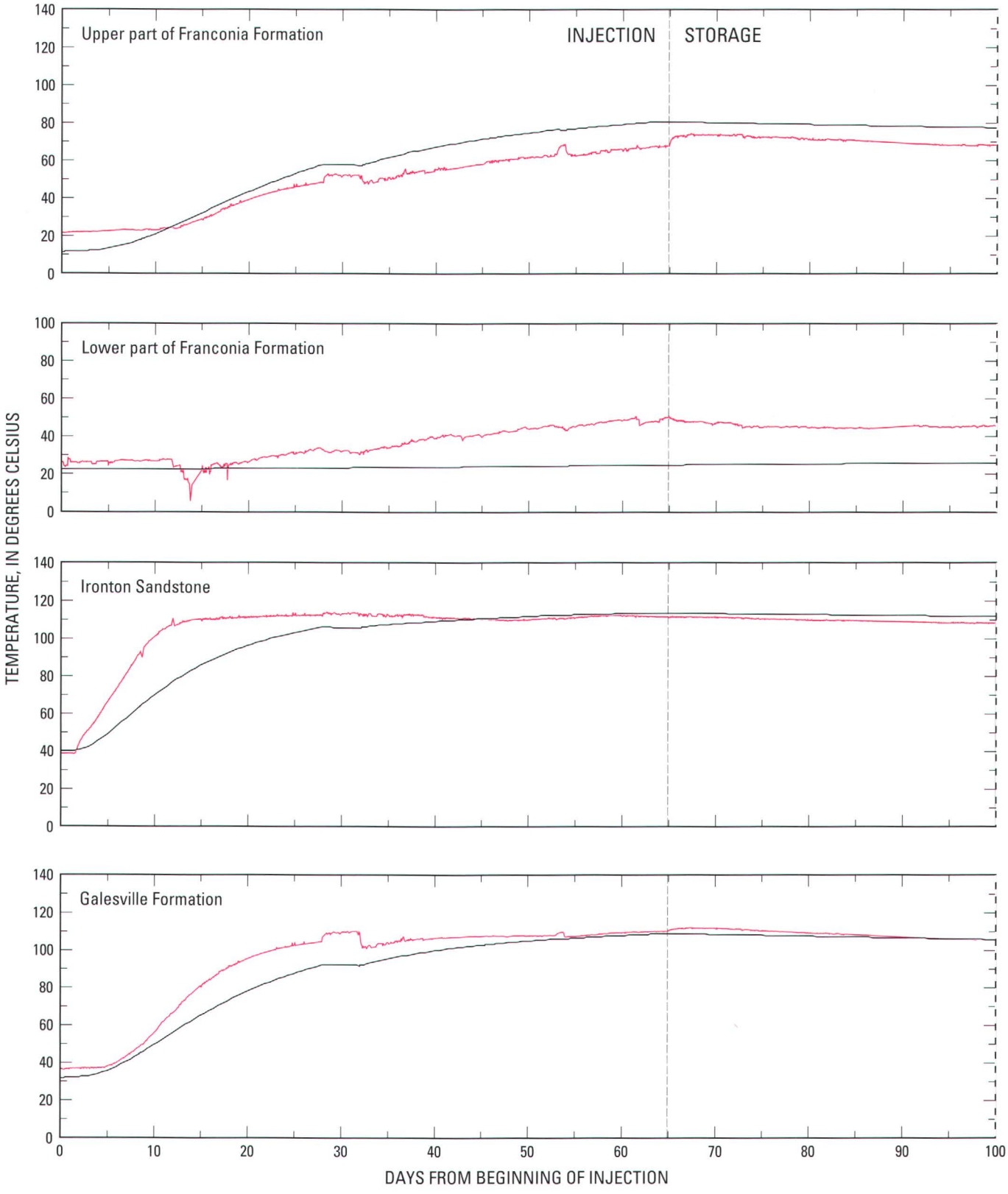

Figure 35. Model-computed and average measured temperatures

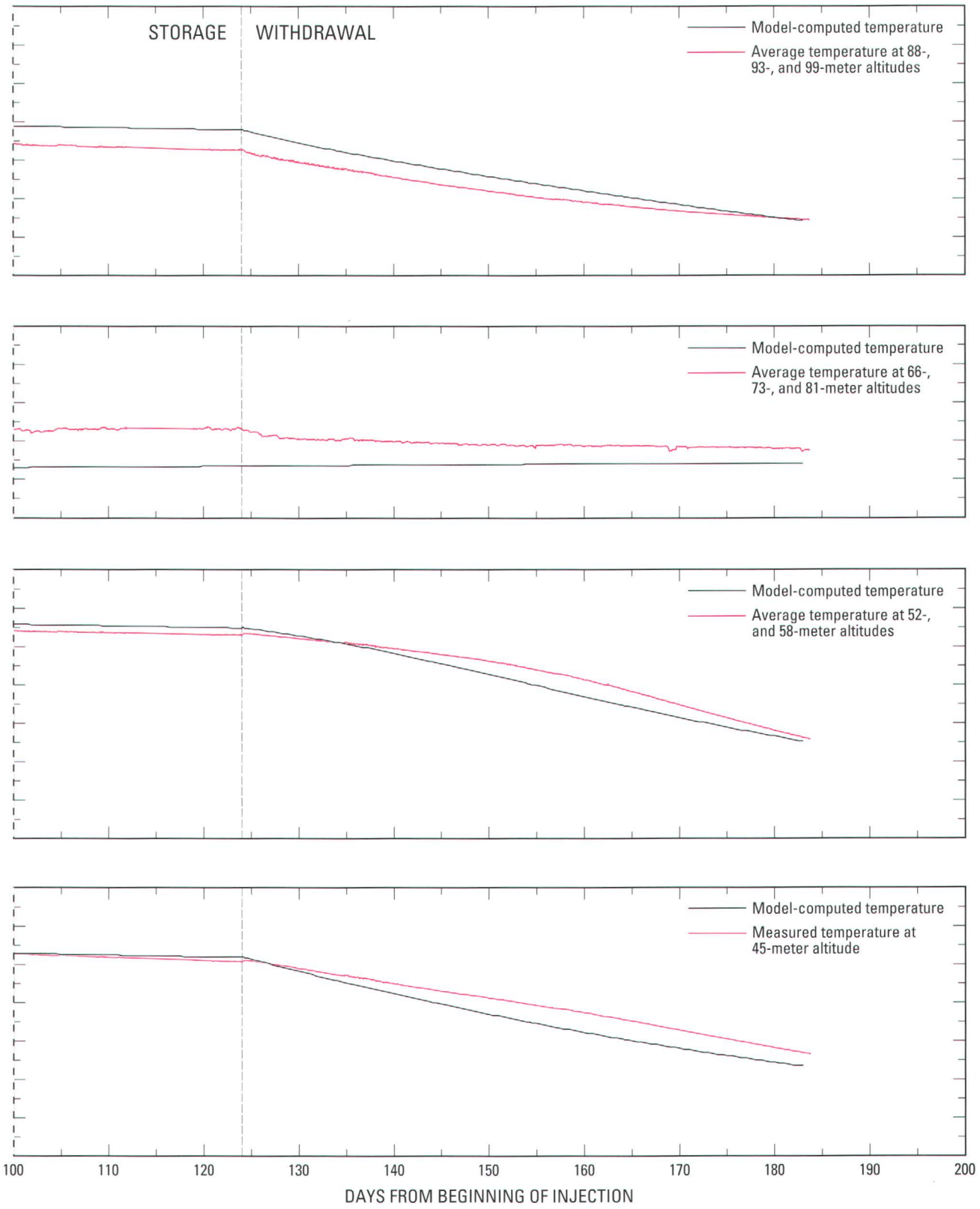

in observation well AM3 during long-term test cycle 2.

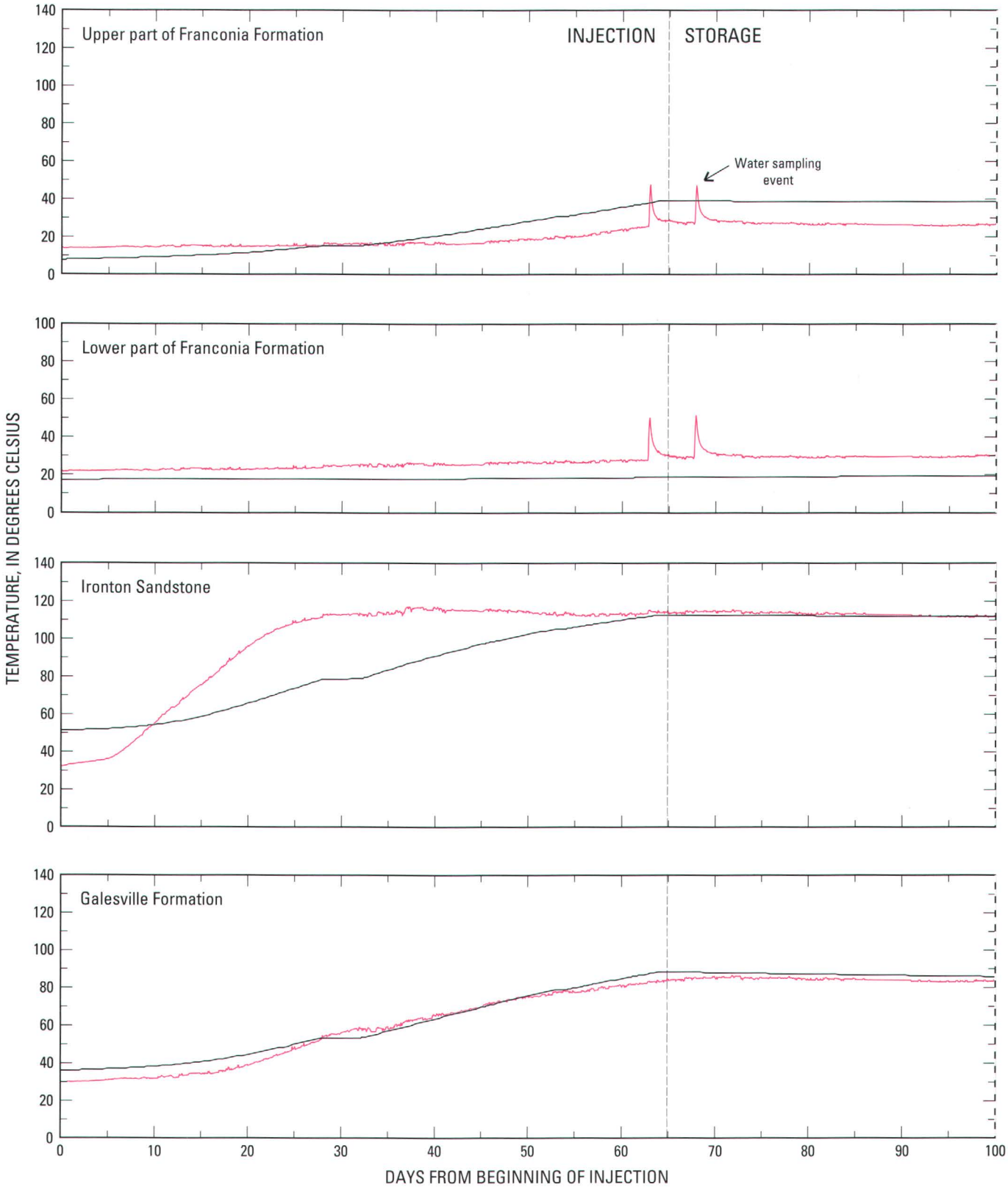

Figure 36. Model-computed and average measured temperatures

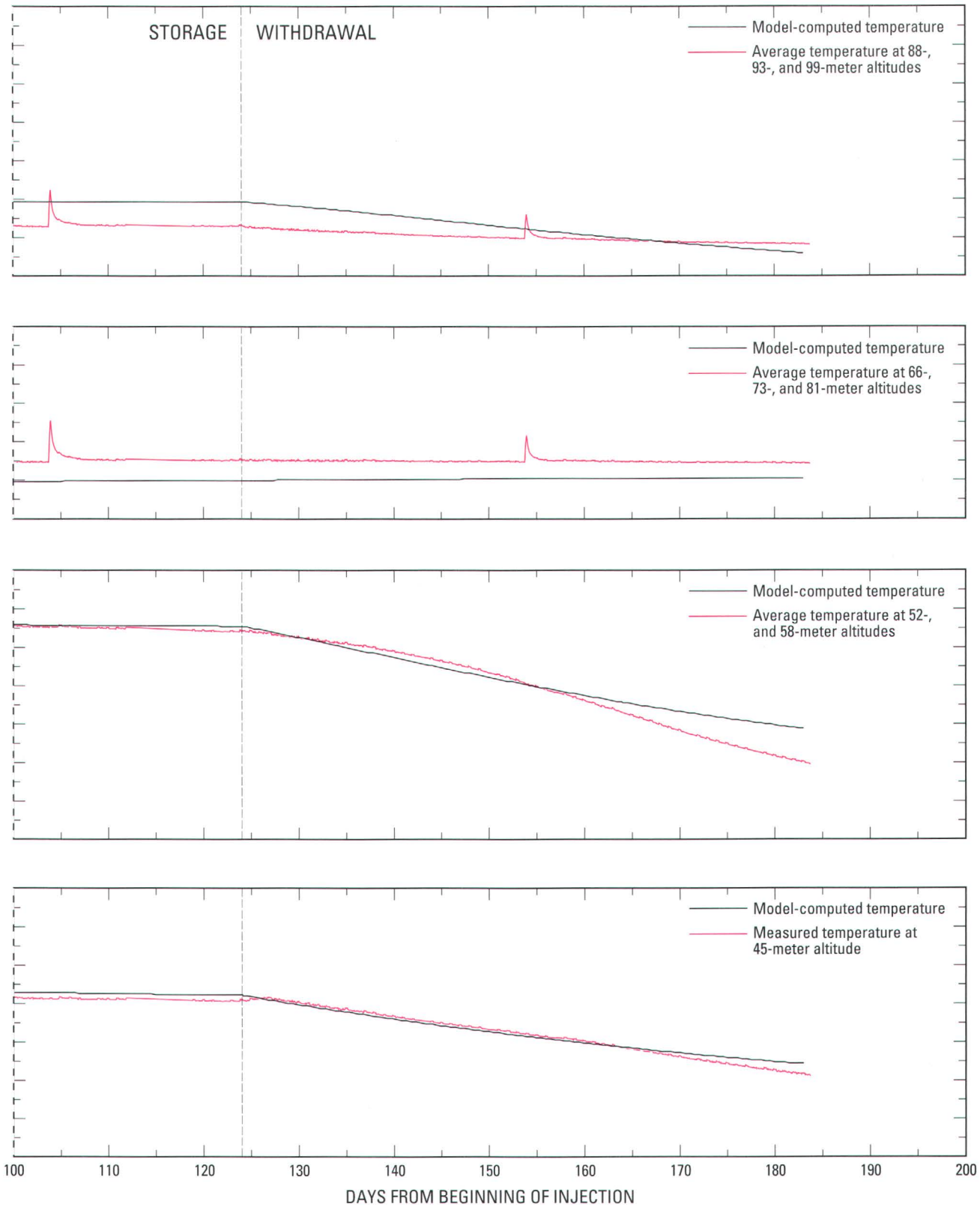

in observation well AM4 during long-term test cycle 2.

Table 8. Altitudes of measurement points where temperatures were averaged to correspond with model layers

Model layer	Stratigraphic unit	Altitude(s) of composited values (meters)
1	St. Lawrence Formation	110, 104
2	Upper part of Franconia Formation	99, 93, 88
3	Lower part of Franconia Formation	81, 73, 66
4	Ironton Sandstone	58, 52
5	Galesville Sandstone	45
6	Eau Claire Formation	38

For the lower part of the Franconia Formation, model-computed temperatures were lower than averaged temperatures at all observation wells. The temperature differences were from less than 5°C to as much as 30°C. This relatively poor approximation of the temperatures measured in the lower part of the Franconia Formation may have resulted from one or more of the following factors: (1) underestimation of the thermal conductivity of the unit or the pipe; (2) more convection transport of heat vertically within the observation well than is accounted for in the model; and (3) leakage between the upper part of the Franconia Formation and the Ironton and Galesville Sandstones, resulting in the transport of heat vertically within the observation well.

The computed temperatures for the model increased more slowly than the averaged temperatures, but ended the injection phases at about the same temperature (within about 10°C). Model-computed temperatures during withdrawal typically were within 10°C of the averaged temperatures. Model-computed temperatures in the Ironton Sandstone were 20–40°C higher than averaged temperatures at well AM2. These averaged temperatures are anomalous in comparison to the averaged temperatures at well AM3, which is at approximately the same radial distance from production well A as well AM2. Well AM2 is on the axis of minimum transmissivity (Miller, 1984). Therefore, it is possible that the model did not accurately simulate the effects of lesser transmissivity near well AM2, causing higher model-computed temperatures. For the Galesville Sandstone, model-computed and averaged temperatures had the best match of all the simulated formations. The timing and magnitude of temperature changes were very close (less than 5°C).

The calibrated nonisothermal model is a tool for evaluating aquifer thermal-energy storage. The model can be used to evaluate the optimum: (1) rates of injection and withdrawal, (2) injection temperature, and (3) duration of injection, storage, withdrawal periods. The model should prove useful in estimating the recovery temperatures of heated-water injection in the Franconia-Ironton-Galesville aquifer and is a valuable tool in computing thermal efficiency of the aquifer.

Results of simulating the long-term test-cycles suggest that the model closely estimated temperatures at the observation wells, except in the low permeability layers. Results of model analyses indicate that the model is accurate in predicting thermal efficiency of the aquifer and temperatures at production well A during periods of withdrawal. The model is less accurate in simulating temperatures at the observation wells because of the effects of aquifer anisotropy. Model accuracy in simulating temperatures at the observations wells could perhaps be improved by obtaining additional information on anisotropy of the Franconia-Ironton-Galesville aquifer and studying its effect on the movement and direction of heat flow for the hydrologic conditions at the ATES site.

SUMMARY

In May 1980, the University of Minnesota began a project to evaluate the feasibility of storing heated water (150 degrees Celsius) in the Franconia-Ironton-Galesville aquifer (183 to 245 meters below land surface) and later recovering it for space heating. The University's steam-generation facilities supplied high-temperature water for injection. This Aquifer Thermal-Energy Storage system had a doublet-well design in which the injection and withdrawal wells were spaced approximately 250 meters apart. Water was pumped from one of the wells through a heat exchanger, where heat was added or removed. This water was then injected back into the aquifer through the other well.

Two long-term test cycles were conducted during which high-temperature water (at 108.5 degrees Celsius and 117.7 degrees Celsius, respectively) was injected for periods of about 59 days duration. Periods of storage

were 61.0 and 59.1 days, and periods of withdrawal were 58.0 and 59.7 days, respectively. Approximately equal rates of injection and withdrawal of about 18 L/s were maintained for each test cycle. Withdrawal temperatures averaged about 75 and 85 degrees Celsius, respectively.

Temperature graphs for selected depths at individual observation wells indicate that the Ironton and Galesville Sandstones received, stored, and yielded more thermal energy than the upper part of the Franconia Formation. Vertical-profile plots and time-graphs during storage indicate that the effects of buoyancy flow were minimal within the aquifer. Temperature graphs indicate that the shortest arrival times for temperature fronts, and the hottest temperatures measured at all observation wells, were in the Ironton and Galesville Sandstones. The next shortest arrival times, and somewhat cooler temperatures, were in the less permeable upper part of the Franconia Formation. The latest arrival times for temperature fronts were measured in the lower part of the Franconia Formation. Because the lower part of the Franconia Formation was not screened, heat within this part of the aquifer was transported by conduction. Significant heat was conducted into the lower part of the Franconia Formation. However, the percentage of total injected heat that remained in the lower part of the Franconia Formation after withdrawal was insignificant. Very little heat conduction was observed in the upper St. Lawrence Formation and Eau Claire Formation confining layers to the aquifer. Buoyancy flow within the aquifer was minimal, as evidenced by temperature profiles at individual observation wells during periods of injection, storage, and withdrawal.

A three-dimensional, anisotropic, nonisothermal ground-water-flow and thermal-energy-transport model was used to simulate the two long-term test cycles. Calibration of the model to nonisothermal conditions consisted of comparing model-computed thermal efficiencies and withdrawal-water temperatures to calculated or measured values. The model was calibrated by comparing model-computed results to: (1) measured temperatures at selected altitudes in five observation wells, (2) measured temperatures at the production well, and (3) calculated thermal efficiencies of the aquifer. The only input properties varied during model calibration were the longitudinal and transverse thermal dispersivity, which were simulated at 3.3 and 0.33 m, respectively. The model accurately simulated aquifer thermal efficiencies to within about 1 percent of calculated values. The model accurately simulated withdrawal-water temperatures to within an average of about 3 percent of calculated values. Graphs of model-computed temperatures closely matched graphs of average measured temperatures in most cases. Results of model analyses indicate that the model is accurate in simulating thermal efficiency of the aquifer and temperatures of production well A during periods of withdrawal. The model is less accurate in simulating temperatures at the observation wells because of the effects of aquifer anisotropy.

The calibrated nonisothermal model is a tool for evaluating aquifer thermal-energy storage. The model can be used to evaluate the optimum: (1) rates of injection and withdrawal, (2) injection temperature, and (3) duration of injection, storage, and withdrawal periods. The model should prove useful in estimating the recovery temperatures of heated-water injection in the Franconia-Ironton-Galesville aquifer and is a valuable tool in computing thermal efficiency of the aquifer.

REFERENCES

Bear, Jacob, 1972, Dynamics of fluids in porous media: New York, Elsevier, 764 p.

Clark, S.P., 1966, Book of physical constants: Geological Society of America Memoir 97, 587 p.

Czarnecki, J.B., 1983, Fortran computer programs to plot and process aquifer pressure and temperature data: U.S. Geological Survey Water-Resources Investigations Report 85–4051, 49 p.

Freeze, R.A., and Cherry, J.A., 1979, Groundwater: Englewood Cliffs, N.J., Prentice-Hall, Inc., 604 p.

Helgeson, H.C., Delaney, J.M., Nesbitt, H.W., and Bird, D.K., 1978, Summary and critique of the thermodynamic properties of rock forming minerals: American Journal of Science, v. 278–A, 229 p.

Hellstrom, G., Tsang, Chin-Fu, and Claesson, Johan, 1979, Heat storage in aquifers—Buoyancy flow and thermal stratification problems: Lund University (Sweden), 70 p.

Hoyer, M.C., Eisenreich, S.J., Almendinger, J.E., Perlinger, J.A., Miller, R.T., Lauer, J.L., and Walton, M., 1991a, University of Minnesota aquifer thermal energy storage (ATES) project report on the first long-term cycle: Pacific Northwest Laboratory, PNL–7817, UC–202, 137 p.

Hoyer, M.C., Eisenreich, S.J., Hallgren, J.P., Howe, J.T., Lauer, J.L., Splettstoesser, J.F., and Walton, M., 1991b, University of Minnesota aquifer thermal energy storage (ATES) project report on the second long-term cycle:

Pacific Northwest Laboratory, PNL–7917, UC–202, 137 p.

Hoyer, M.C., Hallgren, J.P., Uebel, M.H., Delin, G.N., Eisenreich, S.J., and Sterling, R.L., 1994, University of Minnesota aquifer thermal energy storage (ATES) project report on the third long-term cycle: Pacific Northwest Laboratory, PNL–9811, UC–202, 126 p.

Intercomp Resources Development and Engineering, Inc., 1976, A model for calculating effects of liquid waste disposal in deep saline aquifers: U.S. Geological Survey Water-Resources Investigations Report 76–61, 128 p.

Kappelmeyer, O., and Haenel, R., 1974, Geothermics with special reference to application: Berlin-Stuttgart, Gebruder Borntraeger.

Martin, W.L., and Dew, J.N., 1965, How to calculate air requirements for forward combustion: Petroleum Engineer, February 1965.

Miller, R.T., 1984, Anisotropy of the Ironton-Galesville Sandstones near a thermal-energy-storage well—St. Paul, Minnesota: Ground Water, v. 22, no. 5, p. 532–537.

_____ 1985, Preliminary modeling of an aquifer thermal-energy storage system, *in* Subitzky, Seymour, eds., Selected Papers in the Hydrologic Sciences: U.S. Geological Survey Water-Supply Paper 2270, p. 1–20.

Miller, R.T., and Delin, G.N., 1993, Cyclic injection, storage, and withdrawal of heated water in a sandstone aquifer at St. Paul, Minnesota—Field observations, preliminary model analysis, and aquifer thermal efficiency: U.S. Geological Survey Professional Paper 1530–A, 55 p.

_____1994, Cyclic injection, storage, and withdrawal of heated water in a sandstone aquifer at St. Paul, Minnesota—Thermal data analysis and nonisothermal modeling of short-term test cycles: U.S. Geological Survey Open File Report 93–435, 70 p.

Miller, R.T., and Voss, C.I., 1986, Design of a finite-difference grid for a doublet-well thermal-energy storage system in an anisotropic aquifer: Ground Water, v. 24, no. 4, p. 490–496.

Norvitch, R.F., Ross, T.G., and Brietkrietz, Alex, 1973, Water resources outlook for the Minneapolis-St. Paul Metropolitan Area, Minnesota: Metropolitan Council of the Twin Cities, 219 p.

Norvitch, R.F., and Walton, M.S., eds., 1979, Geologic and hydrologic aspects of tunneling in the Twin Cities area, Minnesota: U.S. Geological Survey Miscellaneous Investigations Series Map I–1157, 7 plates.

Robie, R.A., Hemminway, B.S., and Fisher, J.R., 1978, Thermodynamic properties of minerals and substances at 298°K and 1 bar (105 pascals) pressure and at higher temperatures: U.S. Geological Survey Bulletin 1452, 456 p.

Sommerton, W.H., Mehta, M.M., and Dean, G.W., 1965, Thermal alteration of sandstones: Journal of Petroleum Technology, May, p. 589–593.

Walton, Matt, 1981, The University of Minnesota aquifer thermal energy storage system, *in* Proceedings of mechanical magnetic, and underground energy storage, 1981 Annual Contractors Review, August 24–26, 1981, Washington, D.C.: Conf–810 833, U.S. Department of Energy, p. 120–126.

Walton, M., Hoyer, M.C., Eisenreich, S.J., Holm, N.L., Holm, T.R., Kanivetsky, R., Jirsa, M.A., Lee, H.C., Lauer, J.L., Miller, R.T., Norton, J.L., and Runke, H., 1991, The University of Minnesota aquifer thermal energy storage (ATES) field test facility—System description, aquifer characterization, and results of short-term test cycles: Pacific Northwest Laboratory, PNL–7220, UC–202, 295 p.

ISBN 0-607-99152-6